Summer 2010

Quantification and localization of gait variability as biomarkers for mild traumatic brain injury

Rosalind Lauren Smith
University of Iowa

QUANTIFICATION AND LOCALIZATION OF GAIT VARIABILITY AS BIOMARKERS FOR MILD TRAUMATIC BRAIN INJURY

by

Rosalind Lauren Smith

A thesis submitted in partial fulfillment
of the requirements for the Master of
Science degree in Biomedical Engineering
in the Graduate College of
The University of Iowa

July 2010

Thesis Supervisors: Assistant Professor Salam Rahmatalla
Associate Professor Deema Fattal

Graduate College
The University of Iowa
Iowa City, Iowa

CERTIFICATE OF APPROVAL

_____

MASTER'S THESIS

_____

This is to certify that the Master's thesis of

Rosalind Lauren Smith

has been approved by the Examining Committee
for the thesis requirement for the Master of Science
degree in Biomedical Engineering at the July 2010 graduation.

Thesis Committee: _____
Salam Rahmatalla, Thesis Supervisor

_____
Deema Fattal, Thesis Supervisor

_____
Edwin Dove

_____
Nicole Grosland

_____
David Wilder

To my parents,
for believing in me.

ACKNOWLEDGMENTS

I would like to acknowledge and thank the individuals at the MRI Research Facility and the 3D Bio-Motion Research Lab at the University of Iowa for their expertise and assistance with this project. In particular, I would like to acknowledge John Meusch for his assistance in the collection and post processing of the motion capture data and for the inspired conversations. Also, Ricardo Jorge, Jinsuh Kim, and Toshio Moritani for their collaborative work with the imaging protocol and analysis, especially Jinsuh Kim for his reporting of the MRI-DTI findings. I would like to thank Joe Ekdahl and Vincent Magnotta for their assistance and patience scheduling MRIs.

I would like to acknowledge my advisors, Salam Rahmatalla and Deema Fattal, and thank them for teaching me the value of hard work and a positive attitude. I would also like to acknowledge the members of my committee, Edwin Dove, Nicole Grosland, and David Wilder, for their presence and involvement in my education and for their continual support and guidance.

I would also like to pray for the U.S. military and the individuals who so willingly serve and protect our country. It is my hope that this work contributes to the ever growing knowledge of mild traumatic brain injury, and that someday these courageous men and women will benefit from improved diagnosis and treatment and lead lives free of the persistent and debilitating effects of mild traumatic brain injury.

ABSTRACT

Motion capture technology and Magnetic Resonance Imaging with Diffusion Tensor Imaging (MRI-DTI) were used in this work to detect subtle abnormalities in patients with mild traumatic brain injury (MTBI). A new concept, termed dynamic variability, is introduced in this work to quantify and localize gait variability. Three chronic MTBI patients were recruited from the Veterans Affair Medical Center in Iowa City, IA, and three healthy controls with height, weight, and gender matched to the patients were recruited from the Reserve Officers' Training Corps in Iowa City, IA. Kinematic and kinetic data of the subjects were collected during the performance of three gait testing scenarios. The first test involved single-task walking and was used as a baseline. The second and third tests were dual tasks that involved walking while performing a cognitive or motor task and were designed to magnify gait abnormalities. The results showed that MTBI patients had reduced gait velocity, shortened stride length, and larger step width; findings that are consistent with those published in the literature. The new dynamic variability factor found that, as compared to controls, MTBI patients had more variability in their hip and ankle joint moments. MRI-DTI has been used to detect dysfunction of the major white matter tracts in chronic MTBI patients; although, the sample size of this study was too small to detect a difference between the MTBI and control subjects. The imaging and gait abnormalities are suggestive of frontal lobe-white matter tracts dysfunction.

TABLE OF CONTENTS

LIST OF TABLES

LIST OF FIGURES

LIST OF ABBREVIATIONS

%BW	Percentage of Body Weight
AP	Anterioposterior or Anterior-Posterior
BOS	Base Of Support
COM	Center Of Mass
GRF	Ground Reaction Force
ML	Mediolateral or Medial-Lateral
MRI	Magnetic Resonance Imaging
MRI-DTI	Magnetic Resonance Imaging with Diffusion Tensor Imaging
MTBI	Mild Traumatic Brain Injury
TBI	Traumatic Brain Injury

CHAPTER 1

BACKGROUND MATERIAL

Mild Traumatic Brain Injury

Incidence

Traumatic brain injury (TBI) is one of the most challenging medical problems. It is estimated that 5.3 million Americans, approximately 2% of the US population, suffer from disabilities resulting from TBI [38]. According to the 2003 report to Congress, as many as 1.5 million people sustain a TBI annually in the United States, and mild traumatic brain injuries (MTBI) constitute 70-90 percent of these injuries [6,17]. The incidence of MTBI is an estimated 100-300 per 100,000, making it one of the most common neurologic disorders [6]. Most patients improve without treatment; however, 15 percent of persons experience persistent symptoms for at least one year post-injury [1]. Although mortality is rare, these non-life-threatening symptoms include headache, neck pain, dizziness, imbalance, and cognitive complaints and are a source of significant morbidity to MTBI patients throughout their lives [1,4]. The prevalence of persistent symptoms is estimated at 7-33 percent depending on the work referenced [41].

Definition

MTBI is medically characterized by a head trauma resulting from a blunt force or acceleration/deceleration forces. By definition, MTBI is associated with at least one of the following: i) transient confusion or disorientation (no specified time limit); ii) post-traumatic amnesia for less than 24 hours; iii) transient neurological abnormalities such as focal signs, seizure, or intracranial lesion not requiring surgery; and iv) any loss of consciousness for 30 minutes or less. The Glasgow Coma Scale is evaluated at 13-15 out of 15, after 30 minutes post-injury or upon presentation for healthcare [5]. Thus MTBI is a clinical diagnosis. Neuroimaging technologies, including computed tomography and

magnetic resonance imaging (MRI), do not reveal focal signs or structural abnormalities [1,36,39]. Research into advanced imaging modalities may reveal MTBI brain abnormalities that are not identified using these conventional imaging modalities.

Mild brain injury, mild head injury, and concussion are used interchangeably with MTBI.

Outcomes

MTBI is clinically defined during the acute phase of the injury without consideration of symptoms following the injury [1,36]. Cognitive impairment occurs immediately and may include problems with concentration, attention, memory, and reaction time [41]. Patients with minor head injuries have shown poorer function one month post-injury than uninjured individuals in neuropsychological tests. Performance is significantly different when concentration is required to discriminate rhythmic patterns and when learning new information that is recalled after four hours [13]. After one month [39] and at one year [13,41] no significant difference in neuropsychological outcomes are found; although attentional resource deficits are demonstrated when examining measures of complex attention and working memory [41].

Persistent problems in balance and gait are debilitating in work, school, and social relationships [21] because they are difficult to diagnose and treat. Reports have shown that one-third of MTBI patients are newly unemployed three months post-injury [37]. During routine clinical evaluations, there are often few to no demonstrable abnormalities, even when patients have chronic complaints of dizziness or instability. This raises the question of alternative causes, such as psychological factors or compensation and litigation issues [1,11]. In addition, there are no guidelines for predicting who will develop persistent symptoms or for identifying abnormalities using imaging modalities or clinical gait evaluation. Following a TBI, risk of a second injury is three times greater, [11] so premature return to work and play is of concern.

MTBI carries an economic burden in addition to its cognitive and motor deficits. The Centers for Disease Control and Prevention estimated the cost of TBI to the United States in 1995 was $56 billion. This estimate includes $16.7 billion for the cost of MTBI and considers only injuries resulting in hospitalization or death. As a result, it underestimates the cost of MTBI directly in terms of emergency room and private physician care and indirectly in terms of lost productivity and reduced quality of life [17].

There is substantial need to understand risk factors for MTBI, to capture the magnitude of the injury, to improve the understanding and prevention of persistent symptoms, to develop a tool for screening patients at risk for persistent symptoms, and to develop effective methods of rehabilitating individuals with MTBI [17].

Anatomical Reference

According to anatomical definition, medial is towards the midline; lateral is away from the midline; anterior is towards the front, or ventral, aspect of the body; posterior is towards the back, or dorsal, aspect of the body; superior is above, or towards the head; and inferior is below, or towards the feet.

The anatomical position is a posture obtained by standing with the feet shoulder width apart, arms at the side, and palms facing forward. The sagittal plane divides the body into right and left halves, and rotation in the sagittal plane occurrs about the mediolateral (ML) axis. The coronal, or frontal, plane divides the body into ventral and dorsal halves, and rotation in the coronal plane takes place about the anterioposterior (AP) axis. The third anatomical plane, the transverse plane, divides the body into superior and inferior portions and is perpendicular to the longitudinal axis. The anatomical position and reference planes are depicted in Figure 1-1.

Movement of the lower extremities in the sagittal plane is driven by the flexor and extensor muscles crossing the hip and knee joints. At the ankle these muscles are referred to as plantar flexors (such as when walking on one's toes) and dorsiflexors

(when one is walking on one's heels). Movement in the coronal plane occurs by activation of the abductor and adductor muscles groups of the hip and the invertor (inward) and evertor (outward) muscles crossing the ankle [19].

Balance and Stability

Balance is defined as the inertial forces acting on and generated by the body to prevent falling and maintain upright posture and stability against gravity. Balance control is a dynamic task in which the center of mass (COM), the equivalent mass of all the body segments, must be maintained within the base of support of the body in order to prevent falling.

Standing

Balance during standing is modeled as an inverted pendulum with two strategies of control. In the AP direction, the ankle plantar/dorsiflexors are primarily responsible for controlling balance during small external or internal perturbations. Under strong perturbations or when the feet are not firmly planted on the floor, the hip flexors/extensors respond. Examples of insufficient control at the foot-floor interface include standing on a narrow beam or on a tilting platform that acts as the perturbation. In the ML direction, the major control strategy involves the hip abductors/adductors; the use of ankle invertors/evertors is often insufficient to control balance or stabilize the COM [47].

Locomotion

The study of human locomotion is presented in the literature in terms of basic anatomy, biomechanics, and neuromuscular control. Locomotion is produced by intentionally moving the COM anterior to the base of the support and placing the advancing foot to prevent a fall and maintain dynamic balance. Restabilization occurs during the double support period while one foot is accepting weight on the heel and the

other is pushing off on the ball of the foot [47]. This foot placement is one mechanism for maintaining dynamic balance [40]. Activation of the ankle muscles complements foot placement by adjusting the acceleration of the COM in the AP and ML directions but is insufficient to control balance during stance [47]. During locomotion, the hip flexors/extensors and abductors/adductors control stability in the AP and ML directions, respectively [47].

Assessment

Vestibular, visual, and somatosensory information are integrated in central processing to control balance, and a number of assessments are used to clinically examine different aspects of balance. The Romberg test is classically used to assess postural control while maintaining an upright posture. There are several variations on the Romberg test that exist and help understand the information provided by different sensory inputs. These variations include standing on foam, standing on one leg, and the tandem Romberg (i.e., standing with one foot in front of the other), and they stress the proprioceptive and vestibular systems. Visual information is tested by performing the tests with eyes open and closed [42]. Vereeck and colleagues [42] reported decreased balance performance with age, although the decade of decline varied for the tests considered. They presented limited support for a gender effect with middle-aged men performing better than women on the tandem Romberg test with closed eyes [42].

Balance performance during walking is assessed with the timed up and go, tandem gait, and dynamic gait index tests. The timed up and go test requires subjects to sit in an armchair and, upon instruction, to stand up, walk, turn around, return to the chair, and sit down. Completion time for the timed up and go test increases with age, and is greater in females than males [42]. While performing the tandem gait task, subjects walk heel to toe on a straight line with eyes open or closed. Tandem gait and dynamic gait index performance declined for persons in their seventies [42]. The dynamic gait

index measures performance of eight gait tasks. The tasks test different velocities, inclines, obstacles, and stair climbing. The dynamic gait index may be used to indicate functional balance [42]; although, it did not clearly identify gait deficits in a study of eight TBI patients [29].

Woollacott and Shumway-Cook [49] reviewed the relationship between attention and postural control where attention is defined as processing capacity and the performance of a task requires a portion of the limited attention capacity [49]. Research showed that postural control, once thought to be controlled by reflexes, consumed attentional resources [50]. Attentional requirements for standing may increase with age, and the performance of an additional task may increase instability during balance control, especially in older adults [49].

A study of 20 patients with TBI of differing severity tested balance control while performing an arithmetic task and found decreased postural control in TBI patients. Postural instability was not significantly magnified during the arithmetic task, indicating that attention resources may have been reduced though not limited [21]. The study of attentional resources during standing while performing another task is an example of a dual-task testing scenario.

Gait Evaluation

Clinical gait evaluations often reveal few if any abnormalities in persons with MTBI [2]. Research to capture and identify the subtle instabilities associated with this injury is essential to improving patient diagnosis and treatment. Gait instability is associated with an increased risk of fall. It is quantified by temporal and spatial gait parameters, kinematics, and kinetics. Gait analysis is an important consideration for elderly persons and persons with pathological gait resulting from disorders that are neurological, musculoskeletal, or sensory in origin. In the case of MTBI, additional research is needed to characterize gait abnormalities in patients with persistent symptoms.

Temporal and Spatial Parameters

Temporal and spatial gait parameters include speed, cadence, stride time, stance and swing time, stride length, and stride width and are selectively referenced in gait literature [18,31,40,45,48]. Measures of gait components are presented in two parts: the regular component that is repeated with each stride and the variable component that differs from stride to stride. In general, increased variability measures are associated with falling risk in older adults [48]. Increased stride width variability has been shown in healthy older adults along with a greater stride width [18]; decreased stride width variability was shown to be a predictor of future falls in the elderly population [28] and individuals with Parkinson's disease [18].

Reduced gait speed and shorter stride length are observed in TBI patients [2,29,31,45] and in concussed individuals [8] during level walking. The changes in gait speed are attributed solely to decreased stride length [29] or to a combination of reduced cadence and shorter stride length [31,45]. A trend towards longer stance phase was noted with some occurrence of greater double support time [45]. Increased clearance between the toe and ground, step height, may indicate cautious gait planning [29], and a wider BOS may indicate unstable tendencies [45]. One group reported greater stance time on the unaffected limb and no reduction in BOS in TBI patients [31].

Kinematics and Kinetics

Kinematic measures are concerned with describing the motion of the human in space. Kinematics may represent movement of the whole body or a segment and include linear and angular displacements, velocities, and accelerations. A large number of variables are needed to completely define the motion; the data can be reduced for gait analysis by focusing on the lower body and considering kinematics in the plane of progression and the coronal plane where falls are most likely to occur. COM kinematics are important because of the interaction between the COM and BOS in balance control

and stability. The kinematics of the head, arms, and trunk provide important insight for gait analysis; although, they are not considered in this work.

Kinetics is concerned with the forces that cause movement. The joint forces and moments included in kinetic analysis can be solved inversely if the kinematics, anthropometric properties, and external loads are known [46]. Ground reaction forces (GRF) are commonly considered in gait analysis to investigate and characterize gait pathologies.

Kinematic investigation has shown that displacement, or sway, and velocity of the COM in the AP direction was reduced in persons with TBI as compared to healthy participants and accompanied by an increase in ML displacement and velocity of the COM [2].

In one study, sagittal plane joint angles of the lower limb of TBI patients did not differ qualitatively from healthy individuals [29]. Another study presented greater knee flexion angles at heel strike and excessive knee extension at terminal stance for TBI patients. There was some evidence for reduced push-off based on a decreased plantar flexor power generated at the ankle joint and for a marked increase in trunk flexion compared to healthy persons [45].

Dual Tasks

The study of attentional resources during standing while performing an arithmetic task was introduced as an example of a dual-task testing scenario used to examine attentional requirements. Dual tasks are used in gait analysis to study executive function; task prioritization; and the deficits on balance, task performance, or both. Cognitive and motor dual tasks are common for gait analysis because they mimic real-life situations [8, 35,40].

Divided attention during dual-task walking performance has been found to reduce obstacle avoidance and digit recall in healthy adults [33]. One study showed a trend

towards slower walking during dual tasks with increasing cognitive impairment. They considered a walking while talking task and asked participants to recite male or female names [35]. The elderly population decreased velocity while performing a secondary cognitive task, and standardization of walking speed showed increased COM displacement and stride variability [40]. Without standardization, an increase in COM displacement was not measured.

Common cognitive dual tasks include the following: spelling five-letter words in reverse, subtraction by a constant number, and reciting the months of the year in reverse order [7,8,33]. A study of concussed individuals found slower gait velocity compared to healthy participants, shorter stride time for both groups during the dual tasks, shorter stride length in concussed individuals, and longer stride length for the single task for both groups 2 days after injury. Anterior displacement and velocity of the COM decreased in the dual tasks compared to the single task for both groups. A difference in ML sway was observed only during the dual tasks where increased displacement occurred following concussion. The cognitive tasks also increased ML COM velocity during gait [33]. Another study by the same group found similar results of decreased speed, decreased AP COM displacement, and increased ML COM velocity for both normal and concussed individuals when comparing cognitive dual tasks to single task walking [8].

Dual tasks cause instability following mild brain injury, indicating that reduced attention capacity or increased attentional demands of gait occur following injury [33]. Slower gait velocity and a stronger correlation with fall risk were demonstrated with increasing difficulty of the cognitive dual task [44]. The role of instruction during dual tasks, particularly which task to prioritize, was examined during walking while talking. Participants were asked to recite alternating letters of the alphabet; instructions were to prioritize talking during one trial and prioritize both walking and talking during a second trial. Task performance did not change significantly between the prioritizations;

however, when individuals prioritized talking, measures of gait velocity decreased and stride length increased compared to prioritization on both tasks [44].

Interest in dual-task testing with a secondary motor task is explored in obstacle-crossing scenarios to understand the potential for instability that patients may face during everyday obstacle avoidance. A review of obstacle-crossing literature, specifically in older adults, described slower walking and shorter steps immediately before crossing in the older population as compared to young adults. Kinematic analysis of older adults showed increased trunk motion prior to crossing and greater hip flexion for both the leading and trailing limb during crossing. Differences in ankle eversion and dorsiflexion and hip adduction were also reported. Kinetic differences in older adults were velocity matched to younger participants and showed increased hip abduction moment in the trailing limb during stance. Hip extensor, hip abductor, and knee extensor moments were reduced at a preferred, slower, velocity [16].

Healthy individuals show a trend towards reduced gait velocity during obstacle avoidance compared to significantly reduced speeds in TBI patients. The trailing limb crosses at a slower speed than the leading limb in TBI patients and greater toe clearance has been observed. Similar hip, knee, and ankle kinematics are assumed by TBI and healthy persons in the sagittal plane during obstacle crossing with increased maximum hip flexion during swing for the patients [29]. Another study found significantly greater ML COM sway in TBI and an increase in sway proportional to obstacle height. The same results were found for ML COM velocity. AP displacement and velocity of the COM decreased significantly compared to healthy individuals. The obstacle enhanced dynamic instability based on increased COM motion in the coronal plane; the obstacle increased the falling risk for TBI participants [11].

Catena and colleagues [7] compared the effects of performing a cognitive task and crossing an obstacle on temporal and spatial parameters, COM motion and velocity, and task performance. Both tasks reduced gait velocity; obstacle crossing resulted in longer

stride lengths than the cognitive task. When comparing concussed individuals to healthy adults, the group found slower velocities and longer stride times in concussed individuals and wider step widths during obstacle crossing. Measures of AP COM displacement increased for obstacle crossing and decreased for the cognitive task compared to single task walking; concussed individuals had slower AP COM velocities for each task. Measures of ML COM displacement increased for obstacle crossing compared to the cognitive task and single task walking; concussed individuals had greater ML COM displacement and velocity for each task. The group concluded that the cognitive dual task was more sensitive than the motor dual task in separating injured and healthy participants and suggested that obstacle crossing might perturb gait in general for all persons [7]. In a later publication, participants performed the cognitive task during obstacle crossing, and trail foot clearance in MTBI patients was correlated to the ability to spatially orient attention [9].

O'Shea and colleagues [30] compared a secondary cognitive and motor task by considering the effects on gait and task performance. The selected motor task required participants to transfer coins between two pockets, one placed in front of each hip. The selected cognitive task required participants to count backwards by three. The study compared individuals with Parkinson's disease to a control group and reported changes in stride length, walking speed, and double support percentage time from single task walking to dual task walking. Patients showed a reduced rate of coin transfer and produced more errors during the counting task. The group concluded that both cognitive and motor secondary tasks interfered with gait in patients and that one type did not interfere more severely than the other [30].

Summary of Gait Analysis in TBI

There are only a handful of studies that analyzed gait characteristics in mild to severe TBI patients. First, static balance in mixed-severity TBI was found to be

abnormal with TBI patients exhibiting increased sway [20,21]. In the few studies on dynamic balance/gait in mixed-severity populations of TBI, patients were found to have abnormal gait parameters even in those with normal neurological exams [2], namely, reduced gait speed, sometimes half the speed of controls, and reduced stride length [2,11,24,25,29,31]; reduced cadence and doubled stride time [31]; increased ML sway of COM [2,10]; and slow speed (due to reduced stride length) and increased foot clearance with obstacle crossing, suggestive of cautious behavior (the greater foot clearance was due to placing the trailing foot farther from the obstacle and increasing hip flexion) [29]. Kaufman and colleagues [23] studied 10 chronic TBI patients (0.4-14.4 years), four of whom were MTBI and all of whom had normal neurological and gait exam, and found abnormal static balance (using posturography) and dynamic balance (using motion capture), namely decreased velocity and increased ML sway of COM.

Summary of Gait Analysis in MTBI

Parker and colleagues [32] examined 10 MTBI within 48 hours post-injury and found that their stride and their ML COM sway were significantly less than controls (i.e., they walked more "carefully"); moreover, comparing simple walking (single task) versus dual task (walking while doing the serial seven arithmetic task, or spelling five letter words backwards or reciting months of the year), MTBI patients were found to have reduced velocity, stride length, and stride time to a level similar to severe TBI, and they had increased ML sway of their COM. This instability of MTBI patients incurred with dual tasks reflects potential danger upon returning to work/battle where they need to "think on their feet" [32]. In a follow-up study, 58 MTBI patients were analyzed using motion capture on days 2, 5, 14, and 28 during single task walking and dual tasks (walking while subtracting by sevens, spelling five letter words in reverse, and reciting the months of the year in reverse order). The concussed group had more ML COM sway for the dual task on days 5 and 28 [34].

Imaging

Imaging abnormalities are absent in MTBI patients using clinical imaging techniques; therefore, research aims to reveal brain abnormalities using advanced imaging modalities and analysis techniques. Advanced imaging modalities, such as functional MRI and positron emission tomography, may improve findings and reveal regional brain activation or cortical abnormalities, respectively [36]. A type of computed tomography known as single photon emission computed tomography identified cerebral perfusion abnormalities in 36% of MTBI patients within four weeks of injury. Results were reasonably correlated with the presence of persistent symptoms [21]. Diffusion tensor imaging (DTI) has shown lower white matter fractional anisotropy, particularly in the frontal lobe, in a study of twenty acute MTBI patients compared to control subjects. Poorer executive function was also demonstrated in MTBI patients and associated with frontal white matter abnormality [26].

Objective

The objective of this pilot study was to define a protocol using magnetic resonance imaging with diffusion tensor imaging (MRI-DTI) and motion capture technology and to establish its feasibility in detecting a biomarker for MTBI. Specifically, the study aimed to identify the presence of MRI-DTI abnormalities, to characterize gait instabilities, and to examine the relationship between MRI-DTI abnormalities and gait abnormalities in MTBI patients compared to controls. The long-term objective is to improve the diagnosis, treatment, and prognosis of MTBI and to reduce the resulting disability.

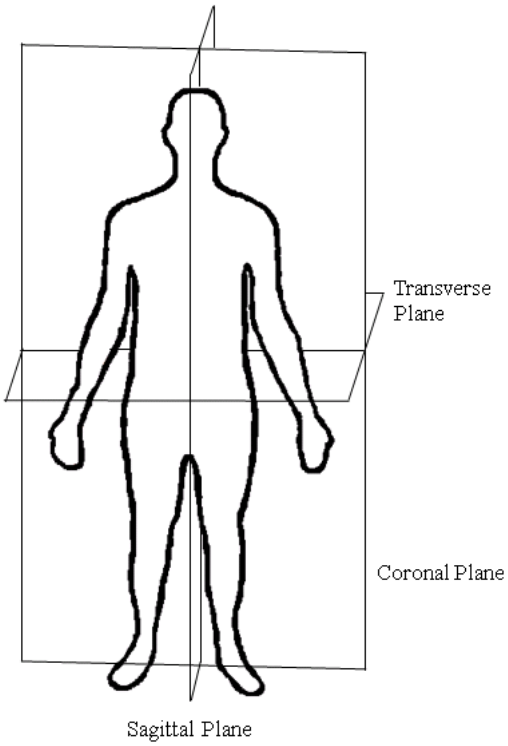

Figure 1-1. Anatomical position and depiction of the three anatomical planes that divide the body.

CHAPTER 2

EXPERIMENTAL PROCEDURES

Subject Population

The subject population was comprised of three MTBI patients and three healthy, height-, weight-, and gender-matched control participants. Chronic MTBI patients were recruited from the Veterans Affair Medical Center in Iowa City, IA. Healthy, normal participants were recruited from the Reserve Officers' Training Corps at The University of Iowa in Iowa City, IA. Exclusion criteria for normal participants were a history of brain injury or complaints of dizziness, lack of balance, or falls. Participation was voluntary, and each subject signed a consent form prior to the study. Consent was obtained from the Institutional Review Board of The University of Iowa and the Department of Veterans Affairs of the VA Medical Center in Iowa City, IA.

The mean height of the MTBI population was 175.8 cm (167-181 cm) with a mean weight of 98.7 kg (72.5-121.5 kg). The average age of the MTBI participants was 26.7 years old (23-29 years old). The mean height of the normal population was 175.3 cm (166.5-182 cm), and the mean weight was 86.7 kg (76-95.5 kg). The average age of the control participants was 22.3 years old (20-25 years old). Anthropometric detail is presented in Table 2-1.

The study recruited chronic MTBI patients 4.6 years (3.7-6.4 years) post-injury. P03 suffered a blast injury resulting in one minute loss of consciousness and eight hours of amnesia. Dizziness and headaches started later the day of the injury or the day after. P04 was injured by an IED (improvised explosive device) and was dazed and confused for 30 minutes. Dizziness started one month later. P05 was injured in a vehicle crash. He suffered 2 minutes of amnesia and dizziness and headaches began after one week. These patients had normal neurological and clinical gait exams with persistent symptoms when they were evaluated in 2009/2010. Injury specifics are detailed in Table 2-2.

Task Design

Participants were asked to walk at a steady, self-selected speed down a 9.5 meter platform. Normal walking was captured as a single task where participants were instructed to walk and make continuous 180 degree turns at either end of the platform until instructed to stop. According to the literature [2,7,8,11,29,31,33,45], MTBI patients have subtle abnormality in their motion that is not visually detected. Therefore, a set of cognitive and motor dual tasks were selected and defined with the intention of magnifying and capturing the subtle abnormalities of MTBI participants during walking.

The cognitive tasks included counting, digit span forward and digit span backward. The counting task required participants to subtract a constant or count backwards by seven starting at 100 or 101. During the digit span forward task, participants were given a series of numbers and asked to repeat them back to the study coordinator. The series of numbers was increased from three to nine digits. The numbers one through nine were used with each number appearing only once in a series. Two sequences were tested for each number of digits. Digit span backward was performed similar to digit span forward, except the participants were asked to repeat the series back to the study coordinator in reverse order. The series ranged in length from three to seven numbers.

The motor tasks were designed to test activities performed in daily life, including asymmetric carrying, symmetric carrying, and obstacle crossing. During asymmetric carrying, participants carried a 15 pound bag in their dominant hand, similar to carrying a shopping or laptop bag. Symmetric carrying required participants to carry a box with a 15 pound load in both hands. Obstacle crossing was designed to challenge the ability to avoid obstacles and interact with steps. An obstacle the size of a standard stair step (20 cm rise height and 23 cm tread depth) was created and was placed in the center of the platform. Participants were instructed to walk normally across the platform, step over the obstacle, and continue walking.

Experimental Design

Motion Capture

The study was conducted in the 3D Bio-Motion Research Lab (3DBMRL) at The University of Iowa using a 16-camera Motion Analysis motion capture system. The Motion Analysis system featured a 4 megapixel resolution with 1-2 frame latency. It is a real-time specific system with Eagle-4 Digital cameras that can collect at up to 500 Hz with a shutter speed ranging from 0-2000 μs. The focal length can be adjusted from 18-52 mm. The lab was equipped with two AMTI force plates positioned in the center of the walking platform twelve inches apart in the direction of movement. The force plates are capable of collecting six degrees-of-freedom. The walking platform and motion capture camera setup are shown in Figure 2-1.

Participants were prepared for the motion capture by wearing a motion capture suit and hospital socks to mitigate slippage chances. Passive reflective markers were placed to highlight bony landmarks and identify segments and joints. Marker placement is important for reducing the occlusions present in the motion capture, improving the clarity of the 3-D image and improving the results obtained through post-processing. The marker placement protocol for this study, presented in Table 2-3, uses definitions following the terminology of the well-defined, classic standards developed by Gray and Lewis [19]. The protocol was designed to capture the major joints present in the human body with a reduced number of spine joints in line with previously identified guidelines and suggestions [3,12]. For example, two markers were placed around the knee; one marker was placed directly on the medial condyle and the other on the lateral condyle. Palpation was used to locate the anatomical landmarks for subject preparation. The marker placement protocol presented is illustrated on a participant in Figure 2-2.

Prior to data collection, participants practiced walking across the platform, and the coordinator marked turn-around points on either end to optimize contact with the

force plates. Baseline cognitive task performance was obtained with the participants seated. Then single-task, normal walking was collected followed by the dual-task scenarios. Task instructions were given at the beginning of each trial as the participant began walking. No instruction was provided regarding which task to prioritize, either walking or the additional cognitive or motor task. Participants self-selected their preferred velocity for each task without feedback from the study coordinator. A break was provided between the cognitive and motor tasks and as necessary for individuals experiencing fatigue or soreness during the physical tasks.

Processing Motion Data

The Motion Analysis system collected marker data at 100 Hz and analog force data at 1000 Hz. Marker data post-processing was completed using Motion Analysis Cortex software. All marker trajectories were labeled and filled using editing tools to complete the data missing during the experiment. The marker trajectories normally encounter some noise; therefore, they were smoothed using a Butterworth filter at 8 Hz cut-off frequency. NIH-approved C-Motion's Visual3D software was used to compute the kinematics and kinetics of the motion and export the data.

Figure 2-3 is a screenshot of motion capture data processed in Motion Analysis Cortex software. The colored circles are the reconstructed and labeled markers tracked from the reflective markers placed on the participant during the motion capture. Figure 2-4 is a screenshot of the Visual 3D skeleton used to calculate and export kinematic and kinetic data. The skeleton was scaled based on the subject's anthropometric measurements and a neutral posture.

MRI-DTI Data

MRI scans were obtained on a whole-body Siemens Tim Trio 3T scanner equipped with a 12-channel head coil. Four image sets were acquired for structural MRI. The T1-weighted image was acquired in the sagittal plane using a 3D MP-RAGE

sequence with the following parameters: TE=2.98ms, TR=2200ms, TI=900ms, flip angle=12 degrees, NEX=1.0, FOV=256x240mm, matrix=256x240, slice thickness=1.0mm. The T2-weighted sequence was acquired using a 3D sagittal turbo spin-echo sequence (SPACE; Sampling Perfection with Application optimized Contrasts using different flip angle Evolution) with the following parameters: TE=406, TR=4000, NEX=1.0, FOV=256x230, matrix=256x230, slice thickness/gap=1.0/0.0mm, turbo factor=121. The FLAIR images was acquired using a 3D T2-prep SPACE sequence in the sagittal plane using the following parameters: TE=476, TR=5000, TI=1800, NEX=1.0, FOV=256x230, matrix=256x230, slice thickness/gap= 1.0/0.0mm. Finally, an axial gradient-echo sequence was obtained (5 mm thickness, 40% distance factor, 20 slices) with TR/TE=500/10, flip angle=20 degrees and voxel size=0.9 x 0.9 x 5 mm, in order to better assess the distribution of diffuse axonal injury.

Diffusion tensor images were acquired using an echo-planar double spin-echo sequence with the following parameters: TE=90ms, TR=9000ms, FOV=256x256, Matrix=128x128, slice thickness/gap=2.0/0.0mm, B-value=1000, number of directions=24, BW=1396Hz/Pixel, and NEX=1.

Processing MRI-DTI

Image analysis was performed using the tools of a locally developed software package: BRAINS2 [27]. This software permits cross-modality image registration, automated tissue classification (i.e., white matter, grey matter, and CSF), automated regional identification, cortical surface generation, volume and surface measurement, 3-D visualization of surfaces, and tracing both cortical and subcortical regions of interest on 2-D image sets and 3-D rendered surfaces with the feature of multi-planar telegraphing.

Processing of the DTI data began with the conversion of the data into NRRD format. Data was preprocessed using the locally developed GTRACT software [10]. Three methods were utilized for analysis of DTI data between groups (i.e., voxel-based

morphometry, ROI-based analysis, and tractography). The same preprocessing was done for all between-groups comparisons.

Table 2-1. Anthropometric data for normal (N) and MTBI (P) participants.

	Age (yr)	Height (cm)	Weight (kg)
N01	25	177.5	88.50
N02	20	166.5	76.00
N03	22	182	95.50
N Avg	22.3	175.3	86.7
P03	23	181	121.5
P04	28	167	72.5
P05	29	179.5	102
P Avg	26.7	175.8	98.7

Table 2-2. Injury details of the chronic MTBI patients.

	Years Post-injury	Injury Description
P03	3.8	Blast injury, 1 minute loss of consciousness and 8 hours of amnesia, dizziness + headaches started later that day or the next day
P04	3.7	IED (improvised explosive device), dazed/confused for 30 minutes, dizzines started 1 month later
P05	6.4	Vehicle crash overseas, 2 minutes of amnesia, dizziness + headaches started 1 week later

Figure 2-1. Walking platform with two force plates mounted in the center and Motion Analysis camera system setup for motion capture.

Table 2-3. Marker placement protocol description.

NAME	DESCRIPTION
RFHD, LFHD	Placed just superior and lateral to each eyebrow
RBHD, LBHD	Placed on the back of the head, one on each side
RMHD	Placed on the right side of the head, above the ear
RC1, LC1	Placed laterally on the level of C1, over the mastoid process
C7	C7 spinous process
RBack	Placed above the medial border of the scapula on the level of T3
T7	T7 spinous process
CLAV	Placed in the center of the clavicles
RCLAV, LCLAV	Placed over each clavical, midway between manubrium and acromion
STRN	Xiphoid process
T10	T10 spinous process
T12	T12 spinous process, follow rib cage back to spine to determine location
LBack	Midway between the lateral edge of the torso and the T12 spinous
L3	L3 spinous process
S1	Superior on the sacrum (S1 process)
RPSI, LPSI	Posterior Suprior Iliac Spine location
RASI, LASI	Placed bilaterally over Anterior Superior Iliac Spines
RHip, LHip	Placed bilaterally over greater trochanter
RSHO, LSHO	Placed over most superior point of the acromion process (shoulder)
RSHOF, LSHOF	Glenohumeral markers on anterior of shoulder, placed midway between
RSHOB, LSHOB	Glenohumeral markers on posteror of shoulder, placed midway between
RProxA, LProxA	On the arm between the shoulder and elbow
RElbow, LElbow	Placed over lateral epicondyle of humerus
RElbowIN, LElbowIN	Placed over medial epicondyle of humerus
RDistA, LDistA	On the forearm between the elbow and wrist
RWRA, LWRA	Placed over wrist radial styloid process (thumb-side)
RWRB, LWRB	Placed over wrist ulnar styloid process (pinky-side)
RHandA, LHandA	Placed over 1st metacarpal head
RHandB, LHandB	Placed over distal end of middle phalange as end effector
RProxL, LProxL	On the leg between the hip and knee
RKnee, LKnee	Placed over lateral condyle of femur
RKneeIN, LKneeIN	Placed over medial condyle of femur
RDistL, LDistL	On the shank between the knee and ankle
RAnkle, LAnkle	Placed over lateral malleolus of fibula
RAnkleIN, LAnkleIN	Placed over medial malleolus of tibia
RHeel, LHeel	Placed on the calcaneus
RMidFoot, LMidFoot	Midpoint along 5th metatarsal (lateral foot)
RToe, LToe	Placed over head of 1st metatarsal (just proximal to 'big toe')

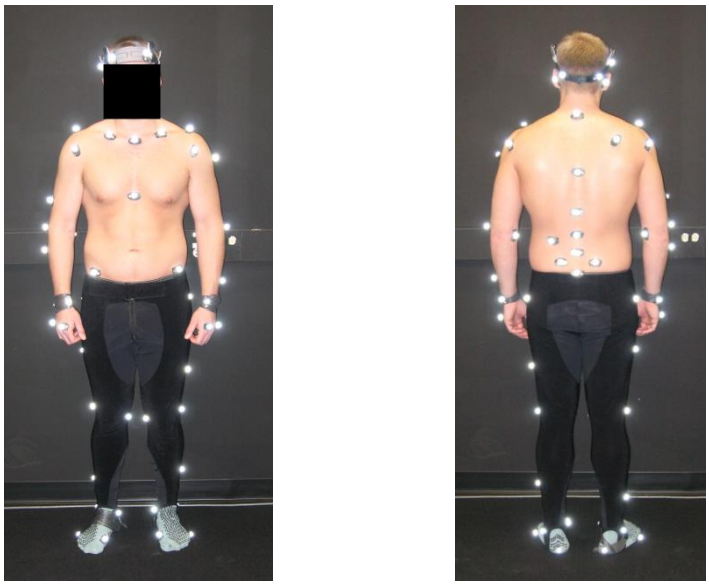

Figure 2-2. Participant wearing the motion capture suit with reflective markers placed according to the marker protocol.

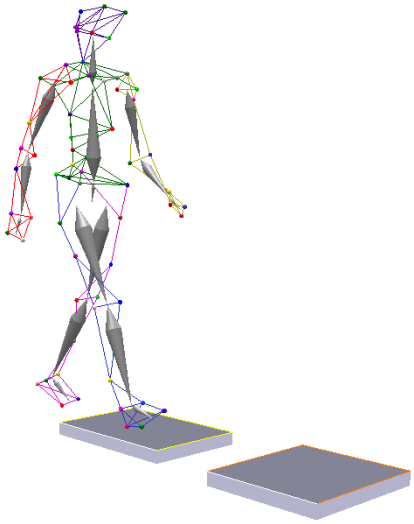

Figure 2-3. Motion data processing in Motion Analysis Cortex software. The data shows a participant at the beginning of the gait cycle in contact with a force plate.

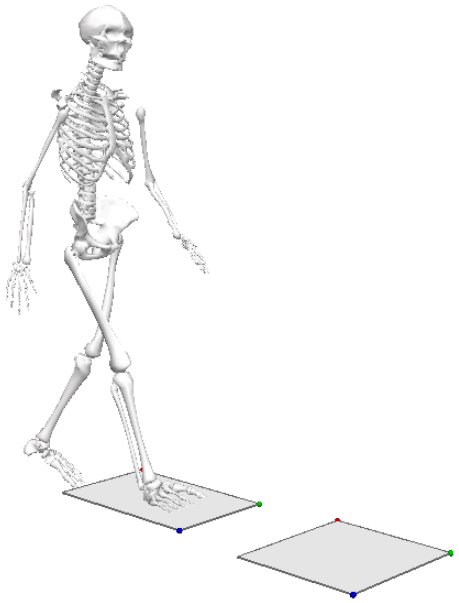

Figure 2-4. Motion capture skeleton used to calculate kinematic and kinetic measures using Visual3D software.

CHAPTER 3

ANALYSIS

The MRI-DTI portion of the study was collaborative work completed by Dr. Jinsuh Kim at the University of Iowa Hospitals and Clinics, Iowa City, IA. Dr. Kim's findings are reported with the results in Chapter 4.

Gait analysis was completed for two gait cycles for each participant and task. Participants walked at a self-selected speed across the platform during the motion capture, making continuous turns at each end. Steady-state gait cycles were selected when participants made contact with the force plate mid-platform and two representative cycles were used for analysis. Participants reported their dominant, or preferred, side, and based on that, data for the dominant limb is presented.

The gait cycle was defined from the instant when the heel of the dominant limb strikes the ground to the subsequent heel strike of that limb. The gait cycle begins in double support with the dominant limb in the lead. This is considered 0% of the gait cycle. The next 10-12% of the gait cycle is considered the initial loading response. As the trailing, non-dominant limb pushes off the ground, the dominant limb enters the single support portion of the stance phase. The single support phase begins at 10-12% of the gait cycle when the trailing toe leaves the ground and ends at 50% percent of the gait cycle when the non-dominant limb contacts the ground and the second double support phase begins. Then the dominant limb pushes off during the pre-swing phase and enters the swing phase around 60-62% of the gait cycle. The gait cycle ends when the dominant limb strikes the ground and the individual re-enters the double support phase with the dominant limb in the lead.

The single support phase is defined from toe off to heel strike of the non-dominant, trailing limb. The single support phase is critical for stability concerns because if the COM falls laterally outside the base of support (BOS) away from the

swing limb there is no mechanism to regain stability and avoid a fall. Therefore, joint moment analysis is presented for the dominant limb single support phase of the gait cycle.

Temporal and Spatial Parameters

Temporal and spatial parameters considered in this work include gait velocity, stride length, stride time, step width, and step height. Spatial parameters measured in the transverse plane are illustrated in Figure 3-1.

Stride length was calculated as the difference in anterior position of the heel marker at the beginning and end of the gait cycle or, in other words, the distance along the line of progression between successive heel strikes of the dominant limb.

Similarly, stride time was the amount of time that occurs between successive heel strikes of the dominant limb.

Velocity for the selected gait cycle was defined simply as stride length, or change in position, divided by stride time, or change in time. Thus, velocity is the distance covered in one gait cycle divided by the time to complete the cycle.

Step width, the distance between the ankle joint centers, was measured perpendicular to the line of progression or in the medial-lateral direction at heel strike. The ankle joint center was calculated as the center of the markers placed on the medial and lateral malleoli.

Step height was measured between the floor and toe marker at mid swing. The toe marker was placed medially on the first metatarsal.

Kinematics and Kinetics

Kinematic and kinetic measures were calculated using C-Motion's Visual3D software. Kinematic measures focus on the COM, which was computed as the equivalent mass of the whole body based on the mass distribution and location of the segments. The displacement, velocity, and acceleration of the COM are considered in the AP and ML

directions to examine motion in the line of progression and laterally where instability may result in a fall.

Kinetic measures focus on the hip and ankle joints, which were shown to function in balance control during standing and locomotion, and on the ground reaction forces (GRF). Joint torques of the hip and ankle were calculated using an inverse dynamic approach where body segment properties including mass and inertia, rotational acceleration of the body segments, and force applied to the feet are known, and the resulting moments at the joint are solved starting at the feet and moving up the body. Flexion/extension joint moments in the sagittal plane and adduction/abduction or inversion/eversion joint moments in the coronal plane were considered for their respective roles in forward progression and lateral stability.

GRF measures were considered in all three directions. The AP and ML components relate to stability in the transverse plane at the foot and the vertical component relates to load bearing during the walking cycle. The peak AP GRF during the initial loading response was quantified in terms of the magnitude and time of maximum loading. These measurements are illustrated in Figure 3-2. The vertical GRF measures include the time of the initial peak loading response, the time at which minimum weight bearing occurs during mid stance, and the difference in force magnitude between peak loading and minimum support. These measures are illustrated using example data in Figure 3-3.

Kinematic and kinetic data were time normalized from 0-100% of the gait cycle (single support phase in the instance of joint moment analysis). Time normalization was calculated as:

$$\% \text{ time} = (t_n - t)/(t_n - t_o)$$

where t_o represented the time at the beginning of the gait cycle (single support phase), t_n represented the time at the end of the gait cycle (single support phase), and t was the time

step of interest. The percentage of the gait cycle (single support phase) at some time t signifies the progression of the participant through the walking cycle (single support phase) and streamlines the comparison between participants.

Dynamic Variability

This chapter introduces the concept of dynamic variability, which is defined as the rate of change in the range of the joint torques during all or a portion of the walking cycle. It considers the population as a whole. To demonstrate this concept, Figure 3-4 shows an example of the plantar/dorsiflexion moment of the ankle for a population of three healthy participants. Each participant is shown in a different color. The walking cycle in this example is the single support phase defined from toe off to heel strike of the swing limb. The time history of the single support phase is normalized from 0-100% as indicated on the time axis.

In order to define the range of the joint moment at a certain time in the walking cycle, a plane, like plane-A shown in Figure 3-4, is drawn perpendicular to the time-moment curves. Distance d_A, shown in Figure 3-5, represents the range of the joint moment at that selected time and is defined as the distance from the largest to the smallest joint moment value inside plane-A. The range of the joint moment at other locations in the walking cycle can be defined in a similar manner to that of plane-A, as demonstrated by plane-B and plane-C in Figure 3-4 and Figure 3-5. The calculated ranges d_A, d_B, and d_C are plotted in Figure 3-6. This plot format is used throughout the results of Chapter 4, and the normal and MTBI population ranges are different colors for comparison.

The dynamic variability at a certain joint of a population was defined as the rate of change of the range between two successive planes. For example, the dynamic variability between plane-A and plane-B was calculated as:

$$DV=(d_A-d_B)/(t_A-t_B)$$

where t_A represented the normalized time where plane-A is drawn and t_B represented the normalized time where plane-B is drawn. d_A was the range calculated in plane-A as the distance from the largest to smallest joint moment value and d_B was the range calculated in plane-B.

Dynamic variability is presented in Figure 3-7 for the example considered. The two columns represent the rate of change of the range between plane-A and plane-B and between plane-B and plane-C.

The dynamic variability does not examine how the mean of the participants changes over time; instead it looks at how the population range changes over time. It then becomes possible to investigate the trend of all the subjects in the whole population and therefore avoid missing any information if considering the mean of the population alone. An individual may show variation from the population as a whole in which case it is useful to examine a subject-specific dynamic variability.

The dynamic variability of a certain individual can be defined in a way similar to that of the population. The only difference between the dynamic variability of the population and of a single subject is in the definition of the range. In this case, the range of a certain joint torque was defined as the distance between the subject's joint moment value and that of the mean of the normal population.

Refer again to the example data presented for three healthy participants in Figure 3-4. Each participant is illustrated in a different color for two selected gait cycles. The mean of the population is illustrated in black. To calculate the specific range for an individual, the cycle repetitions were averaged and the absolute difference was found between the individual mean and the population mean. Similar to the population range, the individual range of joint moments was calculated where plane-A, plane-B, and plane-C were drawn perpendicular to the time-moment curve. Figure 3-8 presents the range of joint moments for the normal population in grey, as was done in Figure 3-6, along with the individual ranges for the three participants in their respective colors.

Dynamic variability is, again, defined as the rate of change of the range between two successive planes. When considering subject-specific dynamic variability, the rate of change of the individual's range was calculated. Results for the example considered are shown in Figure 3-9. The grey column is the population dynamic variability, which was shown in Figure 3-7, and the colored columns are the subject-specific dynamic variability for each of the participants. This plot format is used in Chapter 5 to show the normal population and the individual results for range and dynamic variability of normal and MTBI participants.

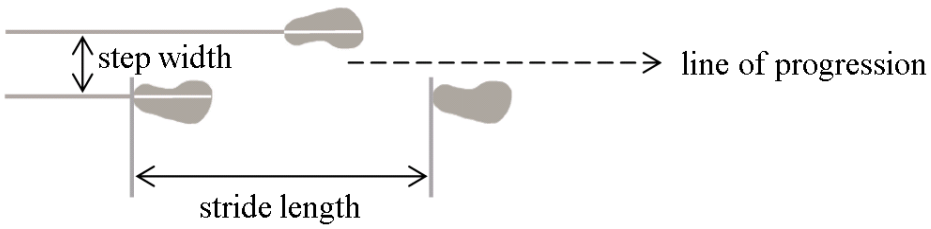

Figure 3-1. Spatial parameters are depicted as solid arrows. Stride length is defined between successive heel strikes and step width between ankle joint centers. Step height (not pictured) is defined between the toe and ground at mid swing.

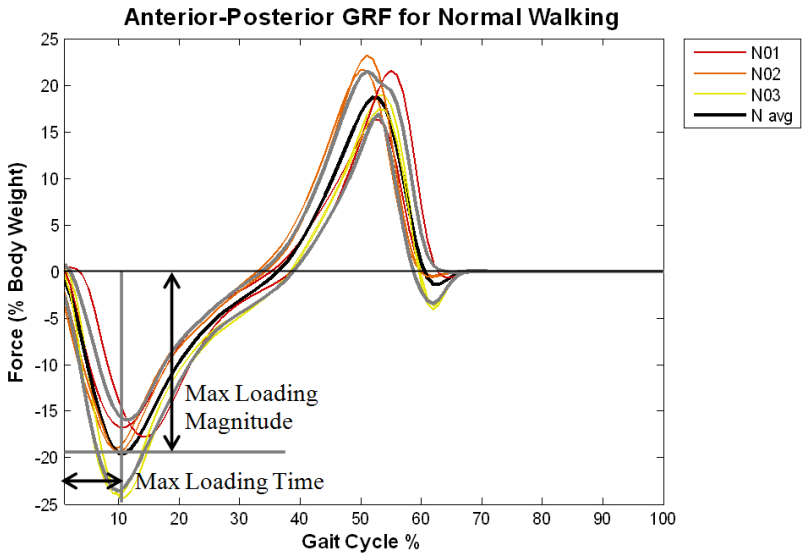

Figure 3-2. AP GRF measures during the initial loading response were quantified as maximum loading time and maximum loading magnitude.

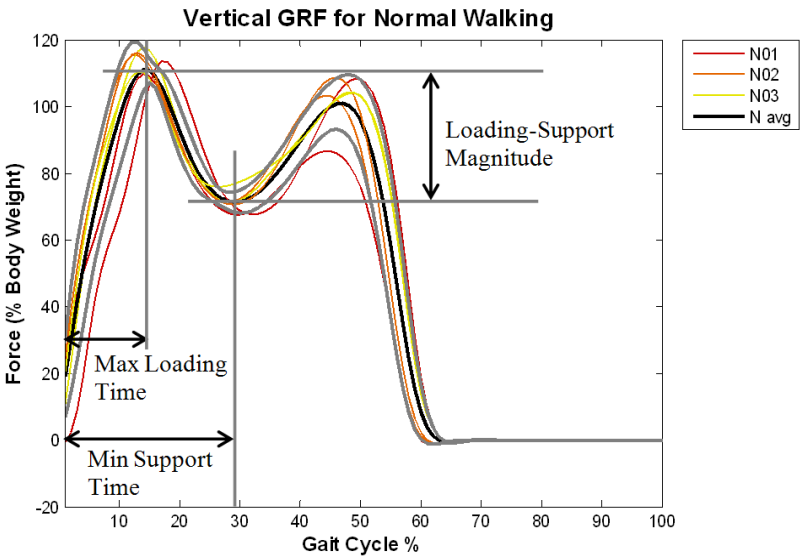

Figure 3-3. Vertical GRF measures include the time of the maximum loading response, the time at which minimum weight bearing occurs during support, and the difference in force magnitude between peak loading and minimum support.

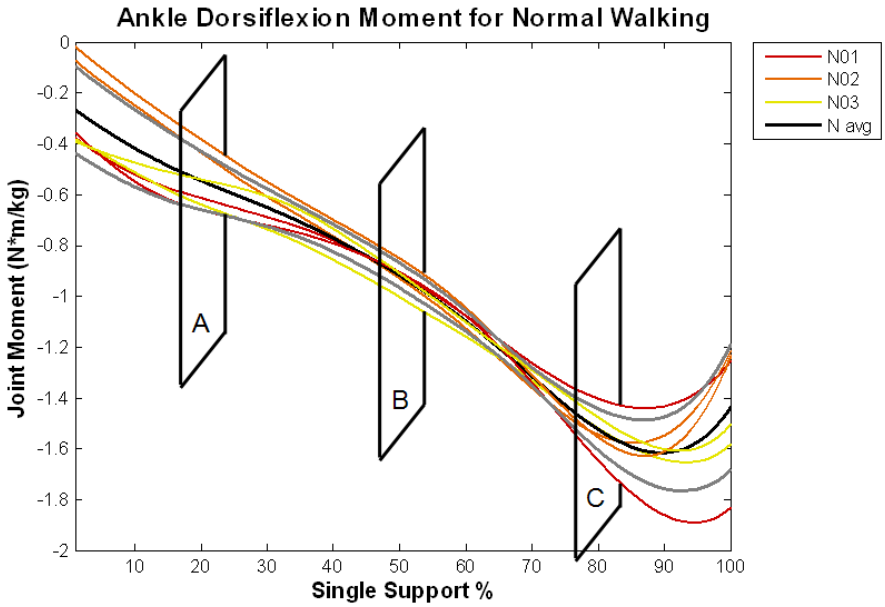

Figure 3-4. Example joint moment plot used to demonstrate dynamic variability analysis. Plane-A, plane-B, and plane-C are drawn parallel to the time-moment curves to define the range of joint moments at those times in the gait cycle.

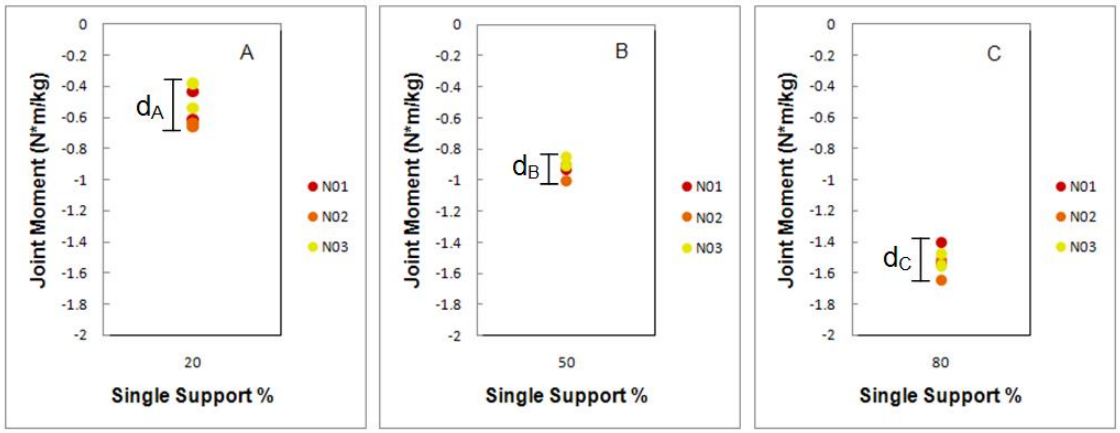

Figure 3-5. The distance d is the measured range of joint moments inside plane-A, plane-B, and plane-C.

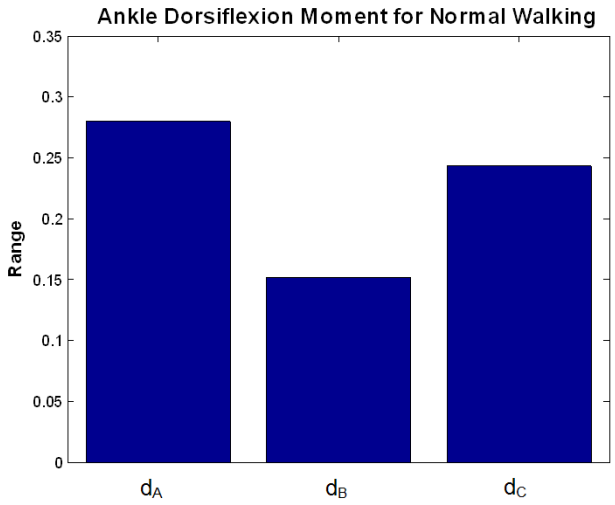

Figure 3-6. Ranges d_A, d_B, and d_C correspond to the joint moment ranges calculated where plane-A, plane-B, and plane-C were drawn through the time-moment curves. Refer to Figure 3-4 for the illustration of the planes and to Figure 3-5 for the calculation of the ranges.

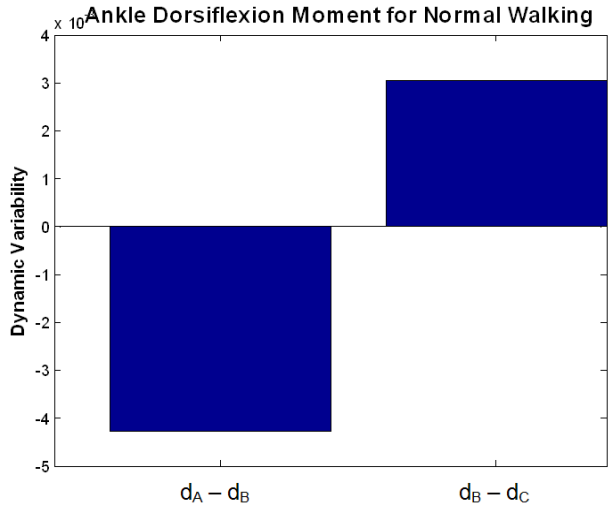

Figure 3-7. Dynamic variability is defined as the rate of change of range d between successive planes at A, B, and C.

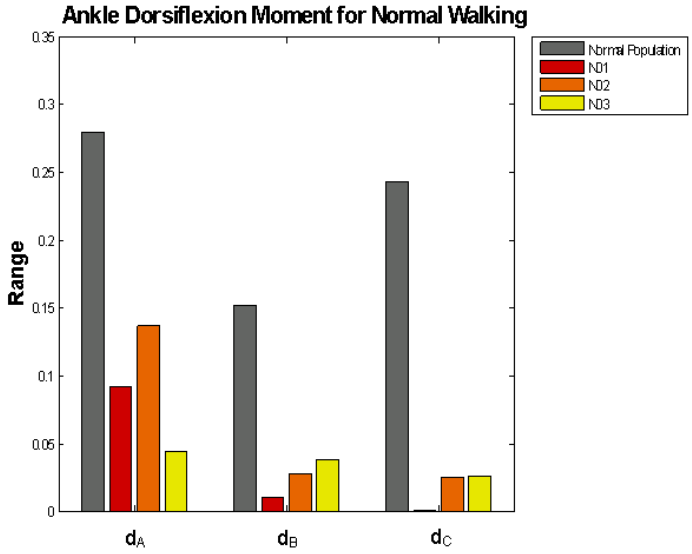

Figure 3-8. Range of individual participants can be defined between the individual's joint moment and mean joint moment for the normal population (grey).

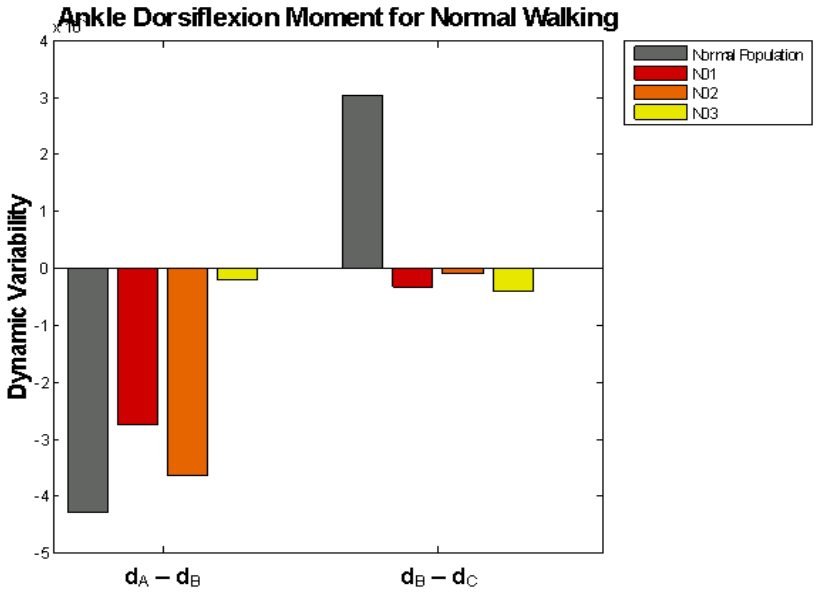

Figure 3-9. Dynamic variability may be defined for individual participants and presented with the dynamic variability of the normal population (grey) for reference.

CHAPTER 4

RESULTS

During the experiments, participants walked at a self-selected speed across the laboratory, making continuous turns at each end. Steady-state gait cycles were selected when the participant crossed the middle of the platform. Two gait cycles were selected for each participant and task. The gait cycle is defined from heel strike to subsequent heel strike of the dominant limb. The single-support phase of the dominant limb is the portion of the gait cycle defined from toe off to heel strike of the non-dominant, swing limb. The leading limb is defined as the forward limb contacting the ground at the beginning of the gait cycle; the trailing limb is behind in double support at the beginning the gait cycle as the following limb and contacts the ground at 50% of the cycle. During the single-support phase, the leading limb is in stance and the trailing limb is in swing. For this study, the leading limb is the dominant limb and all results are for the dominant limb unless otherwise noted. Participants completed the gait cycles at different times; therefore, data were time normalized for comparison.

Due to the large amount of data collected in this study, and for the sake of efficiency and clarity, data for selected tasks are presented in this chapter. Additional results were added to the appendices for future reference. Results are presented for single-task walking and two selected dual tasks, one cognitive and one motor dual task.

For demonstration purposes and to differentiate between the subjects, each participant is illustrated in a different color. MTBI patients are denoted with the prefix ‘P’ and normal participants are denoted with the prefix ‘N’. Control matches and color codes are shown in Table 4-1. The numerical value following each participant indicates the order of recruitment and should not be used to identify MTBI-control matches. MTBI-control matches are P03 (green) and N03 (yellow), P04 (blue) and N02 (orange), and P05 (purple) with N01 (red).

Temporal and spatial parameters were averaged for the two cycles. Kinematics of the COM was calculated for the entire gait cycle. Joint moment kinetics were normalized by participant mass and presented for the single-support phase. Ground reaction forces were presented for the entire gait cycle as a percentage of body weight (%BW).

Single-Task Walking

Temporal and Spatial Parameters

The temporal and spatial gait parameters of the normal and patient populations considered under the current investigation are presented in Table 4-2. The data were consistent with the literature, where the MTBI population had reduced velocity, shortened stride length, and greater step width. Stride time was similar between the populations.

Kinematics

For the kinematics of the motion, due to the large number of gait parameters, the current study investigated the COM during the gait cycle, as it is important in understanding stability and balance and may be representative of the whole-body motion. Thus, the kinematics results of this chapter focus only on the COM. The AP COM displacement and velocity (Figure 4-1 and Figure 4-2, respectively) showed decreased peak AP COM velocity in MTBI participants. Figure 4-3 demonstrates the acceleration of the COM in the AP direction. As shown in the figure, peak AP COM acceleration was reduced in MTBI participants around 15%, corresponding to toe off of the trailing limb, and 50% and 60% of the cycle, closely corresponding to heel strike of the trailing limb and toe off of the leading limb.

The ML COM displacement shown in Figure 4-4 does not show trend differences between populations. Figure 4-5 shows similar ML COM velocity trends and variations among the populations. Figure 4-6 presents the ML COM acceleration in which both

populations show similar variability. This is consistent with the literature. Decreased AP COM displacement and increased ML COM velocity have been reported for patients with TBI [2,8,32,33] when dual-task testing scenarios were used to enhance the subtle abnormalities of MTBI patients and when the data were normalized by gait velocity.

Kinetics

Kinetic joint moment analysis focused on the hip and ankle joint moments in the sagittal and coronal plane. The hip flexors/extensors and abductors/adductors control stability in the AP and ML directions, respectively. The ankle dorsiflexors/plantar flexors and invertors/evertors have fine control of the COM acceleration in the AP and ML directions. Kinetic GRF were analyzed in the AP, ML, and vertical directions.

Hip Flexion/Extension Moment

Hip flexion joint moments for healthy (Figure 4-7) and MTBI (Figure 4-8) participants had similar trends. The range of joint torques for each population is presented in Figure 4-9 at each 10% of the single-support phase. The dynamic variability is presented in Figure 4-10. The range of the normal population at the beginning of single support was small, and the dynamic variability showed a considerable difference between the normal and MTBI populations following toe off from 1-10%, where dynamic variability in the normal population was twice that of the MTBI population and in the opposite direction. MTBI patients had a larger range throughout the first half of single support. The dynamic variability showed differences during the middle of single support between 50% and 70%, where the normal dynamic variability was positive and twice the magnitude of the negative dynamic variability of the MTBI population.

Hip Adduction/Abduction Moment

More variability was seen in hip adduction joint moments in MTBI patients (Figure 4-12) compared to normal, control participants (Figure 4-11). In this case, the

normal population had a smaller range during 10-30% of single support, while the patients had a wider range at this time. The range of hip adduction moment for the population had different trends and magnitudes (Figure 4-13). The dynamic variability showed differences, particularly following toe off of the trailing limb, from 1-10% of the single-support phase (Figure 4-14). Dynamic variability was similar between populations from 10-30% of single support and differed through mid and late stance in either magnitude or direction.

Ankle Dorsiflexion/Plantar Flexion Moment

Trends in ankle dorsiflexion/plantar flexion moment differ between normal (Figure 4-15) and MTBI (Figure 4-16) populations near mid-stance from 30-70% of single support. This difference is captured by the ranges presented in Figure 4-17. The MTBI population had a greater range than the normal population from 10-70% and increased up to 30%, while the normal population range decreased to its minimum value at 70%. Dynamic variability (Figure 4-18) was negative for normal participants in the first 30% of single support as the range became tighter and was positive in patients as the range of the population increased. The dynamic variability of the MTBI patients was considerably more negative in mid stance from 40-60% and considerably less in late stance from 70-100% compared to the normal population.

Ankle Inversion/Eversion Moment

The ankle inversion/eversion joint moment was similar to the normal population (Figure 4-19) for two of the MTBI participants, but results differed for the population as a whole as seen in Figure 4-20. The range of the population increased for MTBI patients (Figure 4-21) throughout single support, while the range of the normal population was relatively constant and increased slightly after 80%. Dynamic variability captured this difference, particularly looking at early to mid stance in Figure 4-22. In early stance, up to 20% of single support, the dynamic variability was positive for the MTBI population

and negative for the normal population. Then, up to 60%, both were positive but MTBI patients had a greater magnitude.

Ground Reaction Forces

For the ground reaction forces, the AP GRF trends showed subtle differences in MTBI participants, noticeably during the landing phase from 0-20% of the gait cycle (Figure 4-23 and Figure 4-24). ML trends differed between populations and were difficult to quantify (Figure 4-25 and Figure 4-26). Vertical GRFs showed subtle differences in weight bearing (Figure 4-27 and Figure 4-28). These differences are quantified in Table 4-3. Peak AP loading during weight bearing occurred at the same time during the gait cycle around 10%; however, loading was reduced in MTBI patients compared to normal participants. Vertical GRF results showed trends towards an earlier peak during landing in normal individuals. Minimum load bearing during mid-stance occurred around the same time in both populations. The drop in force between landing and mid stance was two times greater in normal participants because MTBI participants applied less force at landing and greater force during mid-stance.

Dual-Task Counting

Task Performance

The counting dual task required participants to count backwards by seven starting at 100 during baseline and 101 during walking. Baseline testing was performed with the participant seated. The starting number was modified to preclude recall of the specific pattern. Instructions for the dual task were provided after the participant began walking, and no instruction was provided to prioritize either walking or counting.

The number of arithmetic errors was recorded as a performance measure for the counting task and is presented in Table 4-4. No general performance trends were observed between the normal and MTBI populations.

MTBI patient P03 (green) had only one steady-state gait cycle available while crossing the force plates in the middle of the platform. Consequently, results were limited to one cycle.

Temporal and Spatial Parameters

Temporal and spatial parameters presented in Table 4-5 show decreased velocity and a trend towards shortened stride length and wider step width for the MTBI population. In general, decreased step height and similar stride time were observed in MTBI participants. Compared to single-task walking, gait velocity was decreased in MTBI patients during dual-task counting, and trends showed both slightly reduced stride length and increased stride time.

Kinematics

AP COM displacement trends were similar between the populations (Figure 4-29). The AP COM velocity was decreased in MTBI participants throughout the gait cycle (Figure 4-30), and peak AP COM acceleration was lower than that of healthy individuals, particularly at 10% trailing toe off, 50% trailing heel strike, and 60% leading toe off (Figure 4-31). Referring back to single-task walking in Figure 4-2, AP COM velocity was further reduced in MTBI patients during counting. Peak AP COM acceleration of MTBI participants occurred slightly later than in normal participants. For example, in Figure 4-31, the peak around trailing heel strike occurs just before 50% in controls and slightly after in individuals with MTBI. This difference was magnified during counting compared to single-task walking (comparing Figure 4-31 to Figure 4-3).

ML COM trends did not show differences in the MTBI population in displacement (Figure 4-32), velocity (Figure 4-33), and acceleration (Figure 4-34). The cognitive counting task did not increase ML COM displacement or velocity compared to single-task walking shown in Figure 4-4 and Figure 4-5 or separate the MTBI population in terms of ML COM acceleration (Figure 4-6).

Kinetics

Hip Flexion/Extension Moment

The flexion/extension joint torque at the hip was decreased in magnitude in the MTBI population (Figure 4-36) compared to the normal population (Figure 4-35) at both toe off and heel strike of the trailing limb, corresponding to the beginning and end of the single-support phase. The joint moment ranges differed between the populations (Figure 4-37), and the dynamic variability showed differences from 0-30% of single support (Figure 4-38). Dynamic variability was opposite in direction during early stance from 0-30% and after mid stance from 50-70%. The magnitude of dynamic variability also differed between the two populations at each of these times. The dual-task counting test reduced the range of the hip flexion moment of the normal population in late stance and of the MTBI population throughout single support compared to single-task walking (comparing Figure 4-38 and Figure 4-9).

Hip Adduction/Abduction Moment

MTBI patients showed different characteristics in hip adduction/abduction moment than the normal individuals, as shown in Figure 4-39 and Figure 4-40. MTBI patients had more variability, notably in early stance up to 30% of single support. The range, Figure 4-41, shows similar trends for both populations, but the magnitude of the range is greater in the MTBI population. Dynamic variability was similar throughout the single-support phase except near the beginning and end, which corresponds to trailing toe off and heel strike, respectively (Figure 4-42). The normal and MTBI dynamic variability were closer in magnitude during dual-task counting compared to the results for single-task walking (Figure 4-14) from 10-90%. At the beginning of the single-support phase during counting, the MTBI population dynamic variability had the same direction as the normal population; this was not the case during single-task walking (comparing Figure 4-42 and Figure 4-14).

Ankle Dorsiflexion/Plantar Flexion Moment

The trends of ankle dorsiflexion/plantar flexion moments were similar for normal and MTBI participants, as shown in Figure 4-43 and Figure 4-44, although one cycle for P04 (blue) differed from the MTBI population. This was captured in the increased range of the MTBI population and the differences in dynamic variability presented in Figure 4-45 and Figure 4-46. Results for range and dynamic variability during counting reflected those of single-task walking presented in Figure 4-17 and Figure 4-18 with an increased range in the MTBI population from 10-50%. Dynamic variability of the MTBI population was either opposite in direction or considerably greater in magnitude compared to the normal population in early stance, 0-30%, and mid stance, 40-60%.

Ankle Inversion/Eversion Moment

Figure 4-48 presents ankle inversion moment trends of the MTBI population for comparison to the normal population shown in Figure 4-47. There was a decreased ankle inversion moment at the beginning of single support for patients. The range increased throughout stance in the MTBI population (Figure 4-49), and dynamic variability was greater for the majority of single support as seen in Figure 4-50. At the beginning of single support, the direction of the dynamic variability was different, and at the end of single support, the normal dynamic variability magnitude was greater than the MTBI population. In Figure 4-21 and Figure 4-22, the results for single-task walking showed greater range for the MTBI population during single support and greater dynamic variability for the normal population from 70-90% of single support.

Ground Reaction Forces

The MTBI population had less AP force during the loading response around 10% and pre-swing between 50% and 60% of the gait cycle (Figure 4-51 and Figure 4-52). Peak AP force near the trailing limb heel strike, approximately 50% of the gait cycle, was delayed in MTBI participants. The ML GRF had different characteristics for each

population; however, no specific observations were made (Figure 4-53 and Figure 4-54). The vertical GRF plotted in Figure 4-55 and Figure 4-56 shows a different load-bearing response in the MTBI population that affected the cycle through the push-off phase after 50% of the cycle.

GRF observations for the counting backwards task were quantified in Table 4-6. Forces applied in the AP direction by individuals with MTBI were half those obtained from normal participants. The vertical loading response was delayed in the MTBI population as was the minimum vertical GRF measured during stance. There was less change in force magnitude between these points in time as a result of the decreased force at loading and increased force during stance. Compared to single-task walking, peak AP GRF during landing was reduced during counting for MTBI participants and peak force during push-off was further reduced and delayed. Results from single-task walking are presented for normal participants in Figure 4-23 and for MTBI participants in Figure 4-24. Vertical GRF was more tightly grouped in normal participants during single-task walking (Figure 4-27) compared to counting. For MTBI participants, counting reduced and delayed peak vertical landing force around 20% compared to single-task walking (Figure 4-28).

Dual-Task Asymmetric Carrying

Task Performance

The asymmetric carrying task was a dual motor task selected to represent common daily activities, such as carrying groceries or a computer bag. Participants were asked to carry a 15 pound load in their dominant hand while walking in the laboratory.

Temporal and Spatial Parameters

Temporal and spatial parameters reported in Table 4-7 show decreased velocity in MTBI patients and a trend towards reduced stride length with a range of 1.16-1.50

meters. Average stride time was similar between populations, although results varied among individuals. Step width ranged from 0.073-0.139 meters in the normal population and from 0.079-0.156 meters in the MTBI population, indicating a trend toward increased stride width variability in both populations. Step height varied more among normal participants than MTBI participants; average results were similar.

Carrying parameters were similar to single-task walking parameters presented in Table 4-2. Trends toward decreased step width were observed for the dual carrying task for both populations.

Kinematics

The results of AP COM displacement did not show differences in the patients (Figure 4-57). AP COM velocity, shown in Figure 4-58, was reduced in MTBI participants, as was peak AP COM acceleration (Figure 4-59), particularly at 10% trailing toe off, 50% trailing heel strike, and 60% leading toe off. Comparing these results to single-task walking showed that peak AP COM acceleration in MTBI participants during carrying occurred closer in time to normal participants. Referring to Figure 4-59, the peak at 50% of the cycle during trailing limb heel strike occurred simultaneously for the populations; however, in Figure 4-3 for single-task walking, the peak of MTBI participants at trailing heel strike was delayed from the peak of normal participants.

Figure 4-60 presents ML COM displacement during asymmetric carrying without describable differences between populations. Similarly, ML COM velocity (Figure 4-61) and acceleration (Figure 4-62) do not distinguish the normal and MTBI participants. The same results were shown for single-task walking.

Kinetics

The mass of the bag was added to the hand segment for the inverse dynamic calculations. The normalization of joint moments and GRF included the mass of the bag and were still presented as %BW.

Hip Flexion/Extension Moment

The hip flexion/extension joint moment for normal participants is shown in Figure 4-63. MTBI participants followed a similar range with an increased moment at the beginning of single support (Figure 4-64). The range of the populations (Figure 4-65) was similar throughout single support in trend and magnitude. At trailing toe off, the beginning of single support, the range of the MTBI population was greater than the normal range. The dynamic variability differed in direction from 0-20% with a large difference in magnitudes. For the remainder of single support, the MTBI population produced small dynamic variability (Figure 4-66). Compared to single-task walking (Figure 4-8), the MTBI participants began single support with a larger hip flexion moment. The range difference at trailing toe off was decreased during carrying, and the trend of ranges was closer to the normal population during single-task walking (Figure 4-9). At 10%, the range of normal participants was greater than in normal walking. The difference in dynamic variability between the populations was reduced at 50% mid stance.

Hip Adduction/Abduction Moment

The results for hip adduction/abduction moment in Figure 4-67 for normal participants and Figure 4-68 for MTBI participants show general agreement in trend, although N03 (yellow) shows inconsistency between trials. The range of hip adduction moment (Figure 4-69) was greater in the MTBI population during early single support from 10-30% and less during late stance from 70-100%. The MTBI range was constant throughout single support with a slight decrease early on. The normal population range was low from 10-30%, then increased for the remainder of single support. The dynamic variability is presented in Figure 4-70. Results for the populations were close at mid stance from 40-60% and in terminal stance from 90-100%. In late single support, the normal population had a greater magnitude of dynamic variability. The same was seen

from 0-10%. In early single support from 20-40%, the direction differed between populations. Hip adduction trends for carrying are similar to results shown in Figure 4-11 and Figure 4-12 for single-task walking, except N03 (yellow) shows more consistency between cycles during the single task. During carrying, the range of the MTBI population was reduced and the dynamic variability was closer in magnitude and direction following trailing toe off (0-10%), before trailing heel strike (90-100%), and at mid stance (40-60%). The range and dynamic variability of hip adduction during normal walking are presented in Figure 4-13 and Figure 4-14, respectively.

Ankle Dorsiflexion/Plantar Flexion Moment

The ankle dorsiflexion/plantar flexion joint moment during asymmetric carrying is presented for the normal population in Figure 4-71 and the MTBI population in Figure 4-72. Trends in MTBI participants differed around mid stance from 40-60%. The range results showed similar trends through 80% of single support with a larger range in the MTBI population (Figure 4-73). At the end of single support, the MTBI population range was constant and the normal population continued to increase and had a larger range at the end of single support. The dynamic variability matched well during the first half of the single-support phase (Figure 4-74). At 50% mid stance, the magnitude of the normal population was greater than the MTBI population. There was a considerable difference from 70-100% as well. Both populations had dynamic variability in the same direction, but the magnitude of the healthy population was larger. Referencing the single-task walking results in Figure 4-15 and Figure 4-16, dual-task carrying shows a greater variability in ankle dorsiflexion moment, especially in the normal population. The range of normal walking (Figure 4-17) showed a similar trend for MTBI participants during carrying, and the normal population had an increased range from 10-50% of single support during carrying. The dynamic variability of single-task walking (Figure 4-18) was opposite in direction for most of the first 60% of single support; this was not the case

during dual-task carrying. The normal population had a greater dynamic variability than the MTBI population from 70-100%, and this difference was magnified during carrying.

Ankle Inversion/Eversion Moment

Dual-task carrying results for the ankle inversion/eversion joint moment are shown in Figure 4-75 and Figure 4-76 for the normal and MTBI populations, respectively. In general, the results were similar for the participants, however P04 (blue) showed different characteristics than the other two MTBI patients. These results were also shown in normal walking (Figure 4-20). The joint moment ranges are presented in Figure 4-77. The population ranges matched at 0 and 10%, and then the MTBI population range began increasing and was greater than the normal population. The normal population range began increasing after 40% of single support and remained less than the MTBI range. The dynamic variability (Figure 4-78) was opposite in direction in the first 30% of single support. The normal population was negative as the range decreased and the MTBI population was positive, indicating an increasing range. From 30-60%, the directions were the same and the magnitude of the MTBI range was at least twice as large. After 60%, the normal population range became larger. During single-task walking, the normal population range (Figure 4-21) began increasing later in single support at 80% compared to 50% during carrying. Dynamic variability results of carrying captured the increased magnitude in the MTBI population from 0-60% and the directional difference from 0-20% presented in single-task walking (Figure 4-22). During carrying, the normal population dynamic variability became positive and increased in magnitude earlier than during single-task walking, from 60-70%.

Ground Reaction Forces

The AP GRF is shown for the normal participants in Figure 4-79 and for the MTBI participants in Figure 4-80. The patients applied less AP force than the controls at around 10% of the gait cycle during load bearing. The patients also demonstrated a

reduction and delay during push-off around 50% of the gait cycle. Results were close to those presented in Figure 4-23 and Figure 4-24 for single-task, normal walking.

ML GRF measurements in Figure 4-81 and Figure 4-82 do not show clear abnormalities in MTBI patients due to the variations and subtleties of the data for all participants. The results did show some differences compared to single-task walking for both normal participants (Figure 4-25) and MTBI participants (Figure 4-26). The ML GRF peaks at 10% load bearing and 50% push-off were relatively equal in magnitude during carrying; however, during single-task walking, the peak at 50% push-off was slightly reduced from 10% load bearing.

Figure 4-83 presents the vertical GRF for the normal participants, and Figure 4-84 presents the vertical GRF for the MTBI participants. The normal population was grouped tightly during the majority of the gait cycle. The MTBI participants showed a slower rate of increase during load bearing and a delayed peak force between 10% and 20%. Vertical force around 30% in mid stance was higher in MTBI participants, while force around 50% trailing heel strike was lower. Results were similar to single-task walking (Figure 4-27 and Figure 4-28). Carrying showed larger peak landing force than single-task walking for both populations. Table 4-8 quantifies the GRF observations for AP and vertical loading.

MRI-DTI

In this study, MRI-DTI analysis of the white matter tracts was performed, but the number of subjects was too small to detect the subtle white matter tracts dysfunction. Images are presented in Figure 4-85. A recent MRI-DTI study of 25 MTBI Iowa City veteran patients (i.e., same population pool as the three patients recruited for this study) has confirmed disruption in major white tracts (personal communication, Dr. Jinsuh Kim, University of Iowa).

Table 4-1. MTBI patient and control matches with participant ID and plot color.

Patient ID	Patient Color	Normal ID	Normal Color
P03	green	N03	yellow
P04	blue	N02	orange
P05	purple	N01	red

Table 4-2. Temporal and spatial parameters of the normal walking task

	Velocity (m/s)	Stride Length (m)	Stride Time (s)	Step Width (m)	Step Height (m)
N01	1.26	1.39	1.10	0.094	0.059
N02	1.50	1.49	0.99	0.127	0.050
N03	1.36	1.48	1.10	0.142	0.065
N Avg	1.37	1.45	1.06	0.121	0.058
P03	1.23	1.47	1.20	0.143	0.048
P04	1.20	1.24	1.04	0.078	0.050
P05	1.22	1.28	1.05	0.176	0.059
P Avg	1.22	1.33	1.09	0.132	0.052

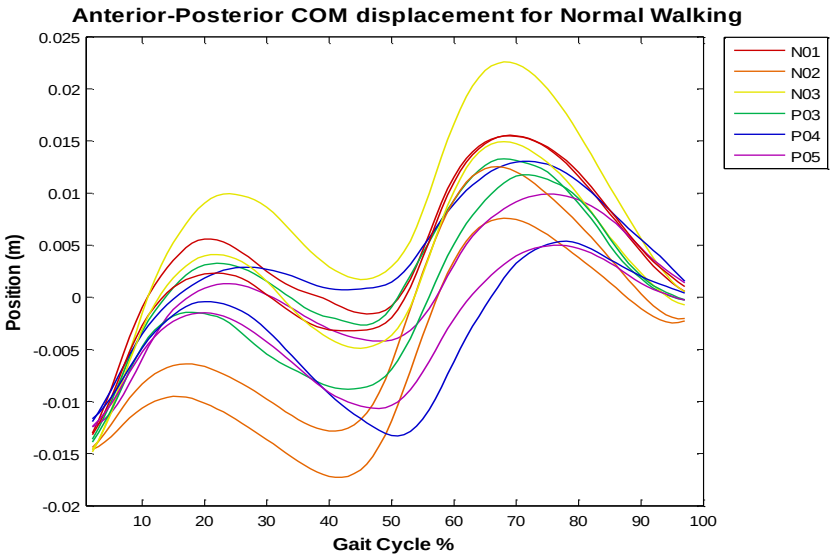

Figure 4-1. AP COM displacement during single-task walking.

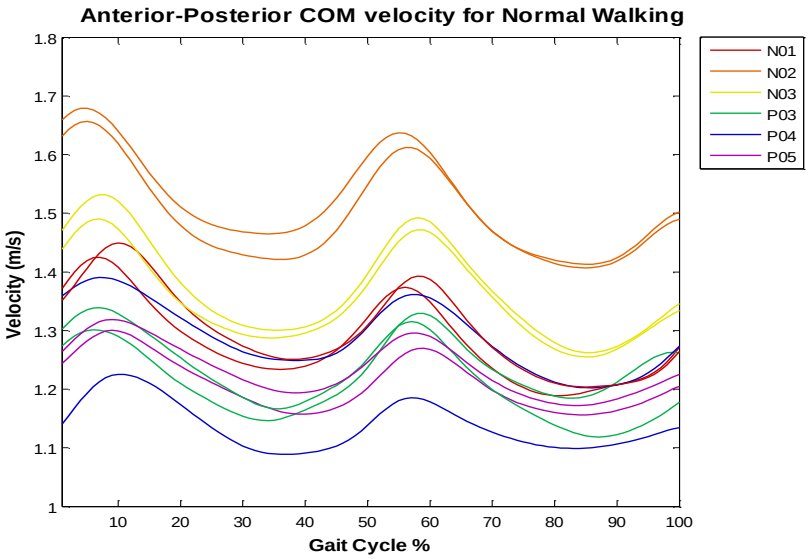

Figure 4-2. AP COM velocity during single-task walking.

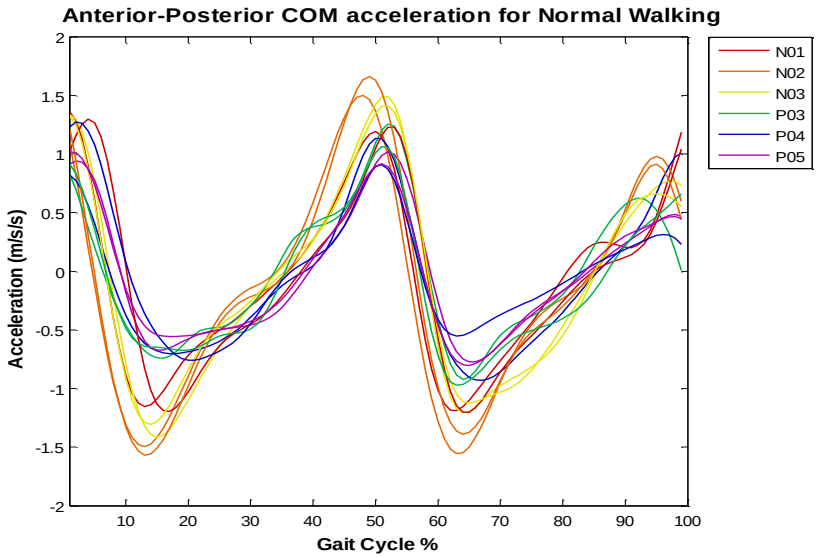

Figure 4-3. AP COM acceleration during single-task walking.

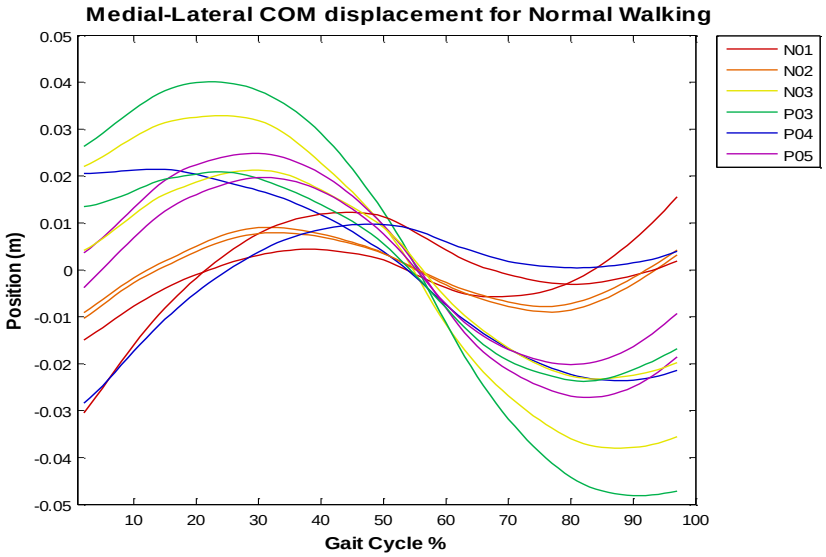

Figure 4-4. ML COM displacement during single-task walking.

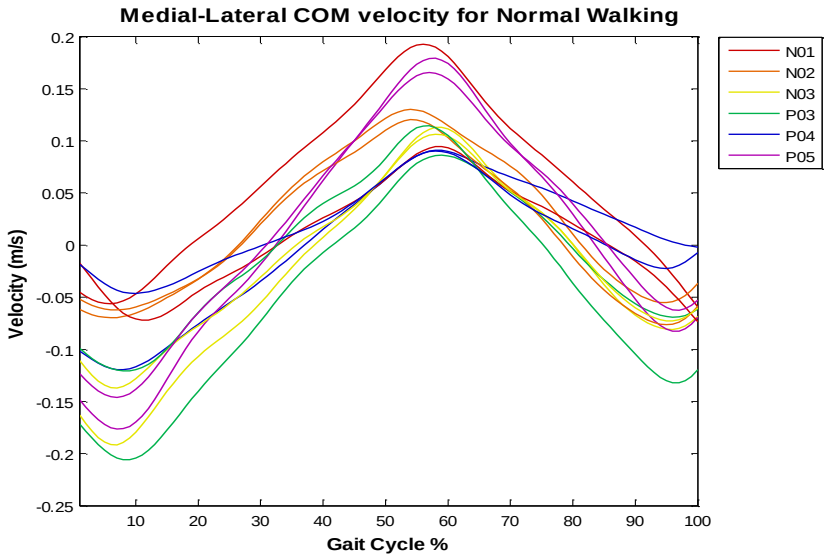

Figure 4-5. ML COM velocity during single-task walking.

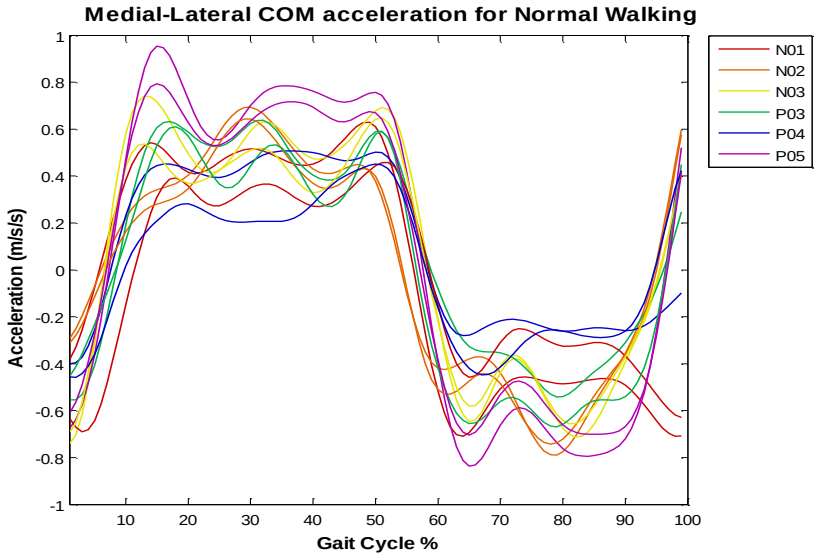

Figure 4-6. ML COM acceleration during single-task walking.

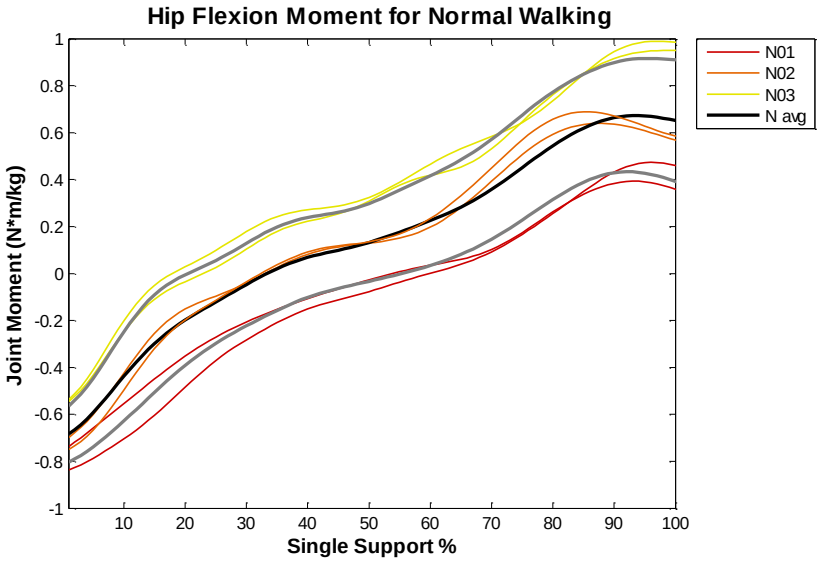

Figure 4-7. Hip flexion/extension joint moment of normal participants during single-task walking.

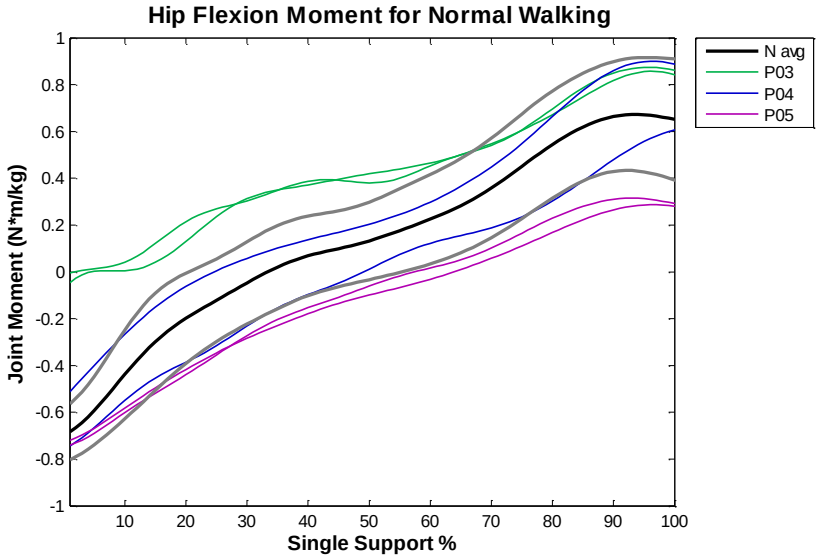

Figure 4-8. Hip flexion/extension joint moment of MTBI participants during single-task walking.

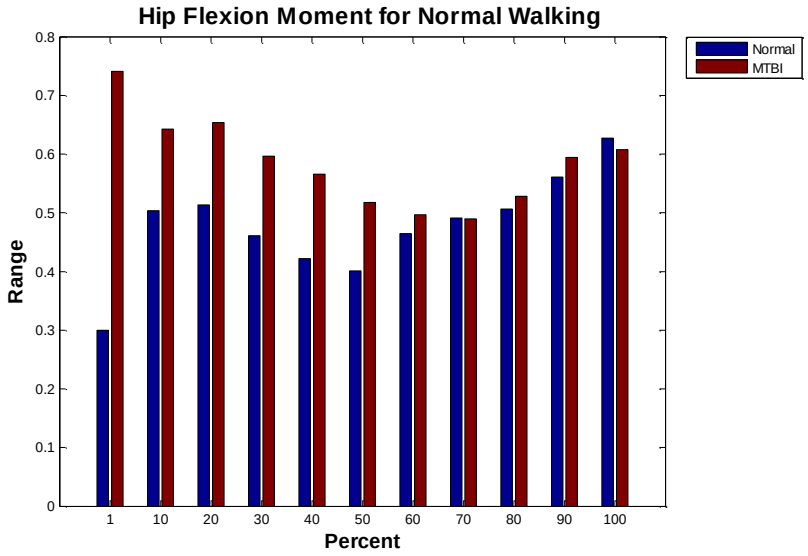

Figure 4-9. Range of hip flexion/extension joint moment of the normal and MTBI populations during single-support walking.

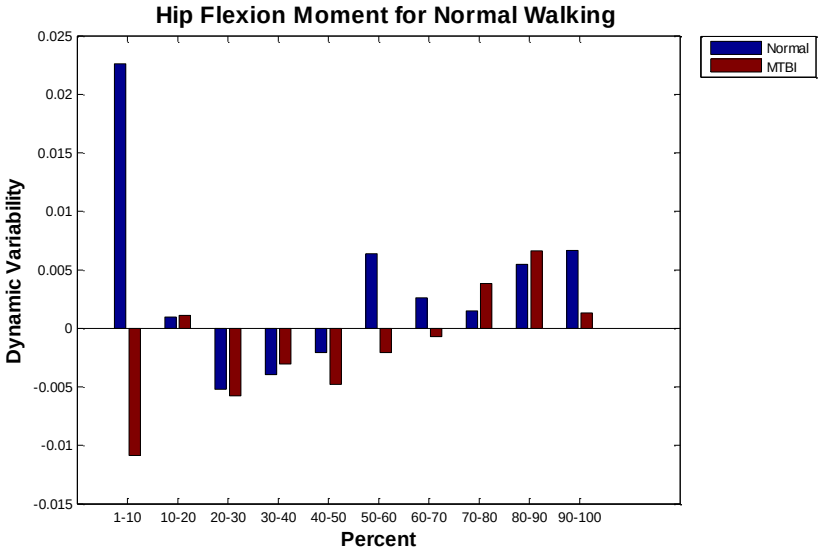

Figure 4-10. Dynamic variability of hip flexion/extension joint moment of the normal and MTBI populations during single-support walking.

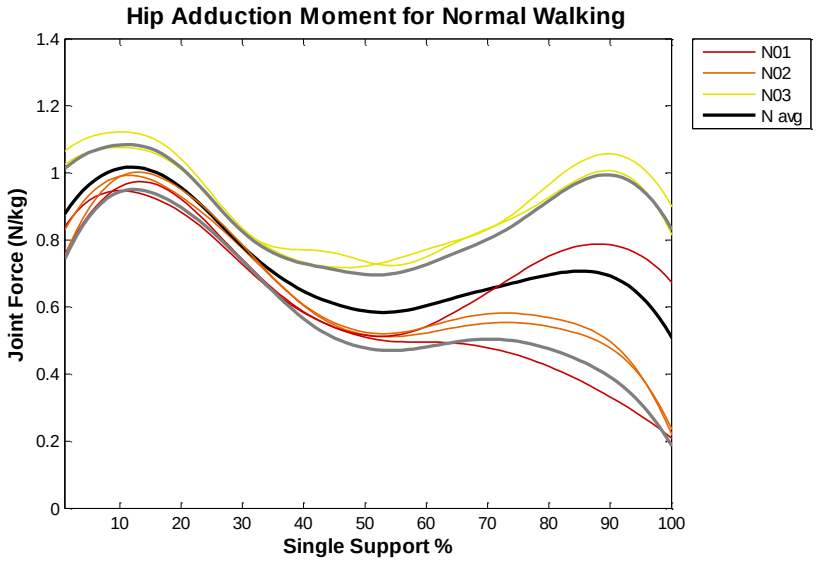

Figure 4-11. Hip adduction/abduction joint moment of normal participants during single-task walking.

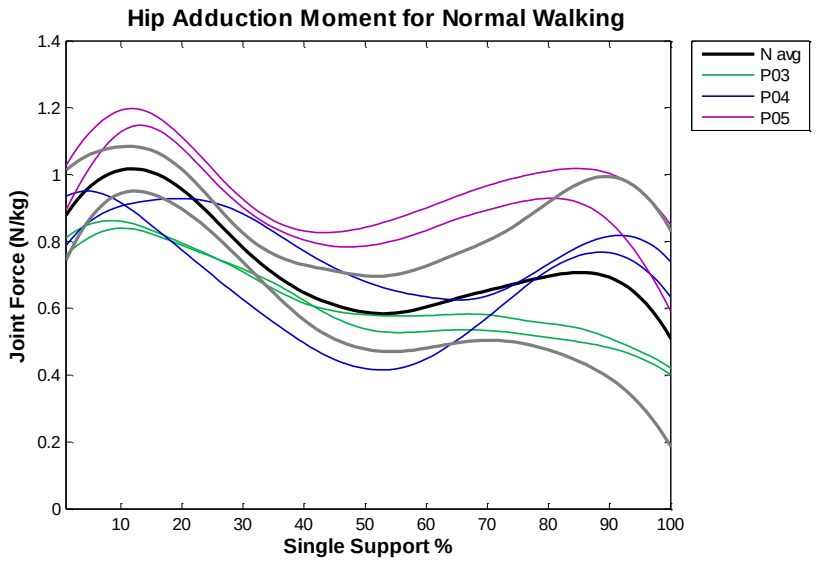

Figure 4-12. Hip adduction/abduction joint moment of MTBI participants during single-task walking.

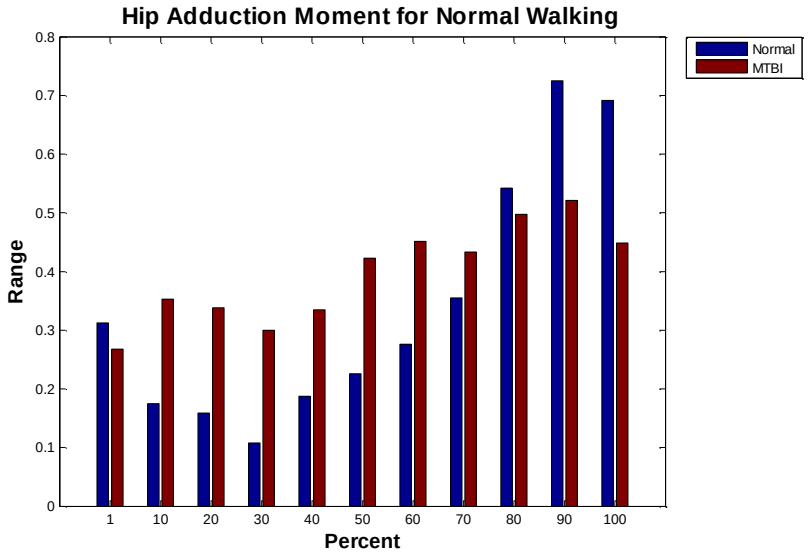

Figure 4-13. Range of hip adduction/abduction joint moment of the normal and MTBI populations during single-support walking.

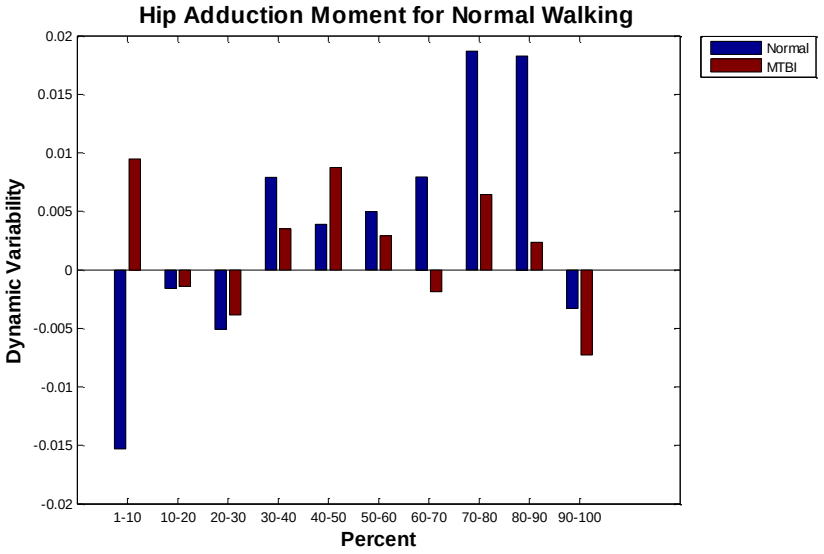

Figure 4-14. Dynamic variability of hip adduction/abduction joint moment of the normal and MTBI populations during single-support walking.

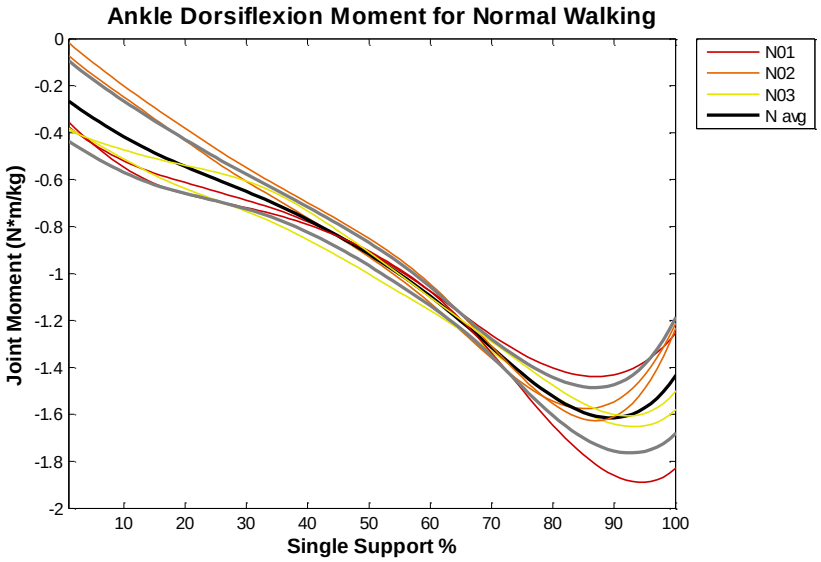

Figure 4-15. Ankle dorsiflexion/plantar flexion joint moment of normal participants during single-task walking.

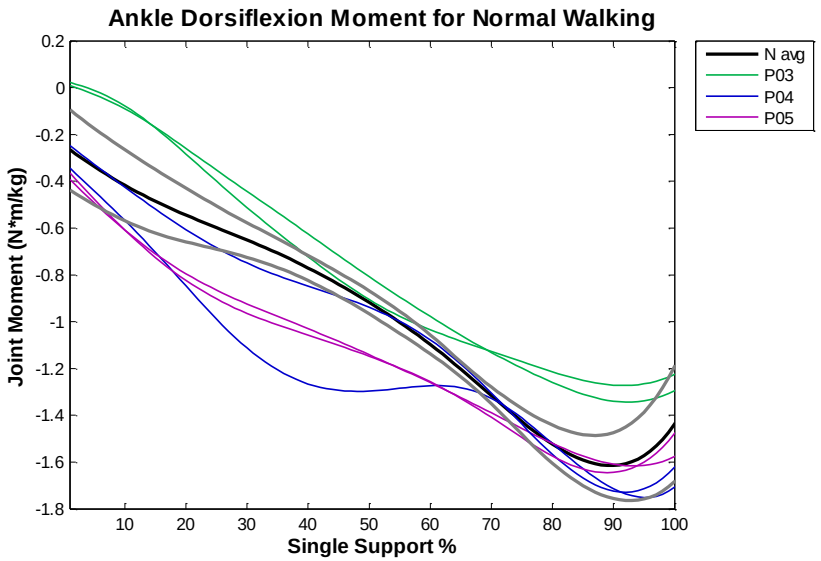

Figure 4-16. Ankle dorsiflexion/ plantar flexion joint moment of MTBI participants during single-task walking.

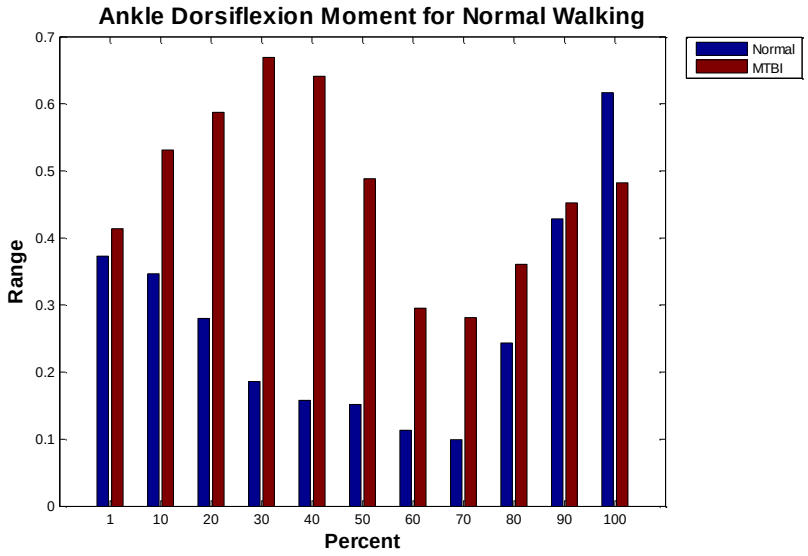

Figure 4-17. Range of ankle dorsiflexion/plantar flexion joint moment of the normal and MTBI populations during single-support walking.

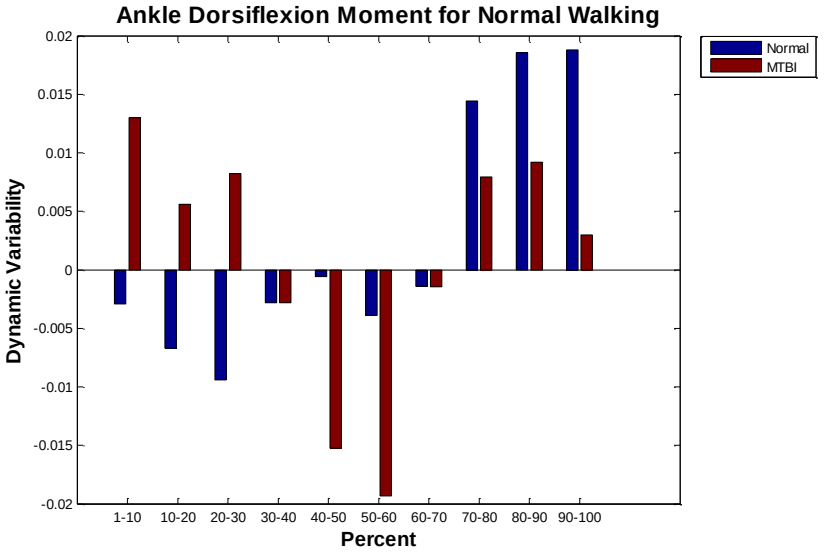

Figure 4-18. Dynamic variability of ankle dorsiflexion/plantar flexion joint moment of the single-task and MTBI populations during single-support walking.

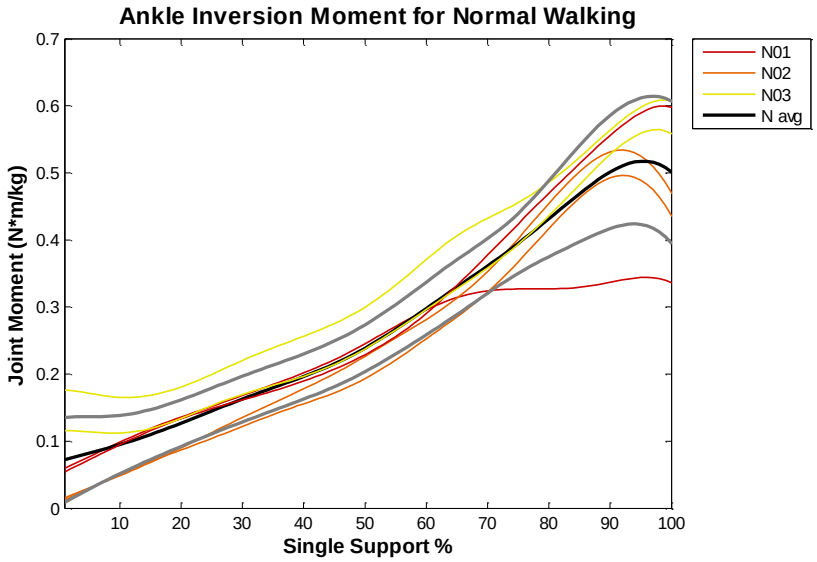

Figure 4-19. Ankle inversion/eversion joint moment of normal participants during single-task walking.

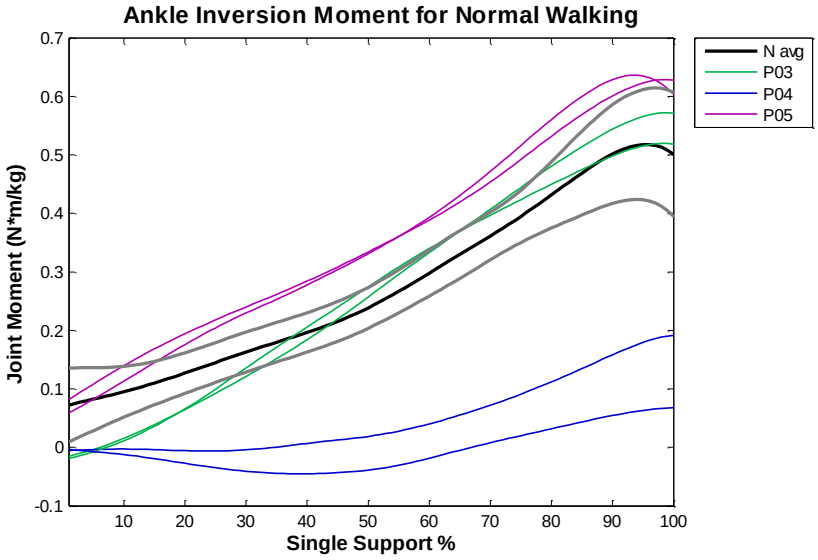

Figure 4-20. Ankle inversion/eversion joint moment of MTBI participants during single-task walking.

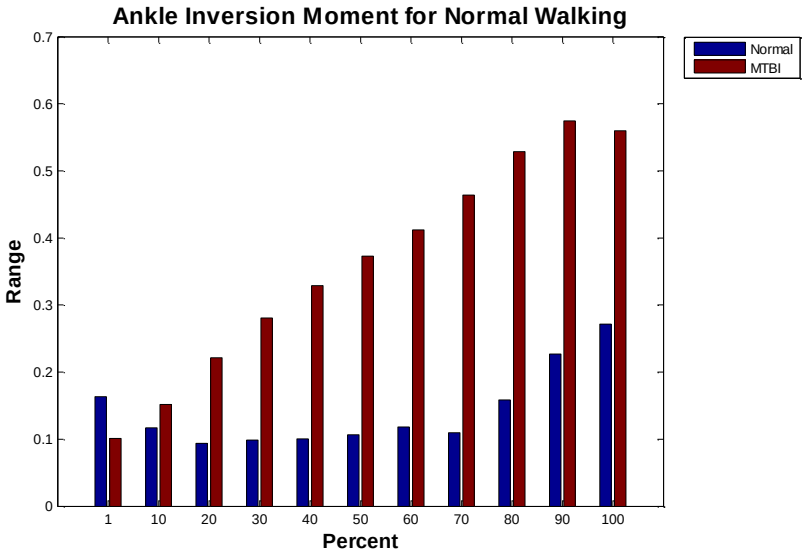

Figure 4-21. Range of ankle inversion/eversion joint moment of the normal and MTBI populations during single-support walking.

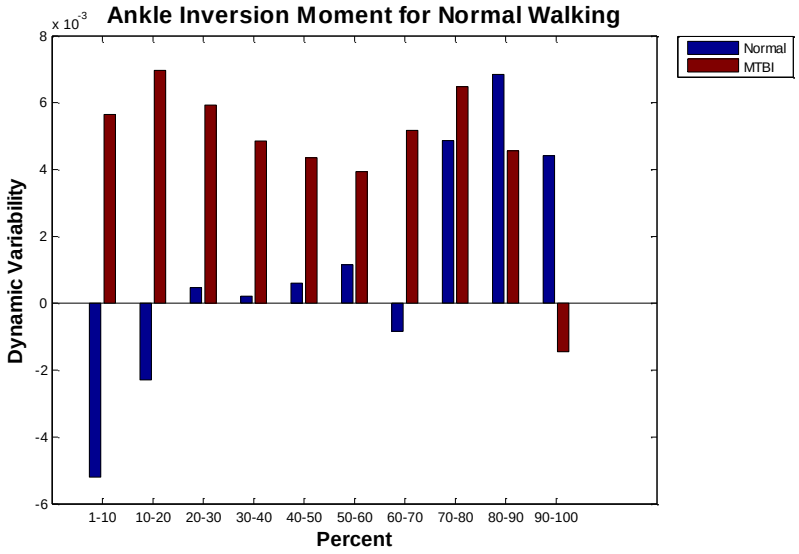

Figure 4-22. Dynamic variability of ankle inversion/eversion joint moment of the normal and MTBI populations during single-support walking.

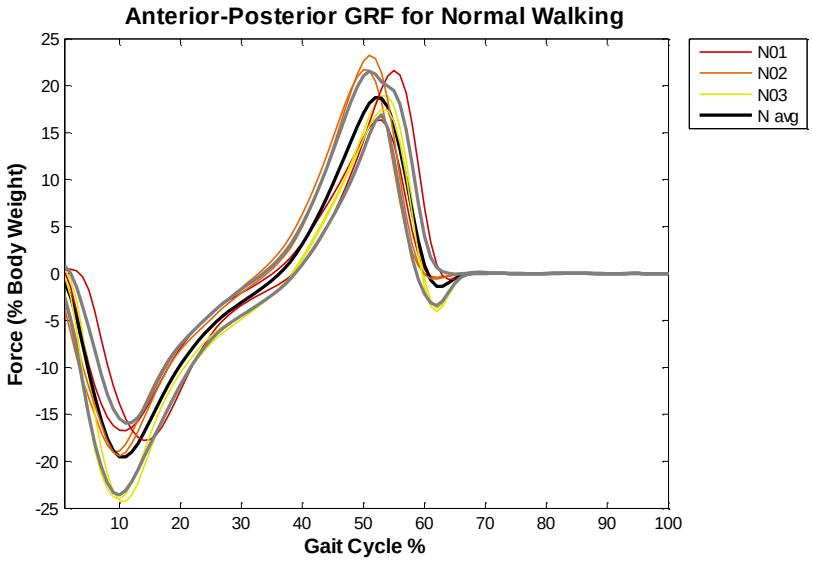

Figure 4-23. AP GRF of normal participants during single-task walking.

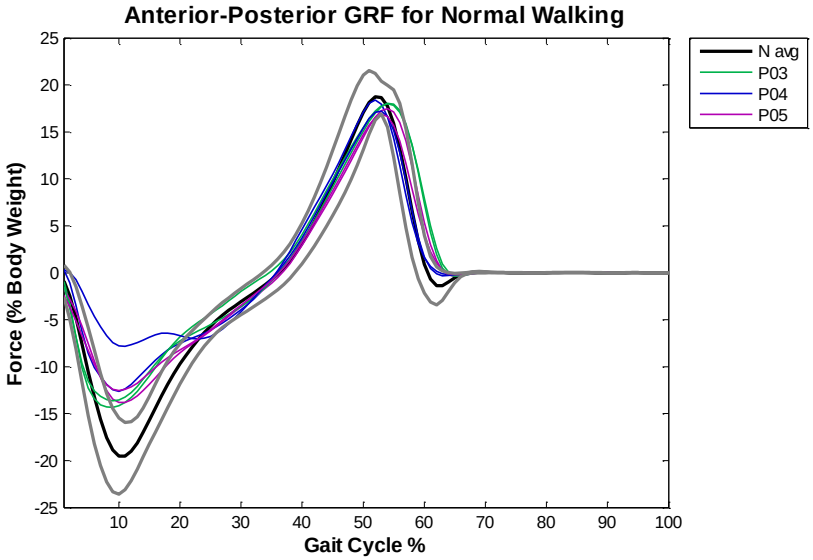

Figure 4-24. AP GRF of MTBI participants during single-task walking.

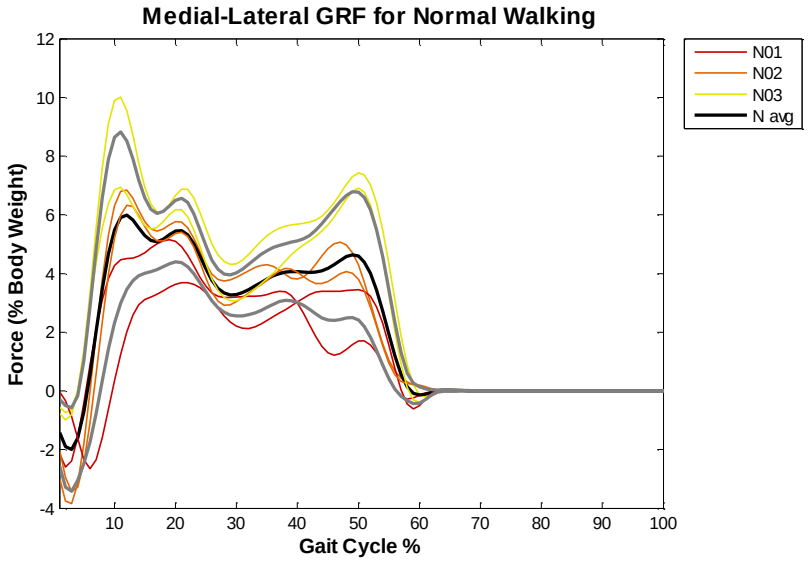

Figure 4-25. ML GRF of normal participants during single-task walking.

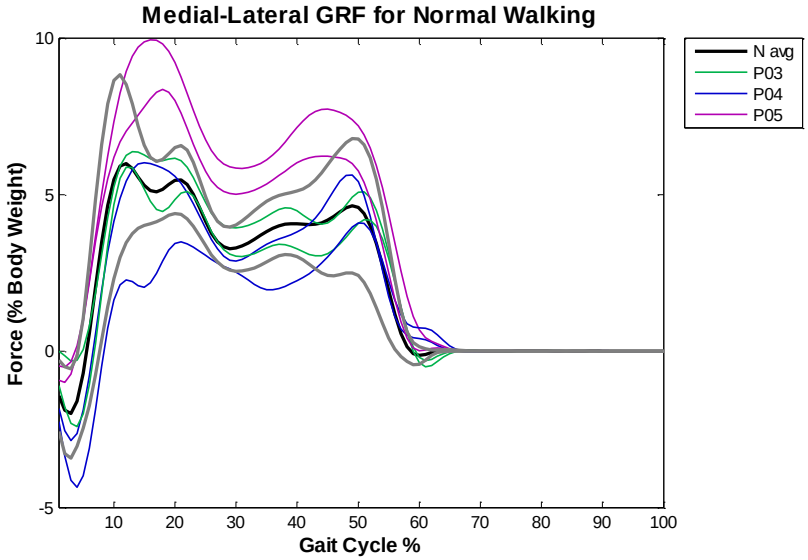

Figure 4-26. ML GRF of MTBI participants during single-task walking.

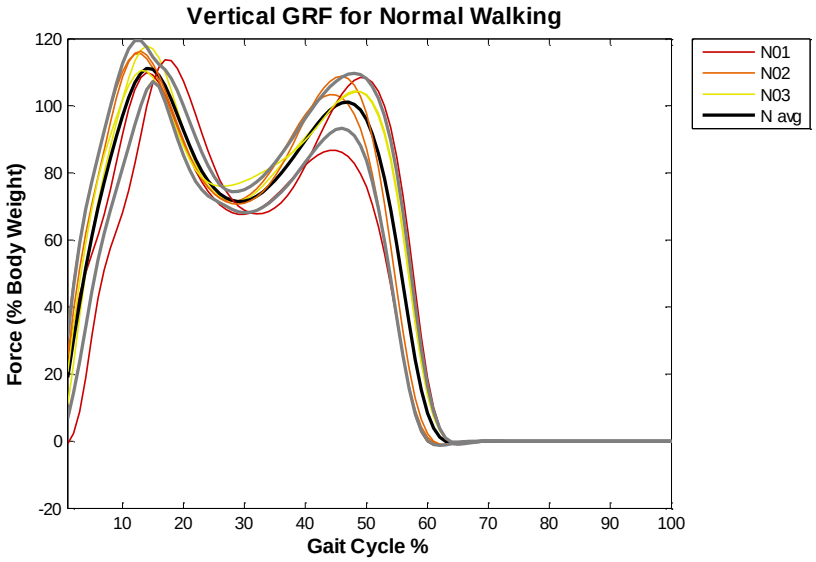

Figure 4-27. Vertical GRF of normal participants during single-task walking.

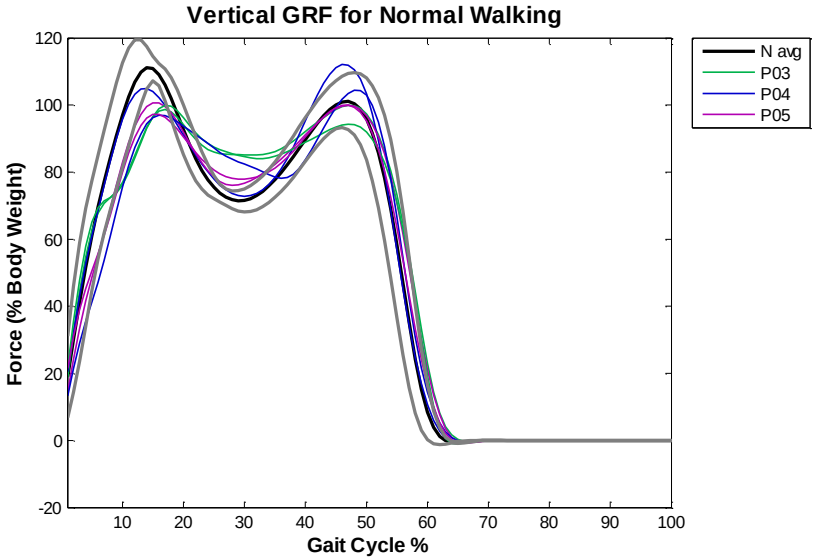

Figure 4-28. Vertical GRF of MTBI participants during single-task walking.

Table 4-3. GRF measures for single-task walking.

	Anterior-Posterior GRF		Vertical GRF		
	Max Loading Time (%)	Max Loading Magnitude (%BW)	Max Loading Time (%)	Min Support Time (%)	Loading-Support Magnitude (%BW)
N01	12.5	-17.2	15.5	31	44.1
N02	9.5	-19.2	13	28.5	44.8
N03	10.5	-24.1	13.5	27.5	40.4
N Avg	10.8	-20.2	14	29	43.1
P03	9	-14.0	17	31.5	14.7
P04	10.5	-10.2	15	33	25.5
P05	10	-13.2	15.5	28.5	22.0
P Avg	9.8	-12.5	15.8	31	20.7

Table 4-4. Number of errors made during walking while counting backwards by seven.

	# Errors	
	Baseline	Walking
N01	0	1
N02	1	3
N03	0	0
P03	0	0
P04	0	3
P05	1	0

Table 4-5. Temporal and spatial parameters of the counting task.

	Velocity (m/s)	Stride Length (m)	Stride Time (s)	Step Width (m)	Step Height (m)
N01	1.33	1.45	1.10	0.087	0.060
N02	1.46	1.50	1.03	0.121	0.052
N03	1.29	1.49	1.16	0.141	0.062
N Avg	1.36	1.48	1.09	0.116	0.058
P03	1.23	1.52	1.24	0.159	0.048
P04	1.02	1.14	1.11	0.078	0.056
P05	1.01	1.14	1.14	0.174	0.049
P Avg	1.09	1.27	1.16	0.137	0.051

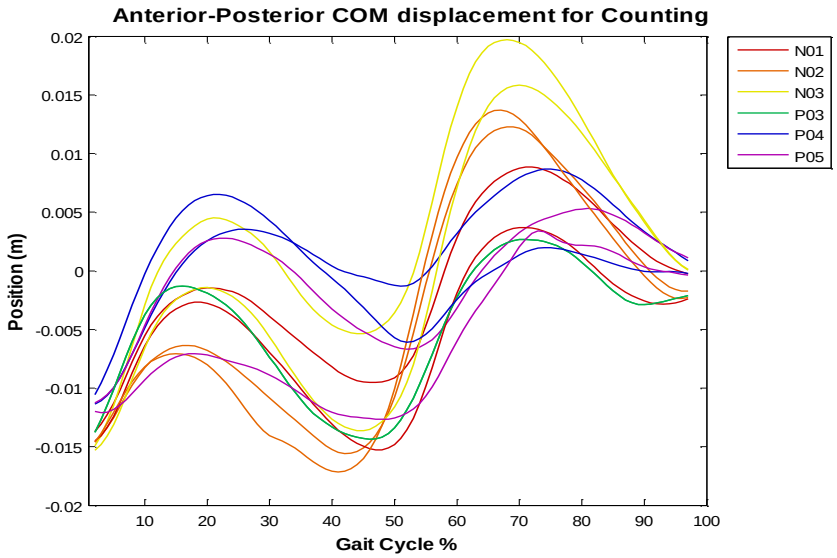

Figure 4-29. AP COM displacement during dual-task counting.

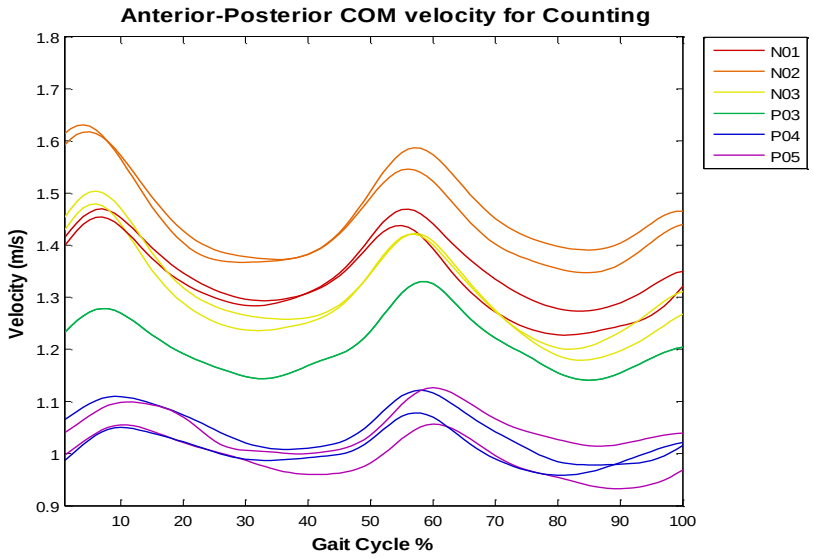

Figure 4-30. AP COM velocity during dual-task counting.

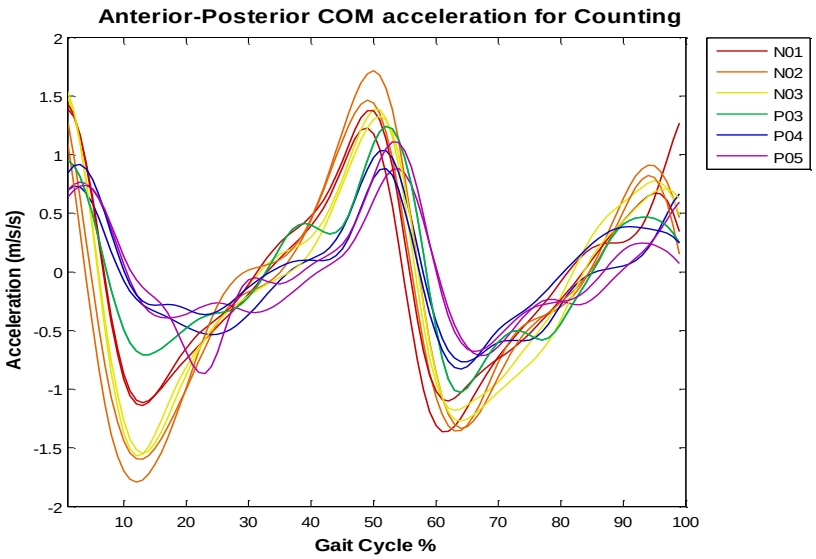

Figure 4-31. AP COM acceleration during dual-task counting.

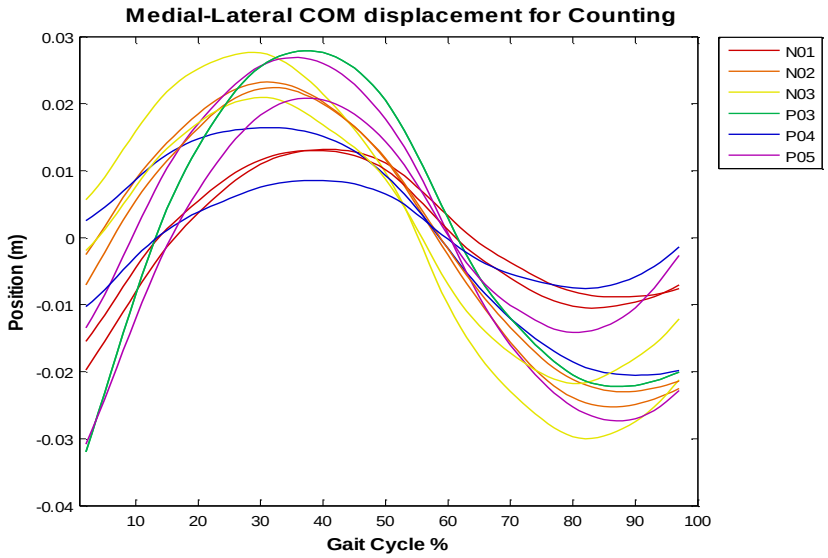

Figure 4-32. ML COM displacement during dual-task counting.

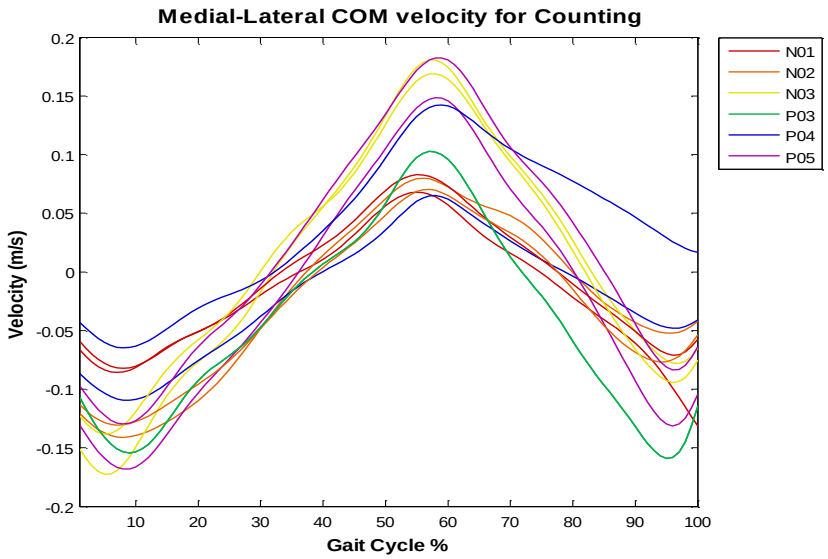

Figure 4-33. ML COM velocity during dual-task counting.

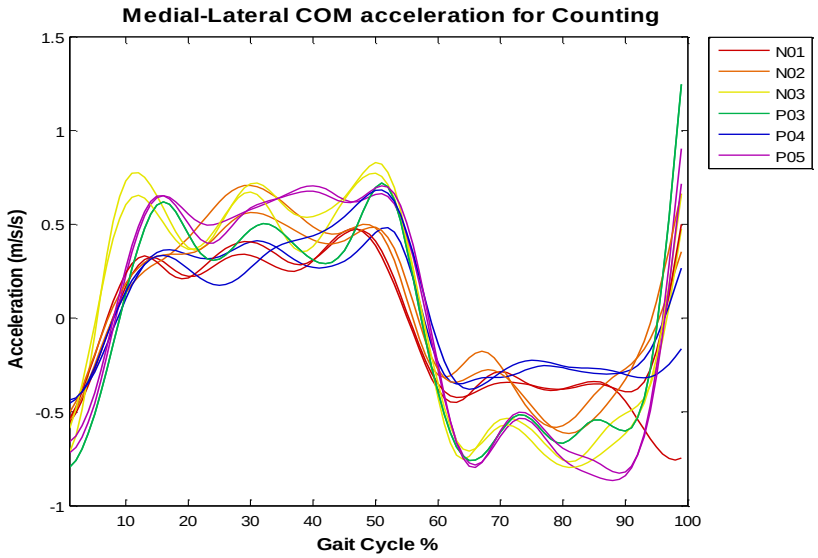

Figure 4-34. ML COM acceleration during dual-task counting.

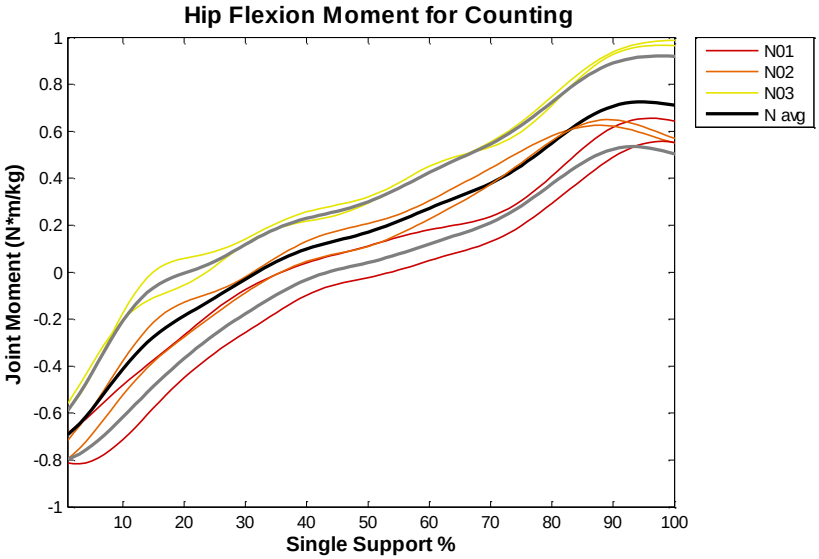

Figure 4-35. Hip flexion/extension joint moment of normal participants during dual-task counting.

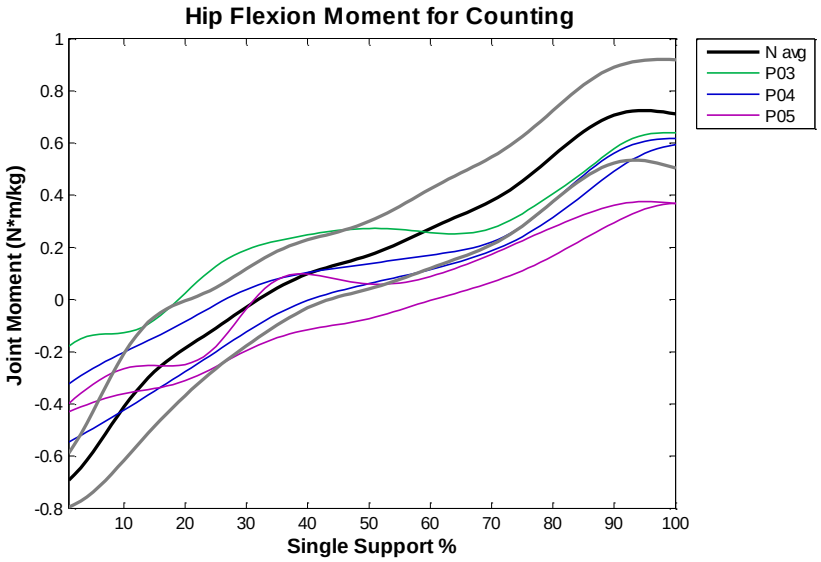

Figure 4-36. Hip flexion/extension joint moment of MTBI participants during dual-task counting.

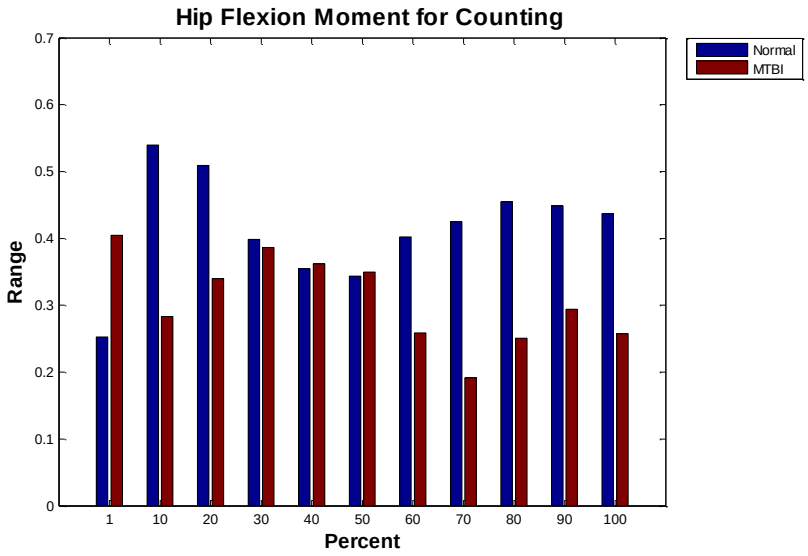

Figure 4-37. Range of hip flexion/extension joint moment of the normal and MTBI populations during single-support counting.

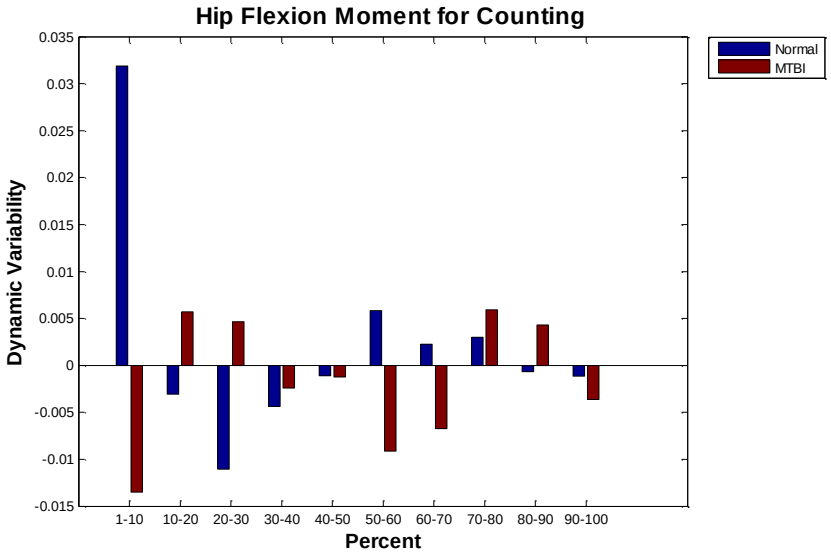

Figure 4-38. Dynamic variability of hip flexion/extension joint moment of the normal and MTBI populations during single-support counting.

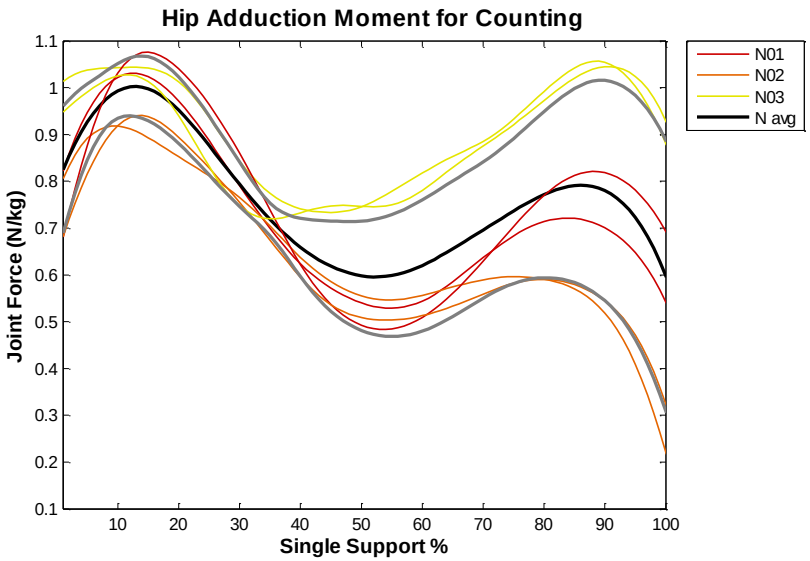

Figure 4-39. Hip adduction/abduction joint moment of normal participants during dual-task counting.

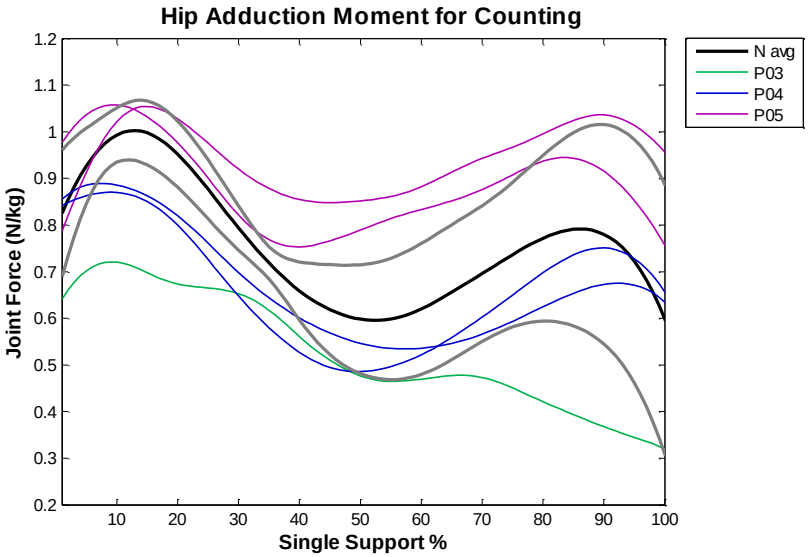

Figure 4-40. Hip adduction/abduction joint moment of MTBI participants during dual-task counting.

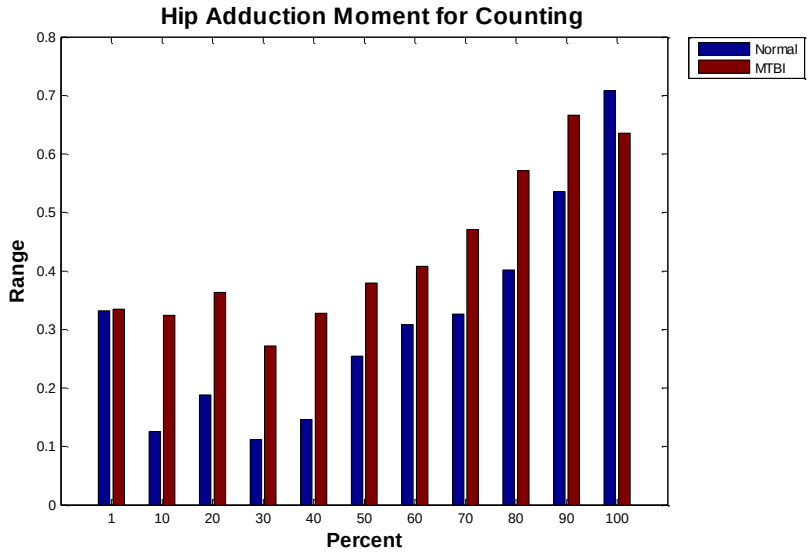

Figure 4-41. Range of hip adduction/abduction joint moment of the normal and MTBI populations during single-support counting.

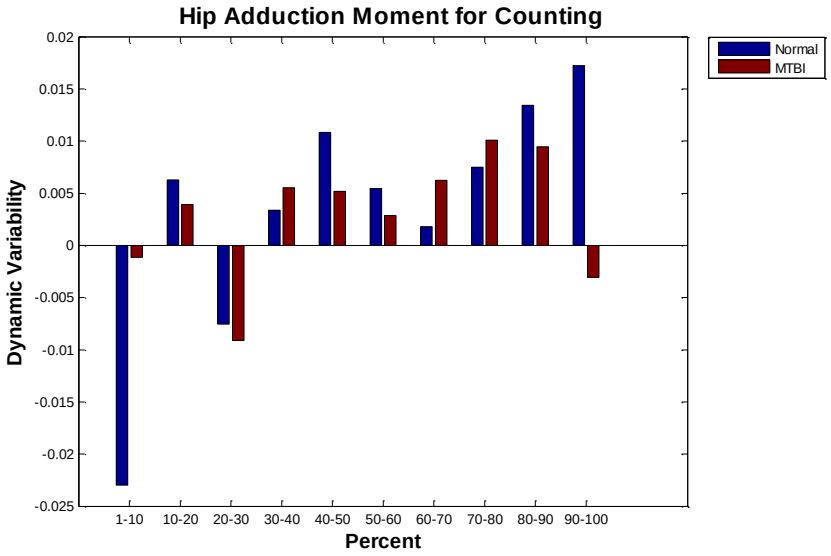

Figure 4-42. Dynamic variability of hip adduction/abduction joint moment of the normal and MTBI populations during single-support counting.

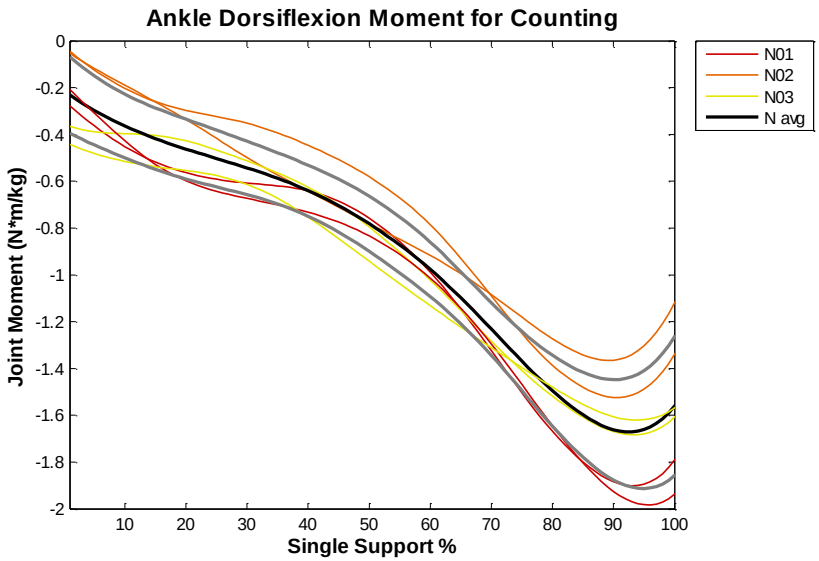

Figure 4-43. Ankle dorsiflexion/plantar flexion joint moment of normal participants during dual-task counting.

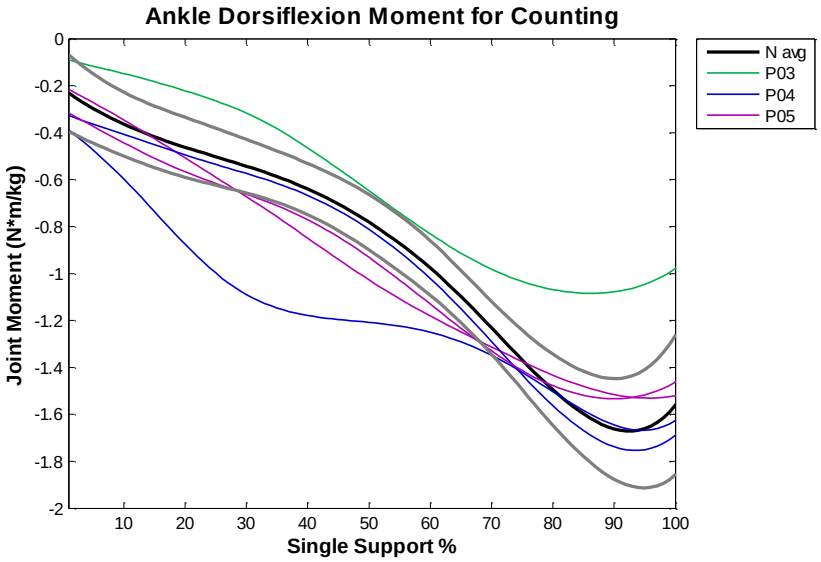

Figure 4-44. Ankle dorsiflexion/plantar flexion joint moment of MTBI participants during dual-task counting.

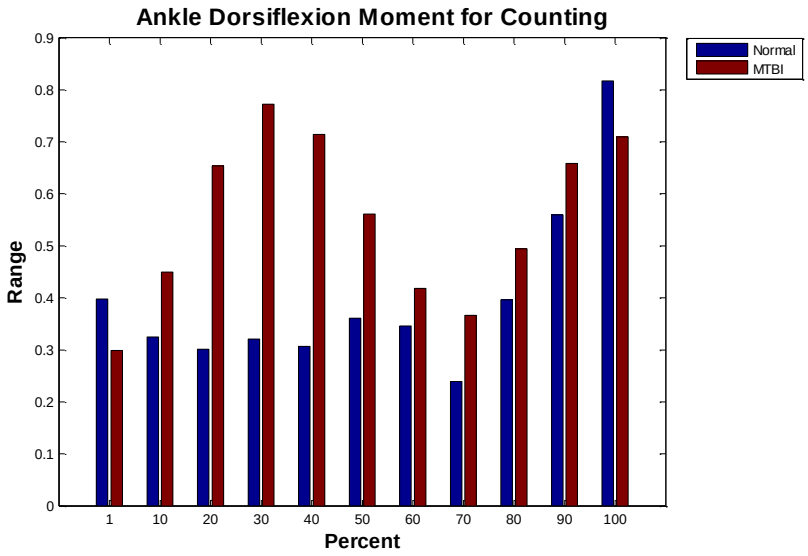

Figure 4-45. Range of ankle dorsiflexion/plantar flexion joint moment of the normal and MTBI populations during single-support counting.

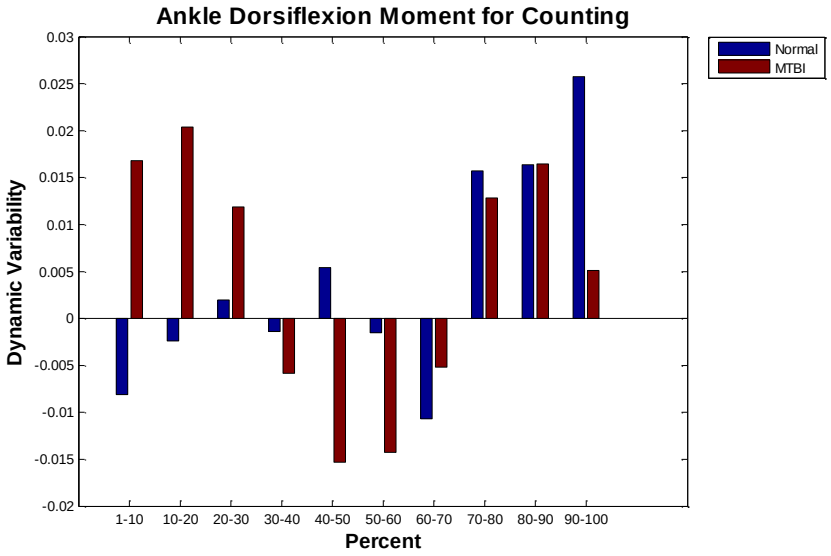

Figure 4-46. Dynamic variability of ankle dorsiflexion/plantar flexion joint moment of the normal and MTBI populations during single-support counting.

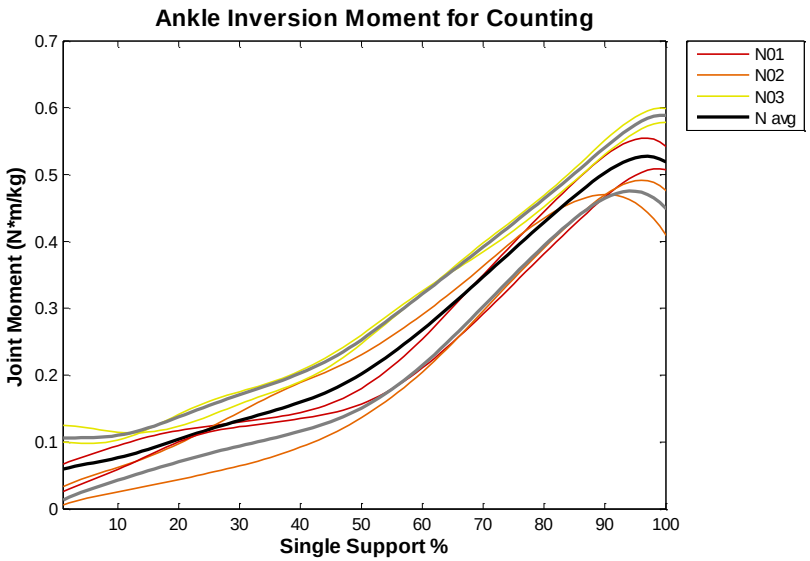

Figure 4-47. Ankle inversion/eversion joint moment of normal participants during dual-task counting.

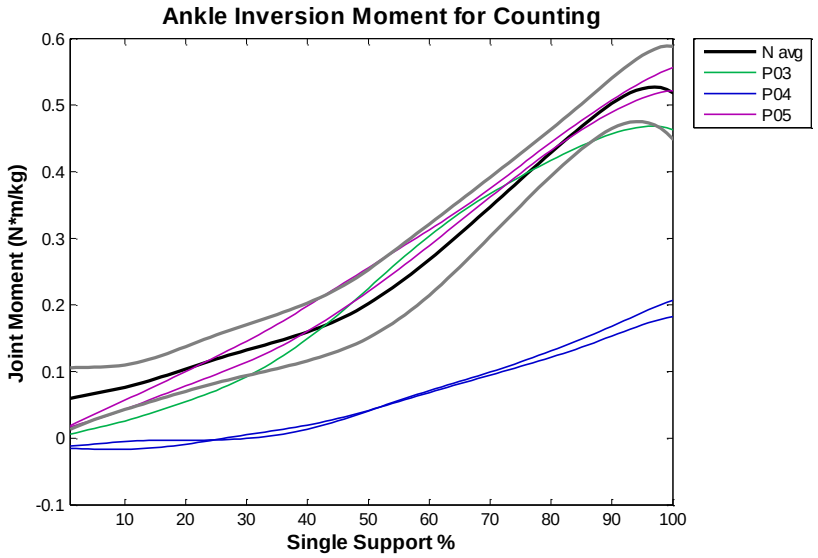

Figure 4-48. Ankle inversion/eversion joint moment of MTBI participants during dual-task counting.

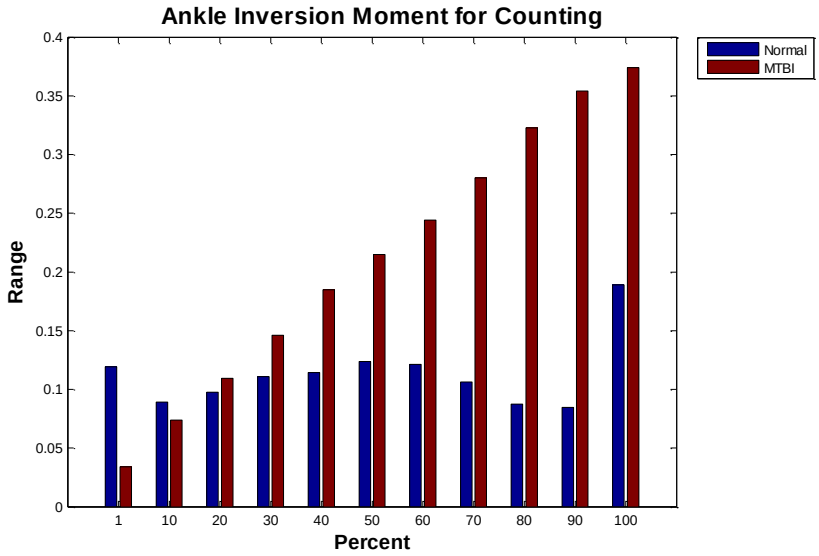

Figure 4-49. Range of ankle inversion/eversion joint moment of the normal and MTBI populations during single-support counting.

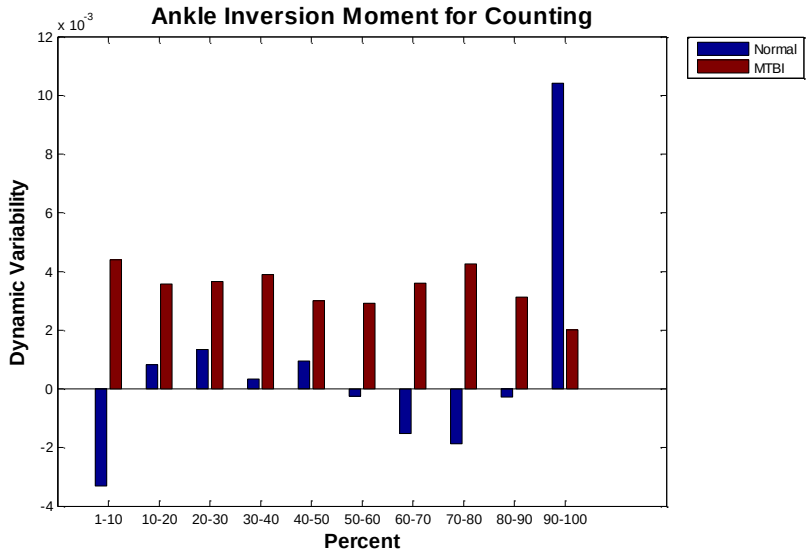

Figure 4-50. Dynamic variability of ankle inversion/eversion joint moment of the normal and MTBI populations during single-support counting.

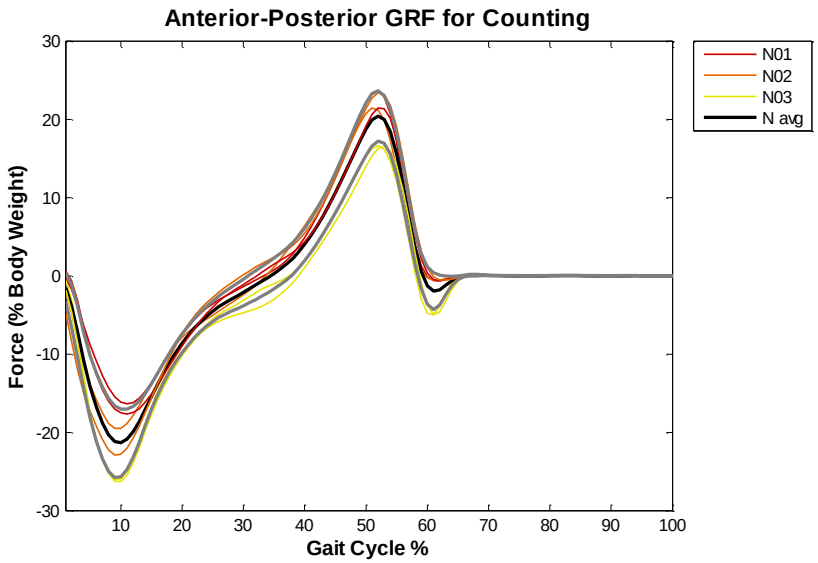

Figure 4-51. AP GRF of normal participants during dual-task counting.

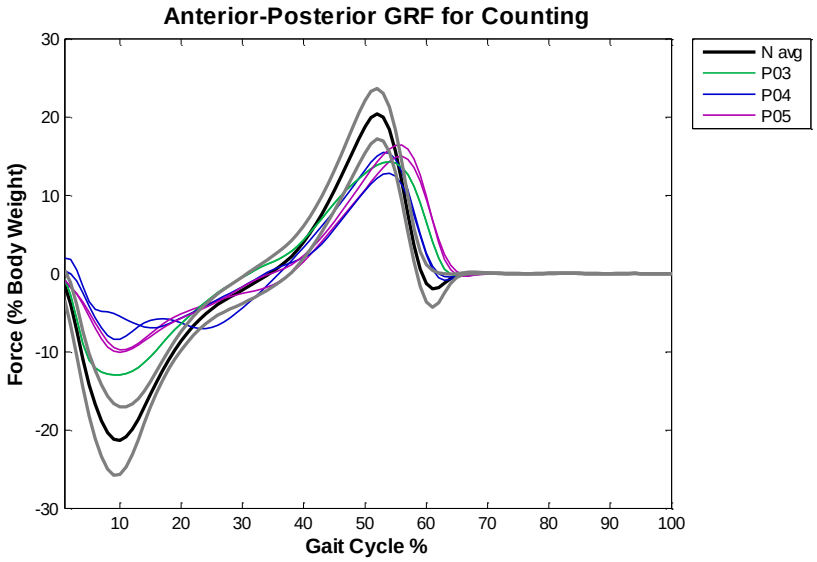

Figure 4-52. AP GRF of MTBI participants during dual-task counting.

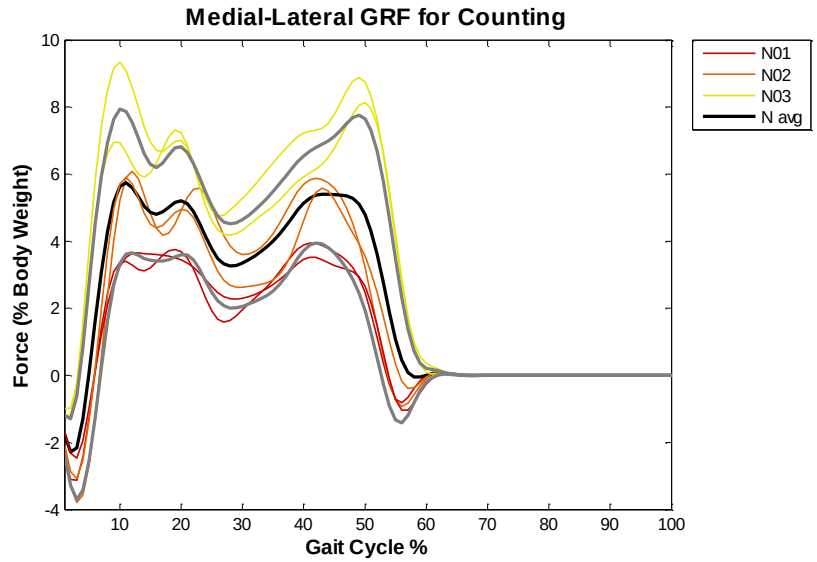

Figure 4-53. ML GRF of normal participants during dual-task counting.

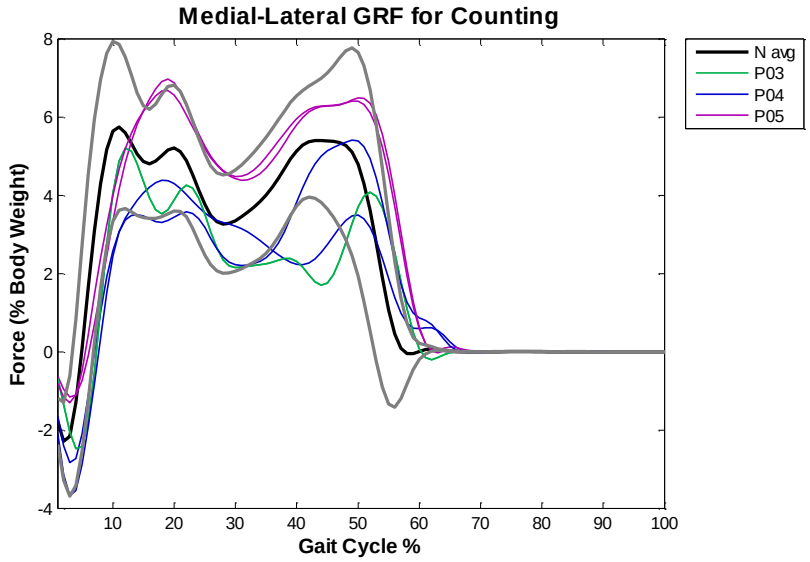

Figure 4-54. ML GRF of MTBI participants during dual-task counting.

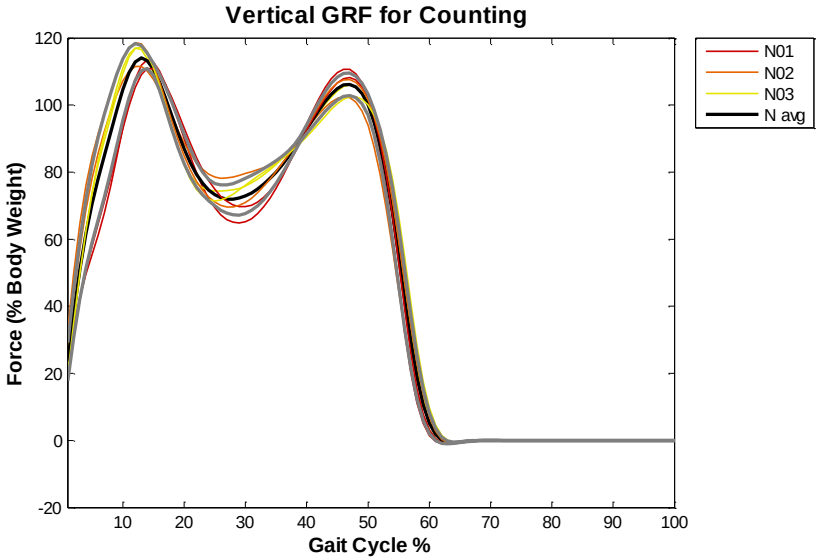

Figure 4-55. Vertical GRF of normal participants during dual-task counting.

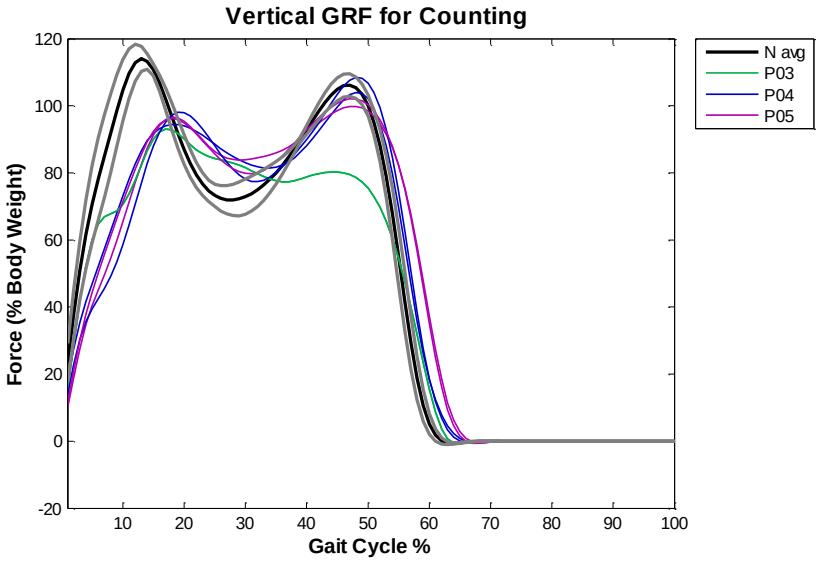

Figure 4-56. Vertical GRF of MTBI participants during dual-task counting.

Table 4-6. GRF measures for dual-task counting.

	Anterior-Posterior GRF		Vertical GRF		
	Max Loading Time (%)	Max Loading Magnitude (%BW)	Max Loading Time (%)	Min Support Time (%)	Loading-Support Magnitude (%BW)
N01	11	-17.0	14	29.5	44.9
N02	9	-21.2	12	26.5	41.2
N03	9.5	-26.2	12.5	25.5	44.2
N Avg	9.8	-21.5	12.8	27.2	43.4
P03	9	-13.0	17	36	15.7
P04	9	-10.7	17.5	35	14.4
P05	12.5	-8.4	18.5	30.5	16.8
P Avg	10.2	-10.7	17.7	33.8	15.6

Table 4-7. Temporal and spatial parameters of the asymmetric carrying task.

	Velocity (m/s)	Stride Length (m)	Stride Time (s)	Step Width (m)	Step Height (m)
N01	1.28	1.43	1.12	0.073	0.061
N02	1.47	1.41	0.96	0.118	0.044
N03	1.30	1.45	1.12	0.139	0.054
N Avg	1.35	1.43	1.06	0.110	0.053
P03	1.25	1.50	1.20	0.133	0.057
P04	1.16	1.16	1.01	0.079	0.054
P05	1.19	1.27	1.07	0.156	0.053
P Avg	1.20	1.31	1.09	0.123	0.055

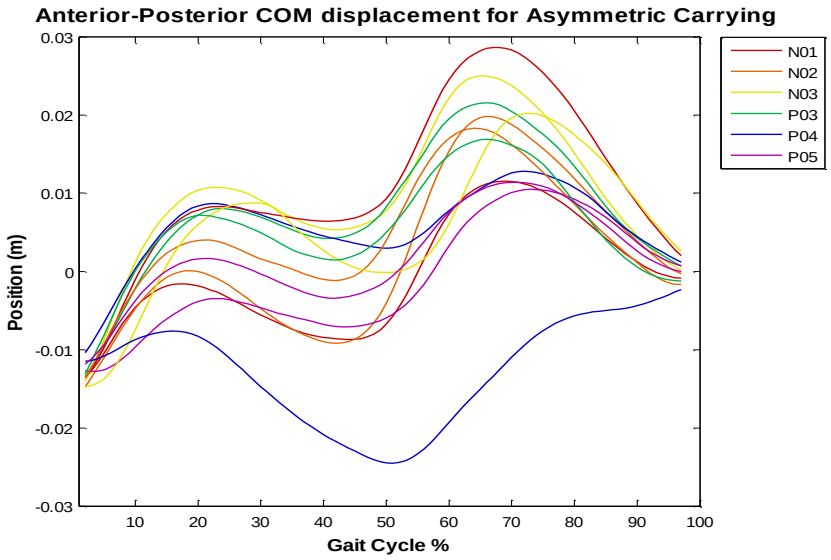

Figure 4-57. AP COM displacement during dual-task carrying.

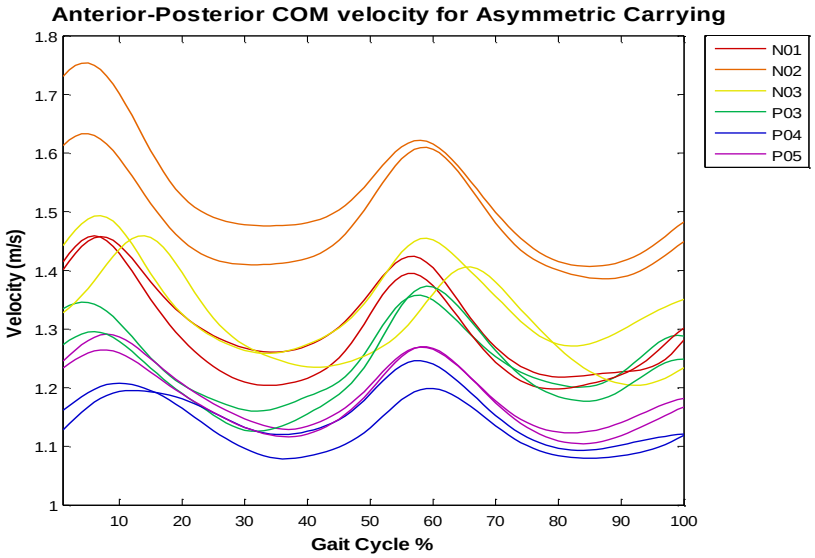

Figure 4-58. AP COM velocity during dual-task carrying.

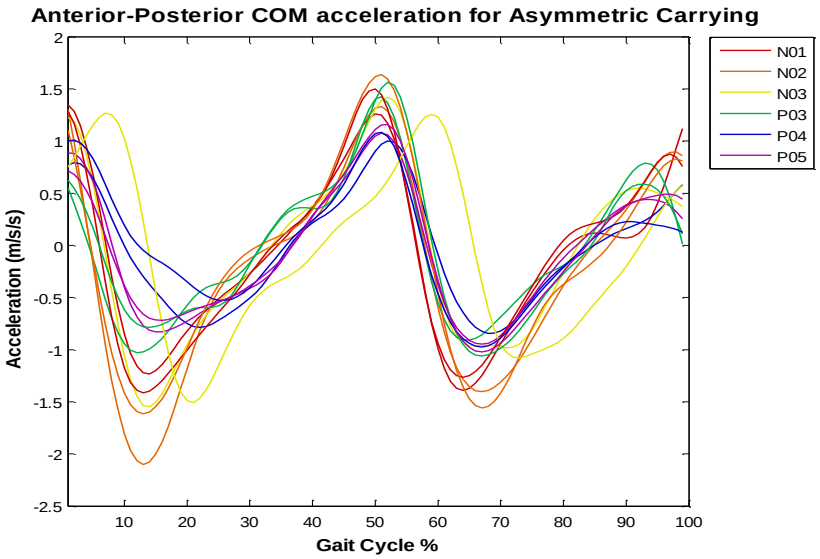

Figure 4-59. AP COM acceleration during dual-task carrying.

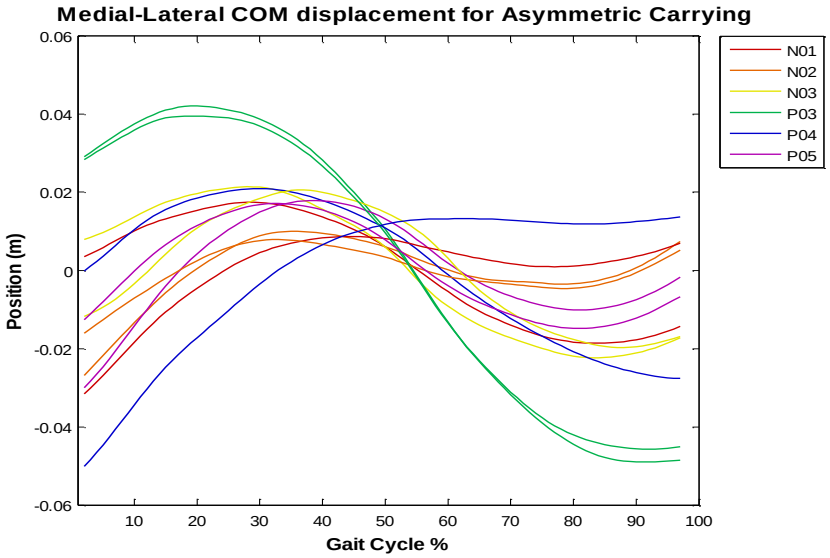

Figure 4-60. ML COM displacement during dual-task carrying.

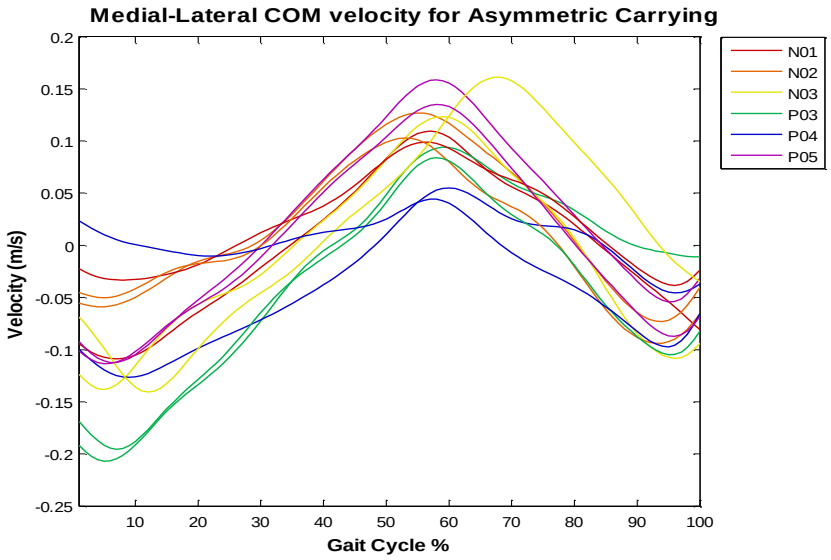

Figure 4-61. ML COM velocity during dual-task carrying.

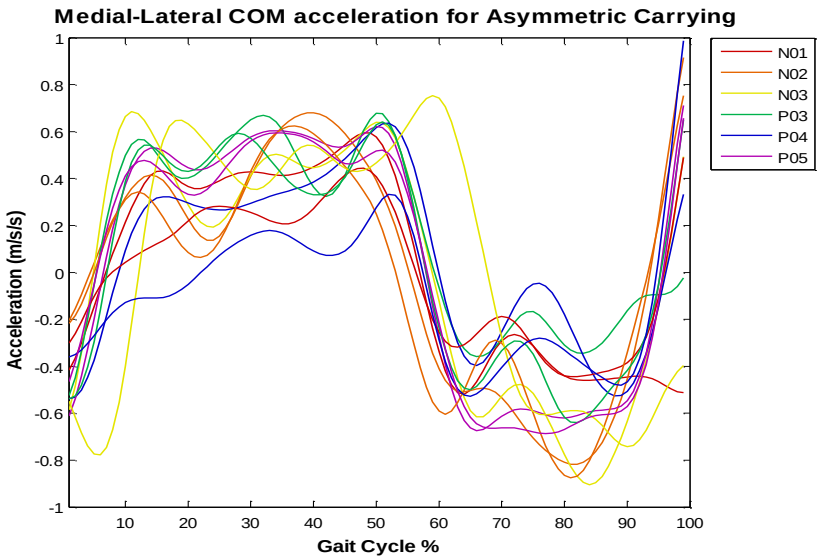

Figure 4-62. ML COM acceleration during dual-task counting.

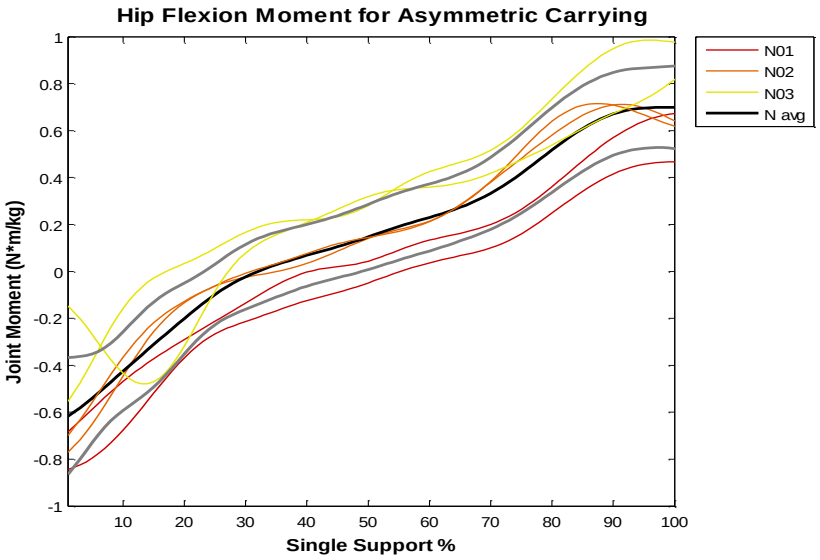

Figure 4-63. Hip flexion/extension joint moment of normal participants during dual-task carrying.

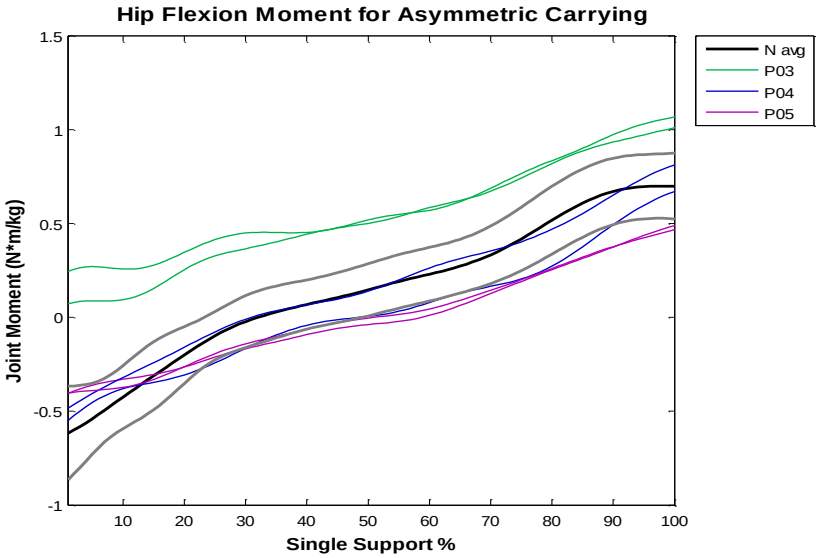

Figure 4-64. Hip flexion/extension joint moment of MTBI participants during dual-task carrying.

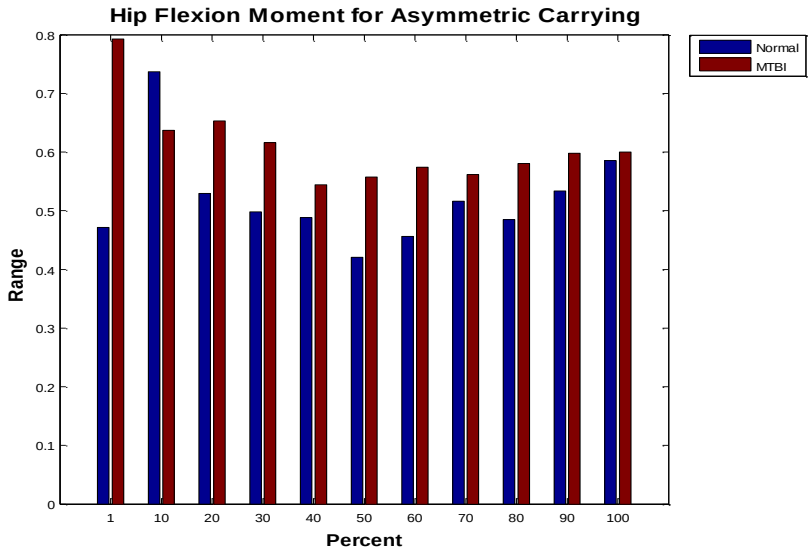

Figure 4-65. Range of hip flexion/extension joint moment of the normal and MTBI populations during single-support carrying.

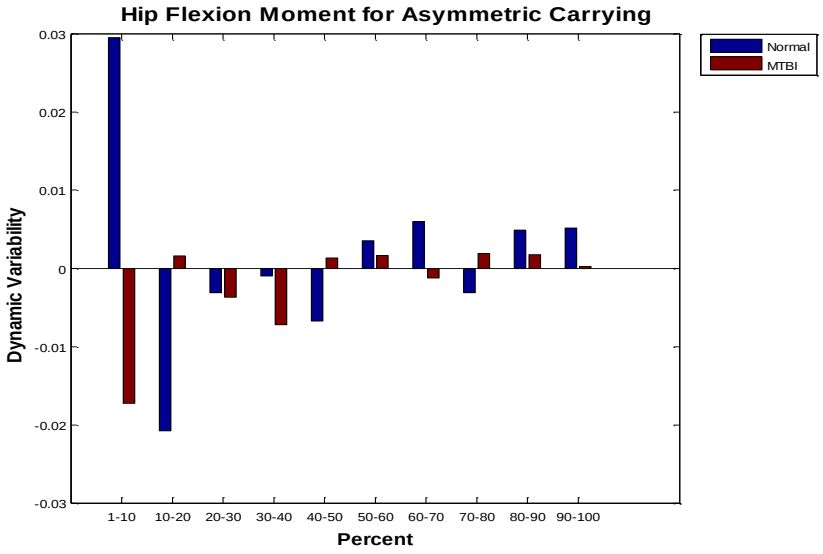

Figure 4-66. Dynamic variability of hip flexion/extension joint moment of the normal and MTBI populations during single-support carrying.

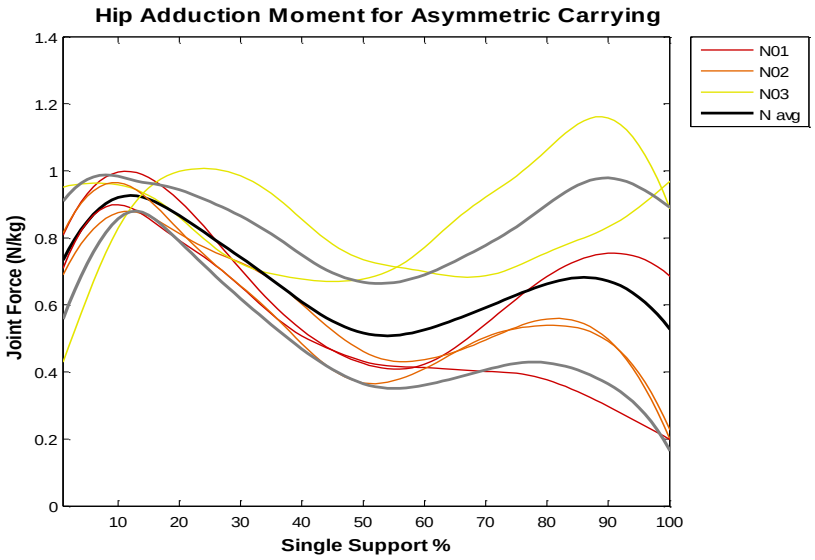

Figure 4-67. Hip adduction/abduction joint moment of normal participants during dual-task carrying.

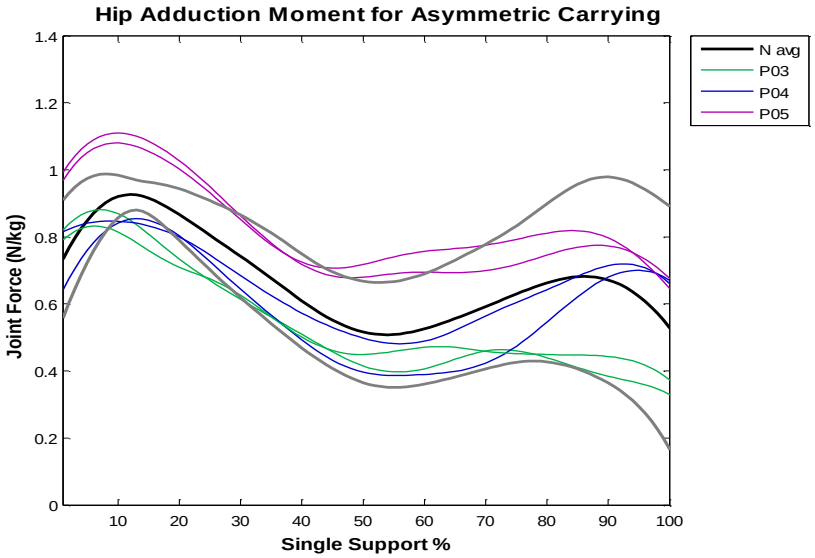

Figure 4-68. Hip adduction/abduction joint moment of MTBI participants during dual-task carrying.

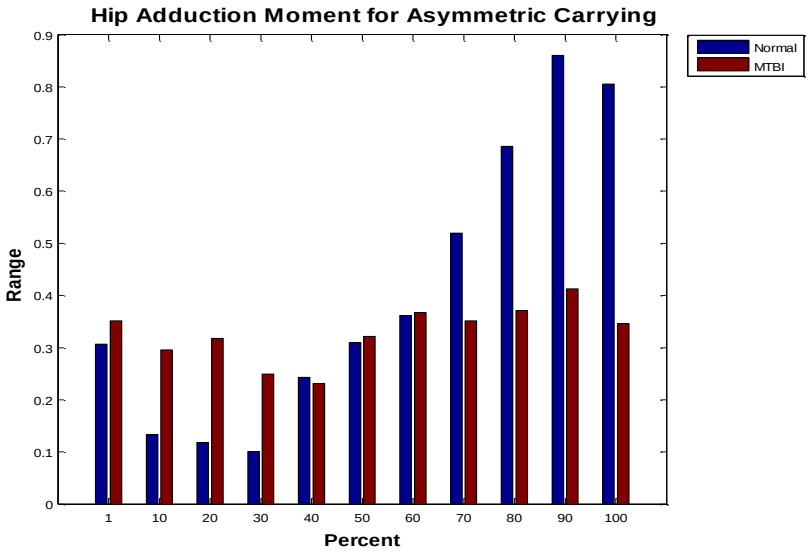

Figure 4-69. Range of hip adduction/abduction joint moment of the normal and MTBI populations during single-support carrying.

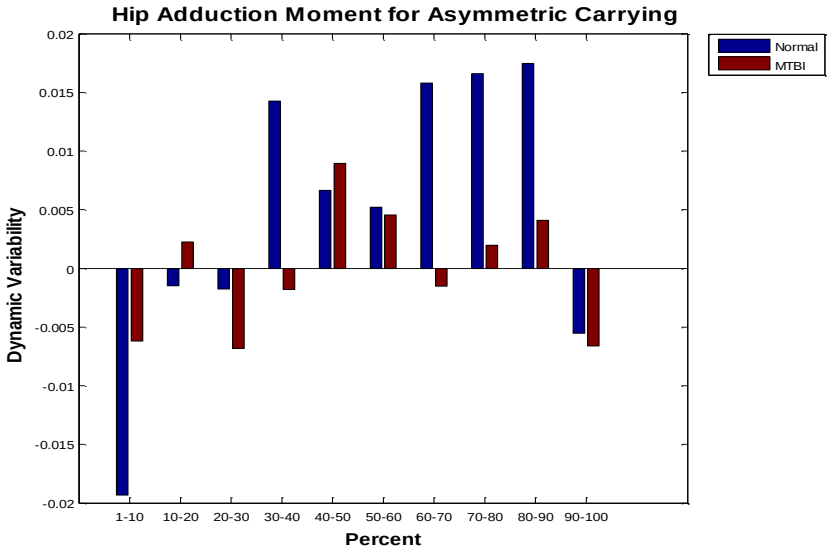

Figure 4-70. Dynamic variability of hip adduction/abduction joint moment of the normal and MTBI populations during single-support carrying.

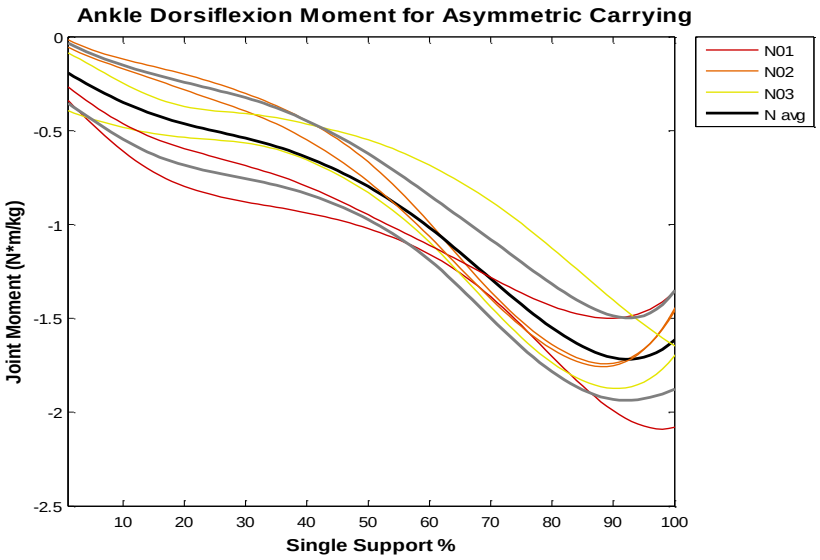

Figure 4-71. Ankle dorsiflexion/plantar flexion joint moment of normal participants during dual-task carrying.

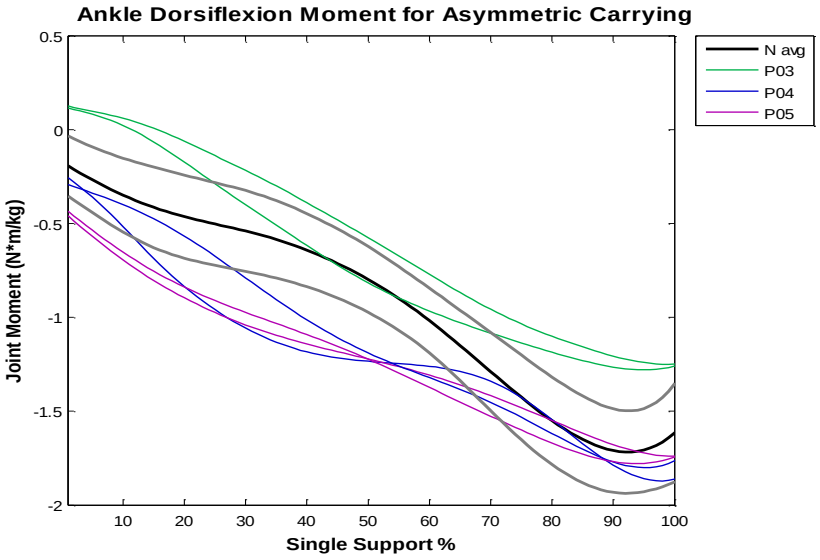

Figure 4-72. Ankle dorsiflexion/plantar flexion joint moment of MTBI participants during dual-task carrying.

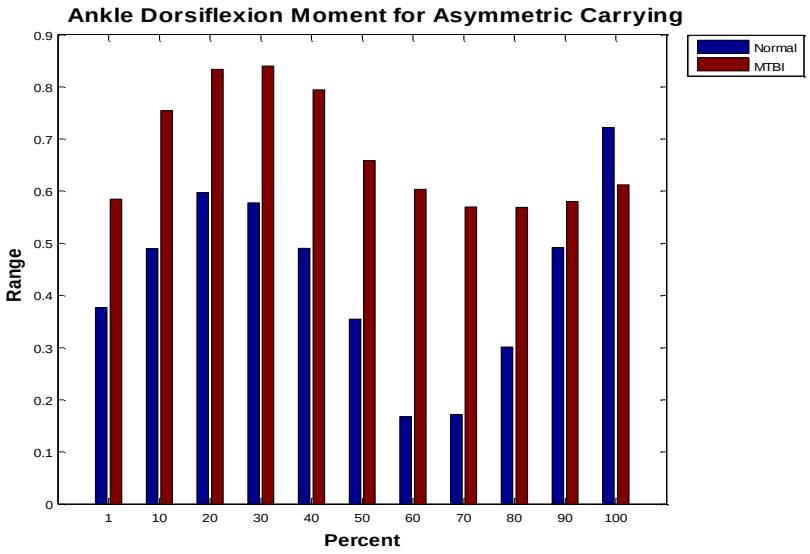

Figure 4-73. Range of ankle dorsiflexion/plantar flexion joint moment of the normal and MTBI populations during single-support carrying.

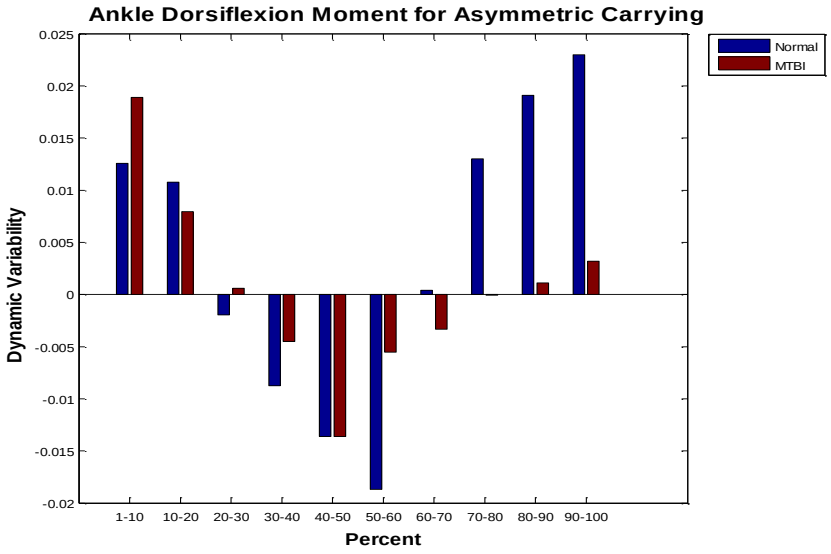

Figure 4-74. Dynamic variability of ankle dorsiflexion/plantar flexion joint moment of the normal and MTBI populations during single-support carrying.

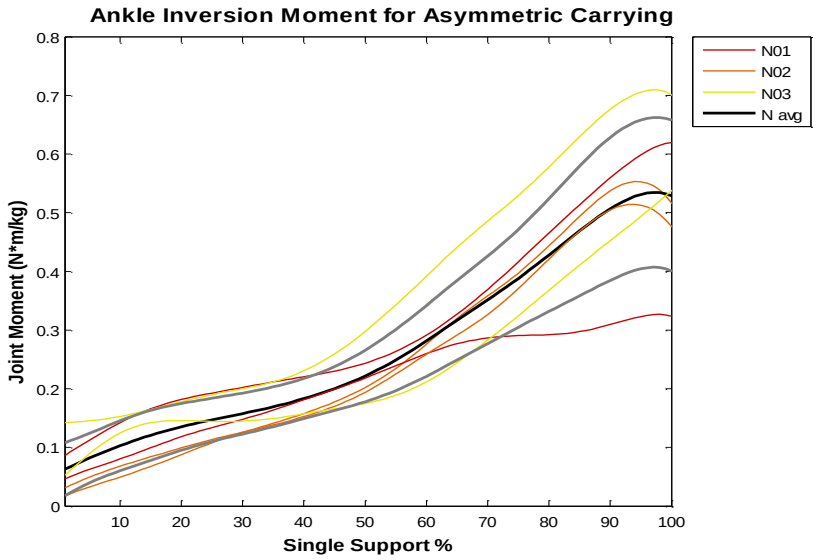

Figure 4-75. Ankle inversion/eversion joint moment of normal participants during dual-task carrying.

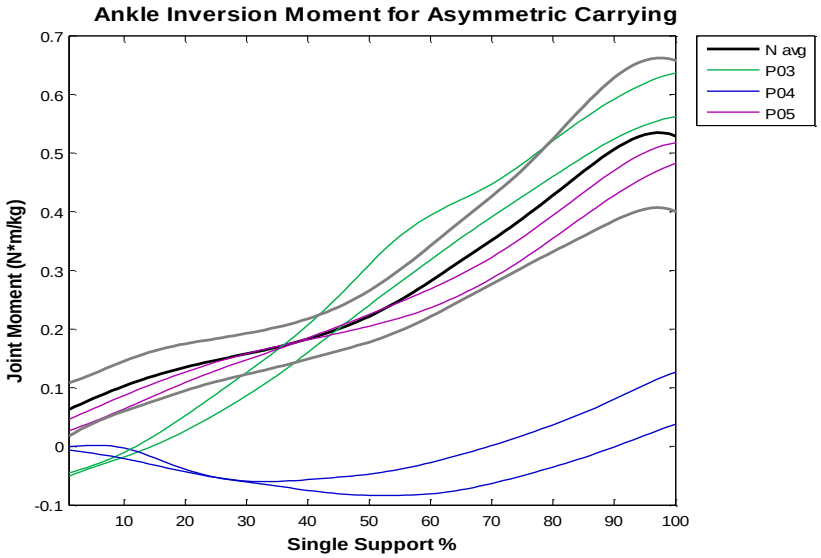

Figure 4-76. Ankle inversion/eversion joint moment of MTBI participants during dual-task carrying.

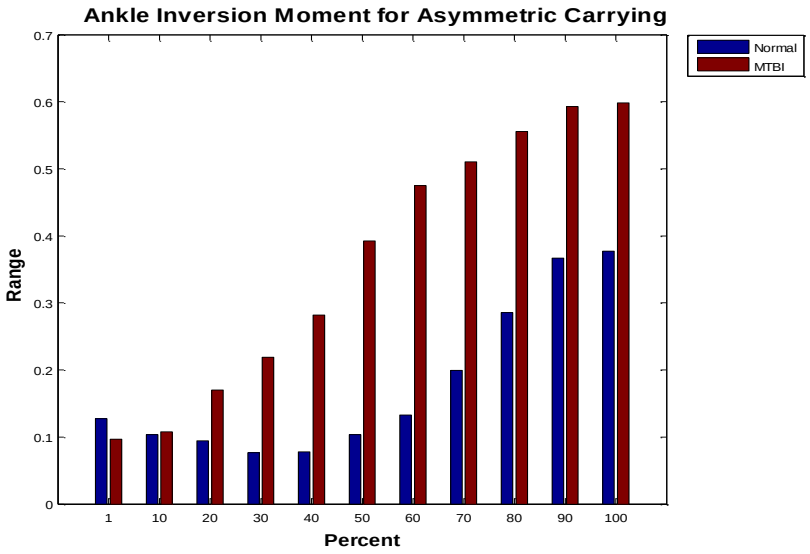

Figure 4-77. Range of ankle inversion/eversion joint moment of the normal and MTBI populations during single-support carrying.

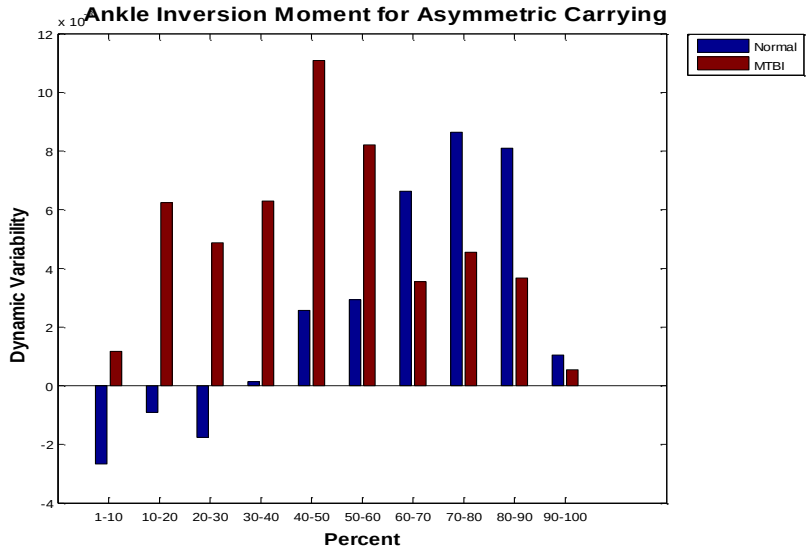

Figure 4-78. Dynamic variability of ankle inversion/eversion joint moment of the normal and MTBI populations during single-support carrying.

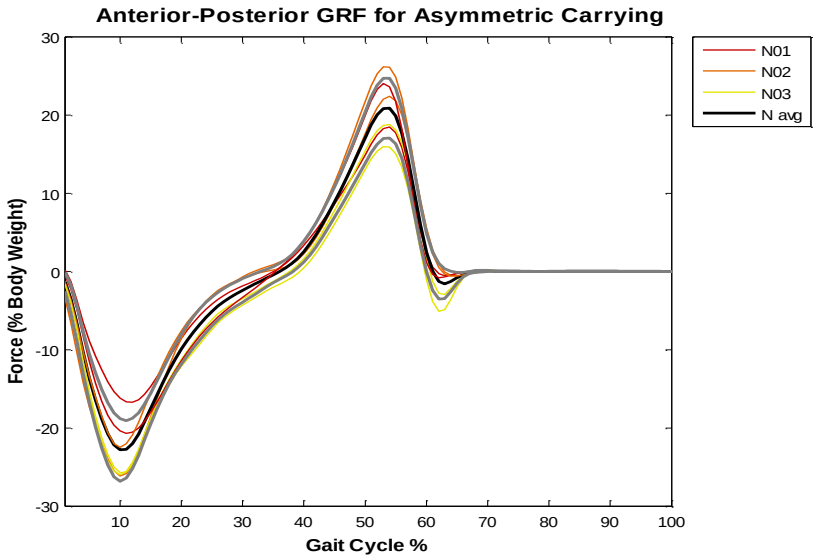

Figure 4-79. AP GRF of normal participants during dual-task carrying.

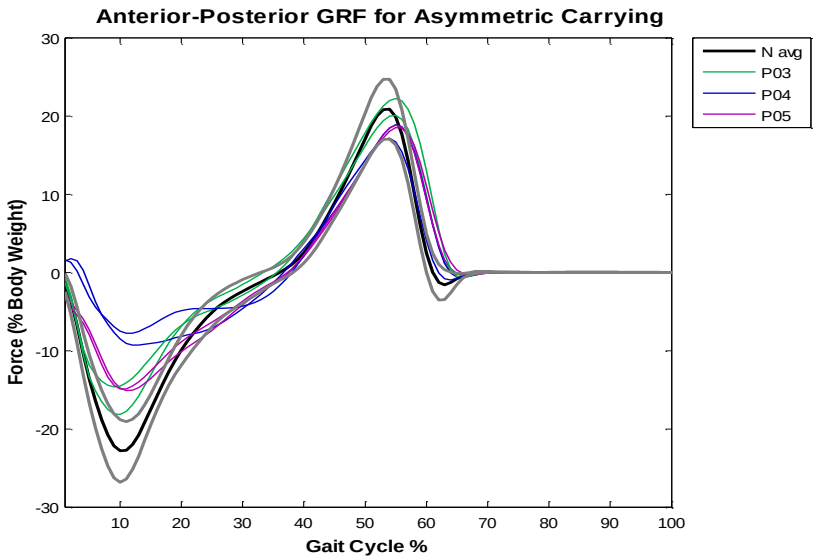

Figure 4-80. AP GRF of MTBI participants during dual-task carrying.

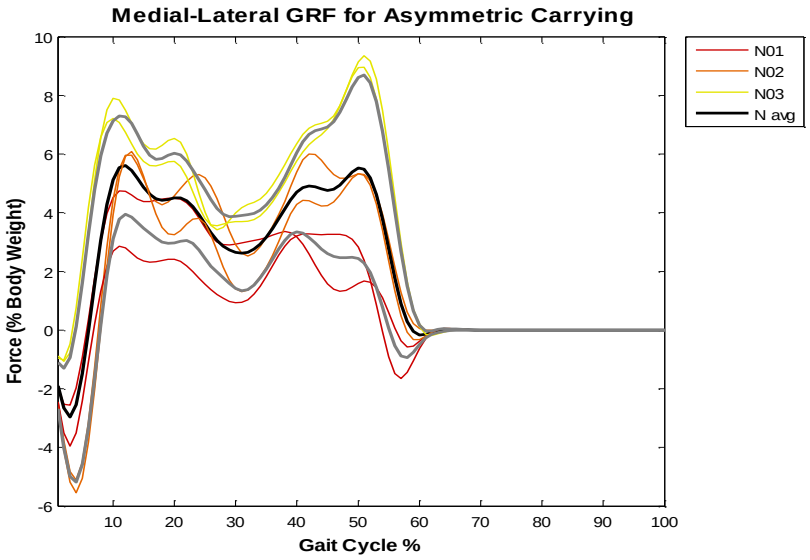

Figure 4-81. ML GRF of normal participants during dual-task carrying.

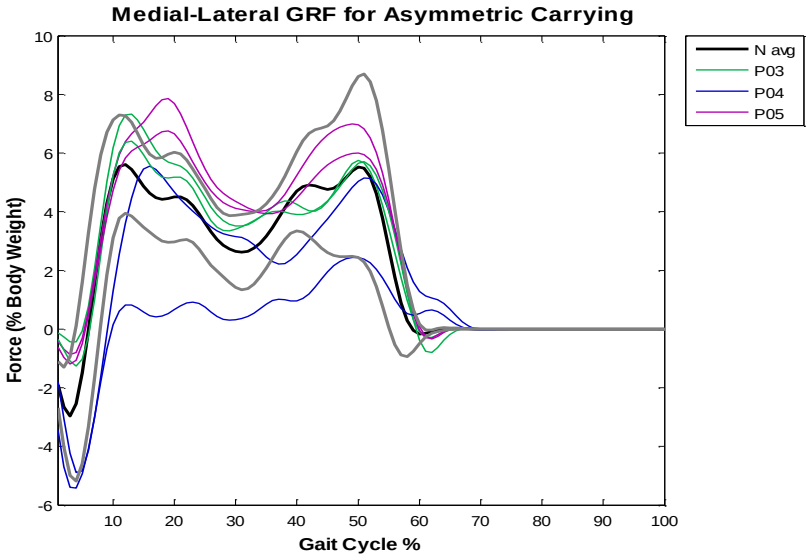

Figure 4-82. ML GRF of MTBI participants during dual-task carrying.

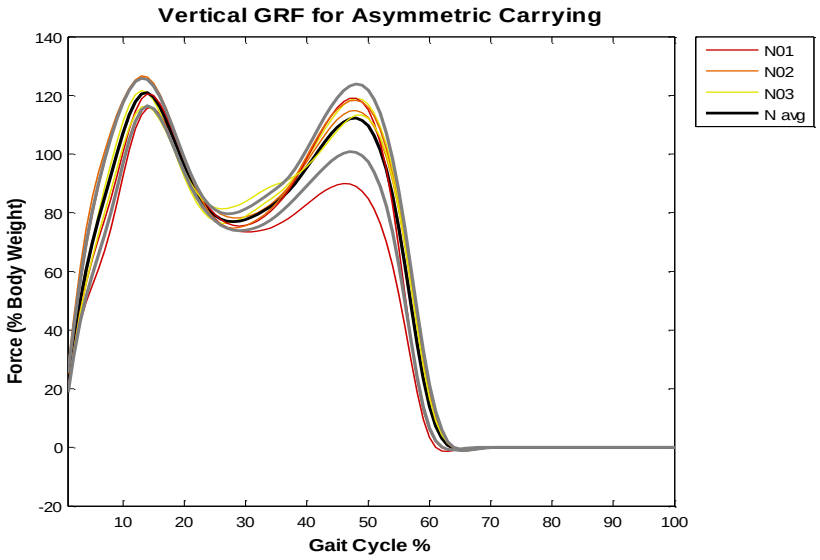

Figure 4-83. Vertical GRF of normal participants during dual-task carrying.

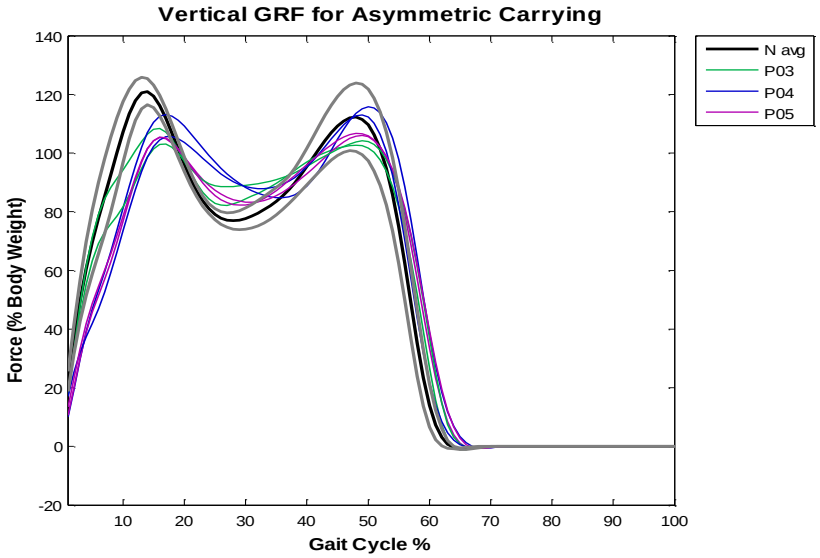

Figure 4-84. Vertical GRF of MTBI participants during dual-task carrying.

Table 4-8. GRF measures for dual-task carrying.

	Anterior-Posterior GRF		Vertical GRF		
	Max Loading Time (%)	Max Loading Magnitude (%BW)	Max Loading Time (%)	Min Support Time (%)	Loading-Support Magnitude (%BW)
N01	11.5	-18.7	14	29.5	43.6
N02	10	-24.3	13	28	49.9
N03	10	-25.9	13.5	26.5	40.1
N Avg	10.5	-23.0	13.5	28	44.6
P03	9.5	-16.4	16.5	27	20.4
P04	11.5	-8.5	17.5	34	23.0
P05	10.5	-15.0	16	30	22.7
P Avg	10.5	-13.3	16.7	30.3	22.0

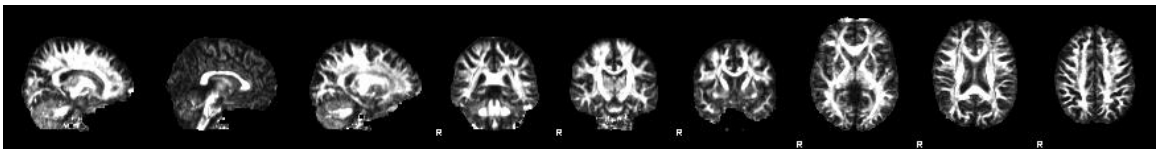

(a)

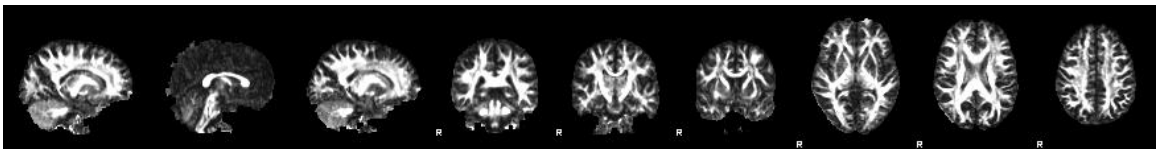

(b)

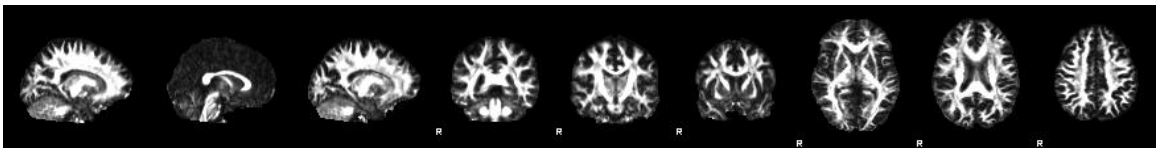

(c)

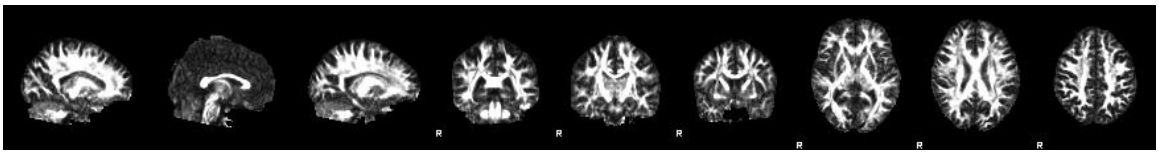

(d)

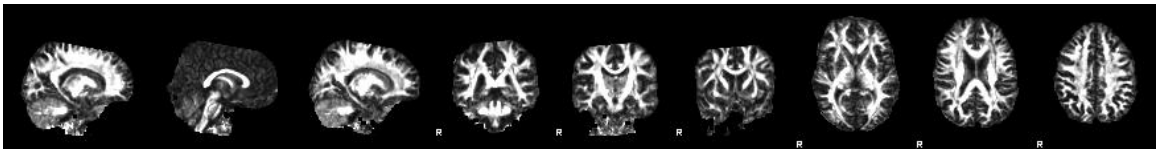

(e)

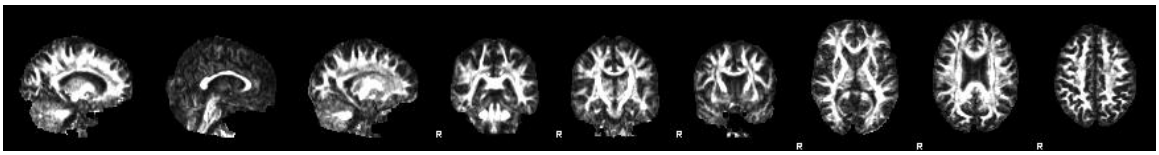

(f)

Figure 4-85. MRI-DTI scans of the participants: (a) N01, (b) N02, (c) N03, (d) P03, (e) P04, (f) P05.

CHAPTER 5

CASE STUDY

The analysis framework for studying gait characteristics of normal and MTBI patient populations was introduced in Chapter 3, and the gait results for the normal and MTBI populations were presented in Chapter 4. As the main goal of this study is to create a protocol to capture abnormal gait behaviors in a single patient with MTBI, and because different MTBI patients encounter different types of injury, this chapter focuses on the steps that need to be taken to investigate gait abnormality of a specific MTBI patient.

Case Study Description

This case study considered P04, a right-side dominant, male individual. He was injured by an IED (improvised explosive device) and was dazed and confused for 30 minutes. Dizziness started one month later. His injury happened close to four years before this study; at the time of the study he had normal neurological and cognitive evaluations. He reported to the study coordinator that he experienced dizziness and lack of balance a few times per month with no occurrence of fall. The patterns of dizziness and instability were reportedly random. P04 is color-coded in blue for the kinematic and kinetic results presented here and in Chapter 4.

Task Performance

The same tasks selected in the results section of Chapter 4 are discussed here for the case study. Single-task walking was considered together with a cognitive dual task and a motor dual task. The cognitive dual task required participants to count backwards by seven starting at 100 during baseline and 101 during walking. This task is referred to as counting. Baseline testing was performed with the patient seated. The motor dual task was an asymmetric carrying task selected to represent common daily activities, such as

carrying groceries or a computer bag. The patient was asked to carry a 15 pound load in his dominant hand while walking in the laboratory. Instructions for the dual tasks were provided after the patient began walking, and no instruction was provided to prioritize either walking or the dual task.

P04 committed zero errors during the backwards counting task at baseline and three errors while walking and performing the counting dual task.

Temporal and Spatial Parameters

Temporal and spatial parameters are presented in Table 5-1 for P04 and the mean of the normal population for the three tasks under investigation: normal walking, counting, and carrying. Parameters were averaged for the two steady-state gait cycles.

P04 had reduced velocity compared to the normal population for all three tasks and a decrease in gait velocity during counting compared to single-task walking. Stride length was shortened for all three tasks compared to the normal population. A shorter stride length was measured in P04 during both dual tasks compared to single-task walking. Stride time was similar to the normal population with some reduction during carrying. Step width for P04 was constant across the tasks and always less than the normal population. His step width was also smaller than other MTBI participants, suggesting a different gait strategy than is typical of MTBI patients. The mean step width for the normal participants was greatest during normal walking; step width decreased during counting and decreased further during carrying. Step height was decreased for P04 during normal walking and similar to the normal average during counting and carrying. Step height was lowest during single-task walking suggesting a cautious adaptation during the dual tasks.

Kinematics

The current study considered investigating the motion of the COM during the gait cycle as the focus of kinematic analysis because it is related to stability and balance and

may be representative of whole-body motion. Kinematics of the COM is presented for the entire gait cycle.

During normal walking, the AP COM displacement, velocity, and acceleration of P04 were similar to other MTBI participants and compared to the normal participants showed similar trends in AP COM displacement (Figure 4-1) and reduced AP COM velocity (Figure 4-2) and AP COM acceleration (Figure 4-3). He had ML COM displacement consistent with other patients (Figure 4-4). The peak ML COM velocity of P04 was reduced slightly when compared to other MTBI participants (Figure 4-5), as was peak ML COM acceleration (Figure 4-6).

During the counting dual task, P04 had increased peak AP COM displacement around 20% in early single support (Figure 4-29) compared to other normal and MTBI participants. Two different trends in AP COM displacement were observed for P04 during carrying (Figure 4-57). No notable differences in his ML COM acceleration were found during counting (Figure 4-34). During carrying, his ML COM acceleration was reduced compared to other MTBI patients in the first part of the gait cycle (Figure 4-62).

Kinetics

Kinetic analysis concentrated on the hip and ankle joint moments in the sagittal and coronal plane. Results included joint moment trends, the range of joint torques, and the dynamic variability, which is defined as the rate of change of the ranges. Subject-specific dynamic variability is presented in this chapter. Joint moment kinetics were normalized by participant mass and presented for the single-support phase. The single-support phase of the gait cycle is defined for the dominant limb from toe off to heel strike of the non-dominant, swing limb.

Ground reaction forces examined the anterior-posterior and medial-lateral components, which are related to stability in the transverse plane at the foot-ground interface, and the vertical component, which is related to load bearing during the walking

cycle. Ground reaction forces are presented for the entire gait cycle as a percentage of body weight (%BW).

Hip Flexion/Extension Moment

P04's hip flexion/extension joint moment presented in Figure 4-8 for normal walking is similar to the normal population shown in Figure 4-7. Subject-specific range and dynamic variability were calculated at 20%, 50%, and 80% of the single support phase during early, mid, and late single support. Results for the individual range (Figure 5-1) and dynamic variability (Figure 5-2) during single-task walking were small for P04 and close to normal results. The joint moment trend in early single support during counting differed for P04 (Figure 4-36) compared to the normal population (Figure 4-35) The trends of P04 hip flexion joint moment differed slightly from other MTBI participants during carrying. An increased range of hip flexion moment for P04 during counting and carrying is shown in Figure 5-3 and Figure 5-5, respectively. An increased magnitude of subject-specific dynamic variability is also observed for P04 in Figure 5-4 and Figure 5-6 for the dual-task conditions. The dynamic variability of P04 was opposite in direction during counting from early to mid single support, 20% to 50%. There was an increase in range between these times.

Hip Adduction/Abduction Moment

The hip adduction/abduction joint moment for the participants was presented in Chapter 4 for single-task walking in Figure 4-11 and Figure 4-12, for counting in Figure 4-39 and Figure 4-40, and for carrying in Figure 4-67 and Figure 4-68. Individual range and dynamic variability of the hip adduction/abduction joint moment during single-task walking are shown for P04 and other participants in Figure 5-7 and Figure 5-8, respectively. The individual range for P04 at 20% was greater than normal participants and less than MTBI participants. The range was reduced by 50% of single support. The decrease from 20% to 50% was reflected in the negative dynamic variability of P04,

which was different from the normal participants. The individual range of P04 was greater during counting (Figure 5-9). Results for the joint moment range of P04 during carrying are shown in Figure 5-11. The dynamic variability of P04 varied slightly from single-task walking during counting (Figure 5-10) and carrying (Figure 5-12), but no substantial differences were noted.

Ankle Dorsiflexion/Plantar Flexion Moment

The ankle dorsiflexion/plantar flexion joint moment for the participants was presented in Chapter 4 for single-task walking in Figure 4-15 and Figure 4-16, for counting in Figure 4-43 and Figure 4-44, and for carrying in Figure 4-71 and Figure 4-72. The results of P04 showed variations between cycles for single-task walking and counting. The individual range of P04 during normal walking (Figure 5-13) was elevated at early (20%) and mid (50%) single support and was a normal level at late single support (80%). The individual dynamic variability was opposite in direction from 20% to 50% compared to all other participants and substantially greater in magnitude from 50% to 80% compared to normal ranges. The same is seen for the individual range (Figure 5-15) and dynamic variability (Figure 5-16) during counting. During dual-task carrying, the range of P04 was similar to normal participants at 20% early single support (Figure 5-17); the dynamic variability between 20% and 50% was greater (Figure 5-18) than during single-task walking.

Ankle Inversion/Eversion Moment

The most striking difference between P04 and other MTBI participants was seen in the ankle inversion/eversion joint moment. Results for the ankle inversion/eversion joint moment were presented in Figure 4-19 and Figure 4-20 for single-task walking, Figure 4-47 and Figure 4-48 for counting, and Figure 4-75 and Figure 4-76 for carrying. Joint moment trends for P04 were reduced and relatively constant compared to the other participants. P04 showed a greater joint moment range during single-task walking

(Figure 5-19), and individual dynamic variability was substantially greater than the normal population and other MTBI participants (Figure 5-20). The counting (Figure 5-21) and carrying (Figure 5-23) dual tasks produced similar ranges for P04 throughout single support. The counting task results showed that P04's dynamic variability (Figure 5-22) was closer in magnitude to the other participants between 20% and 50%. Between 50% and 80%, the dynamic variability of P04 was opposite in direction from and larger than all other participants. The carrying task results showed that the individual dynamic variability of P04 (Figure 5-24) was largest in magnitude of all participants; this was consistent with normal walking results.

Ground Reaction Forces

The AP GRF for P04 was reduced at load bearing, approximately 10% of the gait cycle, during single-task walking (Figure 4-24), and more noticeably reduced during dual-task counting (Figure 4-52) and dual-task carrying (4-80). P04 showed trends toward a greater peak vertical GRF than other MTBI participants at 20% and 50% of the gait cycle. GRF results were presented in Chapter 4 for single-task walking (Figure 4-28), counting (Figure 4-56), and carrying (Figure 4-84).

Table 5-1. Temporal and spatial parameters for P04 and the normal population average during single-task walking, dual-task counting, and dual-task carrying.

	Walking		Counting		Carrying	
	N avg	P04	N avg	P04	N avg	P04
Velocity (m/s)	1.37	1.20	1.36	1.02	1.35	1.16
Stride Length (m)	1.45	1.24	1.48	1.14	1.43	1.16
Stride Time (s)	1.06	1.04	1.09	1.11	1.06	1.01
Step Width (m)	0.121	0.078	0.116	0.078	0.110	0.079
Step Height (m)	0.058	0.050	0.058	0.056	0.053	0.054

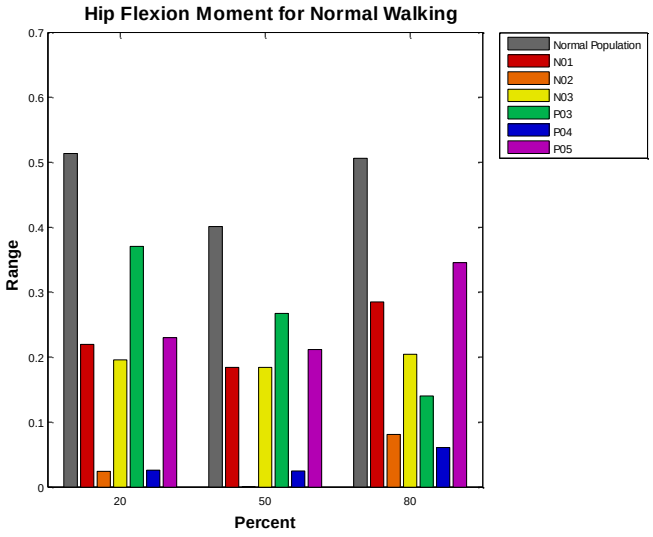

Figure 5-1. Range of hip flexion/extension joint moment of the normal population and individual participants during single-support walking.

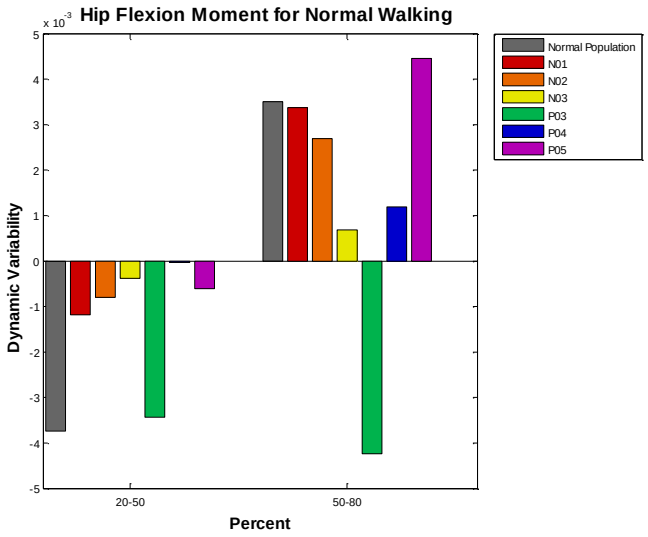

Figure 5-2. Dynamic variability of hip flexion/extension joint moment of the normal population and individual participants during single-support walking.

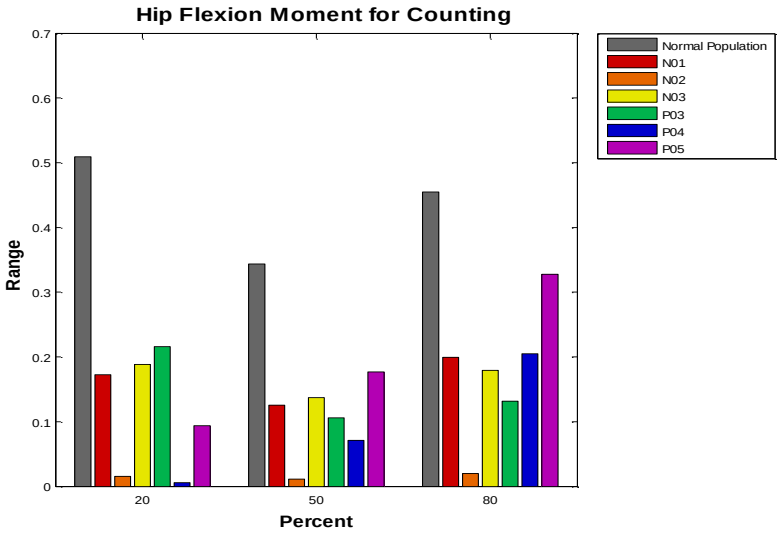

Figure 5-3. Range of hip flexion/extension joint moment of the normal population and individual participants during single-support counting.

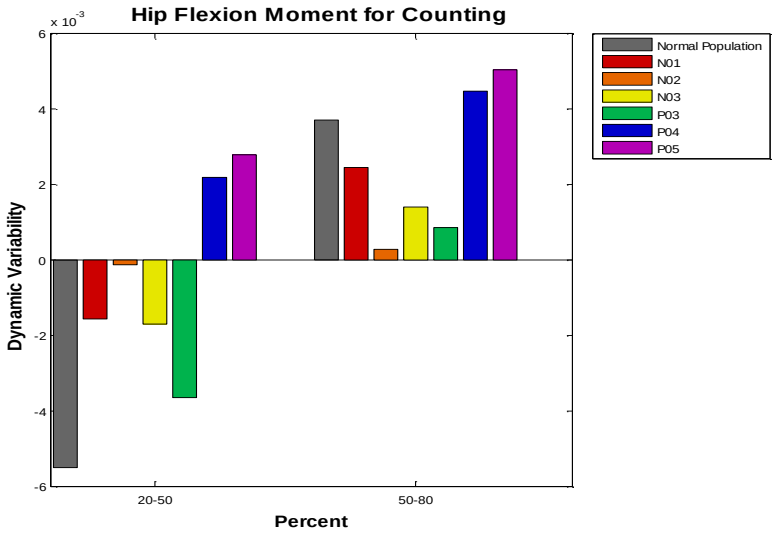

Figure 5-4. Dynamic variability of hip flexion/extension joint moment of the normal population and individual participants during single-support counting.

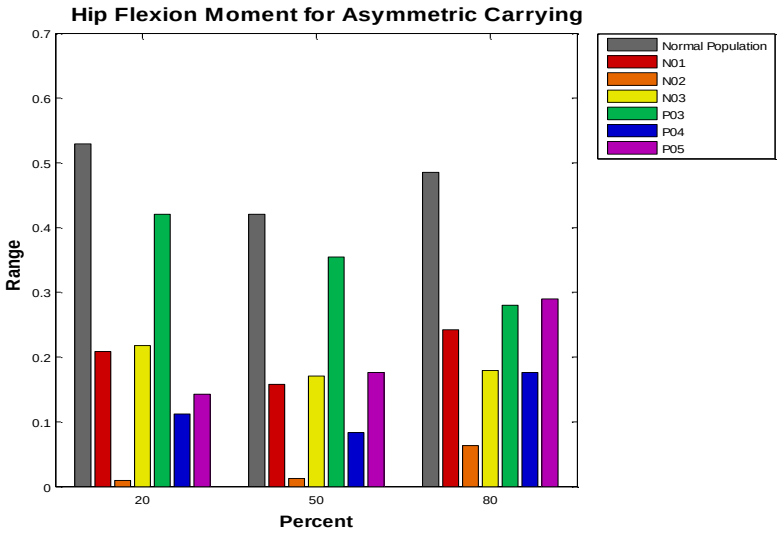

Figure 5-5. Range of hip flexion/extension joint moment of the normal population and individual participants during single-support carrying.

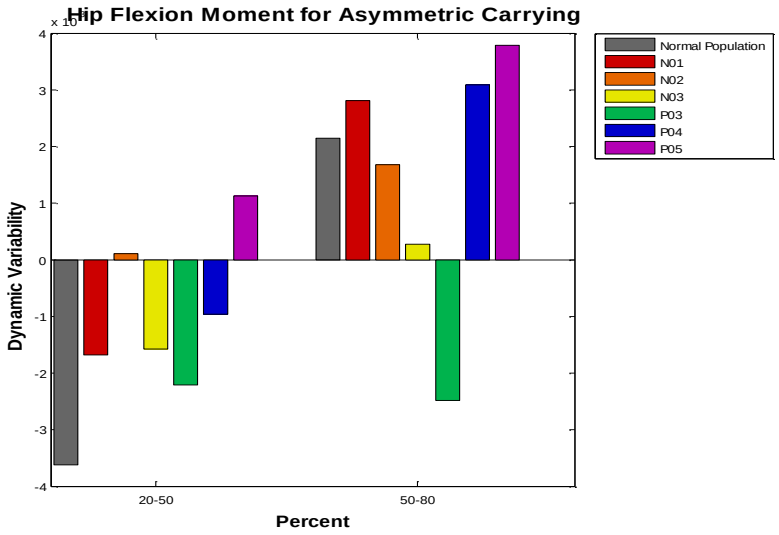

Figure 5-6 Dynamic variability of hip flexion/extension joint moment of the normal population and individual participants during single-support carrying.

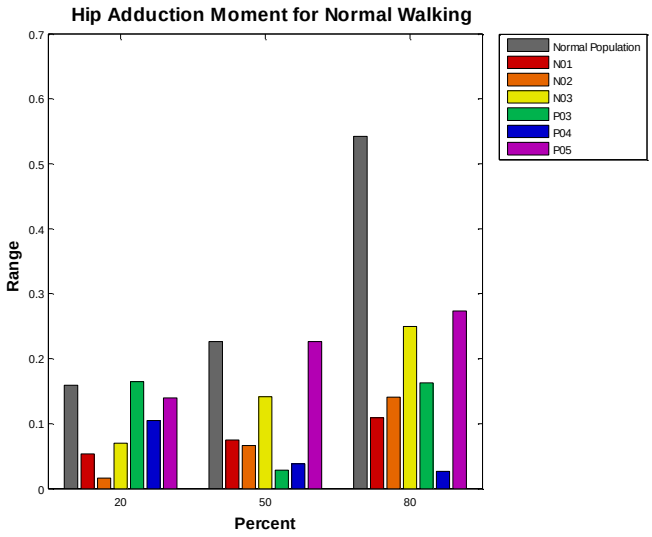

Figure 5-7. Range of hip adduction/abduction joint moment of the normal population and individual participants during single-support walking.

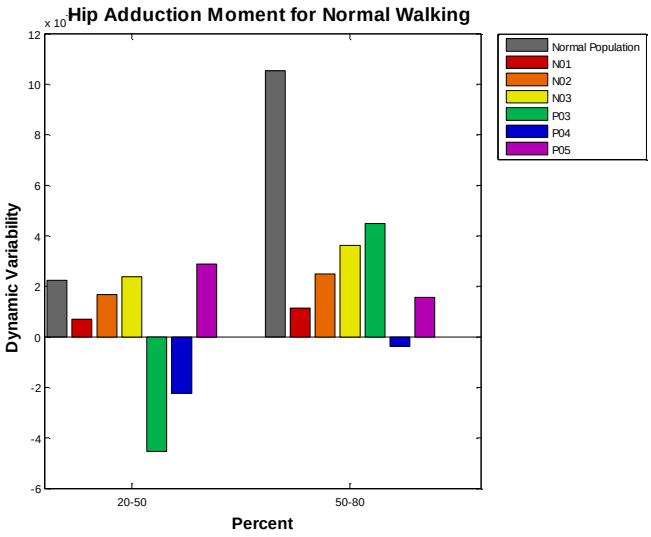

Figure 5-8. Dynamic variability of hip adduction/abduction joint moment of the normal population and individual participants during single-support walking.

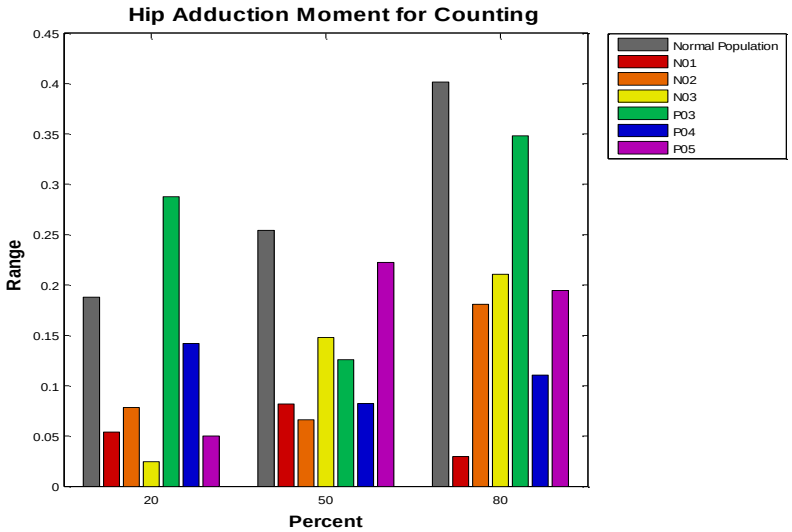

Figure 5-9. Range of hip adduction/abduction joint moment of the normal population and individual participants during single-support counting.

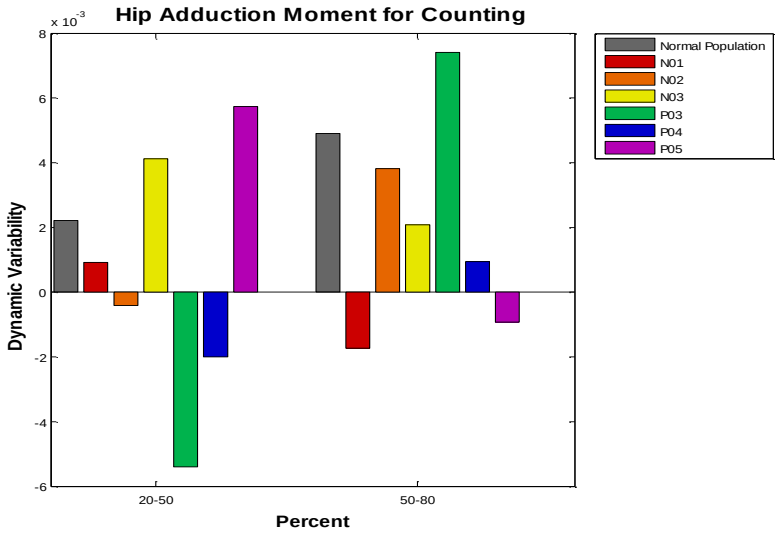

Figure 5-10. Dynamic variability of hip adduction/abduction joint moment of the normal population and individual participants during single-support counting.

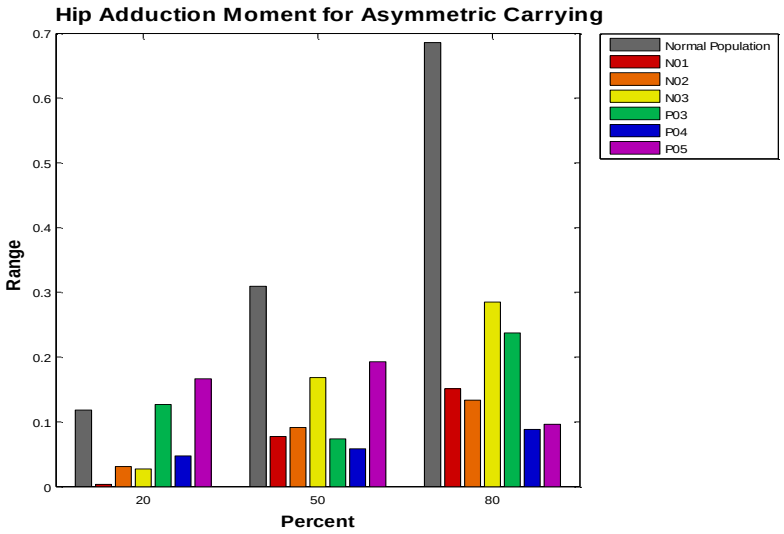

Figure 5-11. Range of hip adduction/abduction joint moment of the normal population and individual participants during single-support carrying.

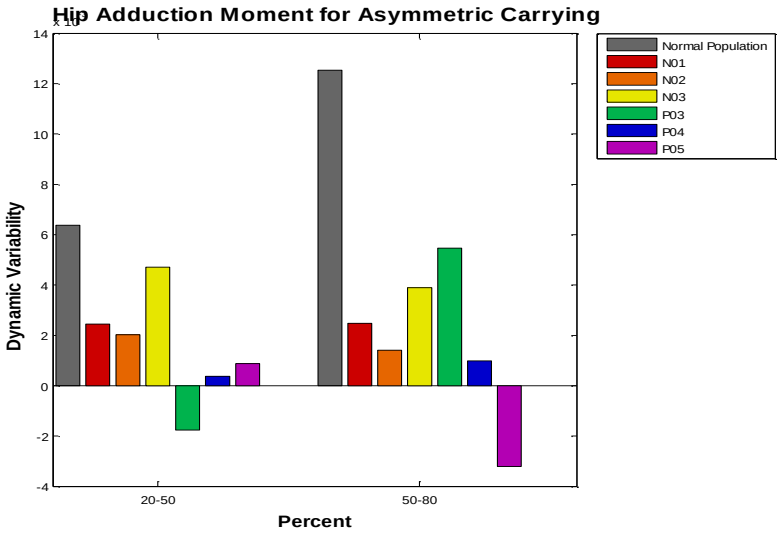

Figure 5-12. Dynamic variability of hip adduction/abduction joint moment of the normal population and individual participants during single-support carrying.

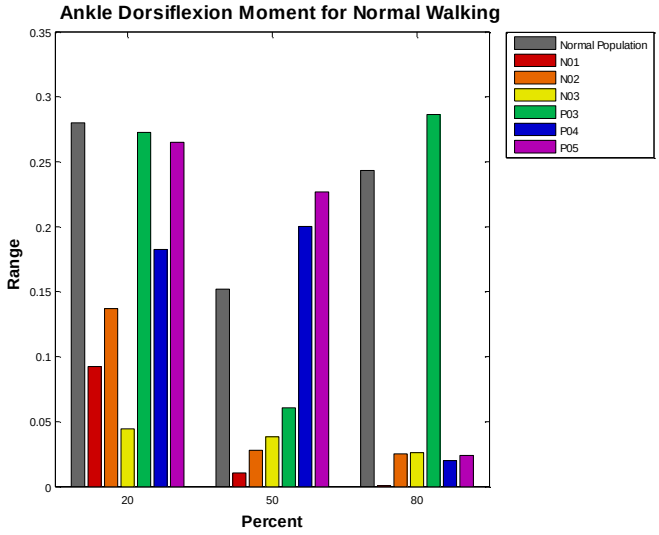

Figure 5-13. Range of ankle dorsiflexion/plantar flexion joint moment of the normal population and individual participants during single-support walking.

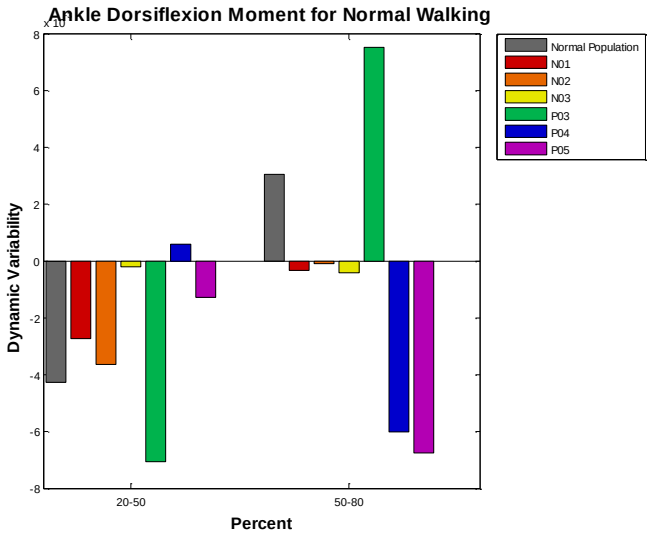

Figure 5-14. Dynamic variability of ankle dorsiflexion/plantar flexion joint moment of the normal population and individual participants during single-support walking.

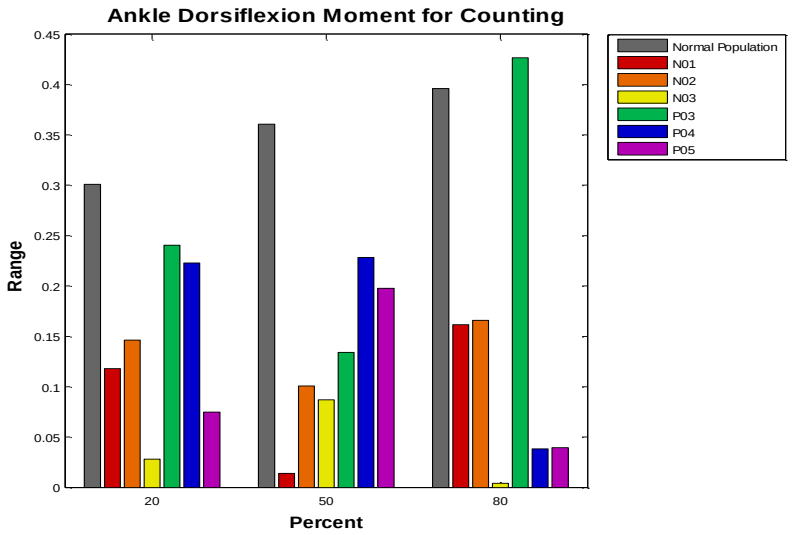

Figure 5-15. Range of ankle dorsiflexion/plantar flexion joint moment of the normal population and individual participants during single-support counting.

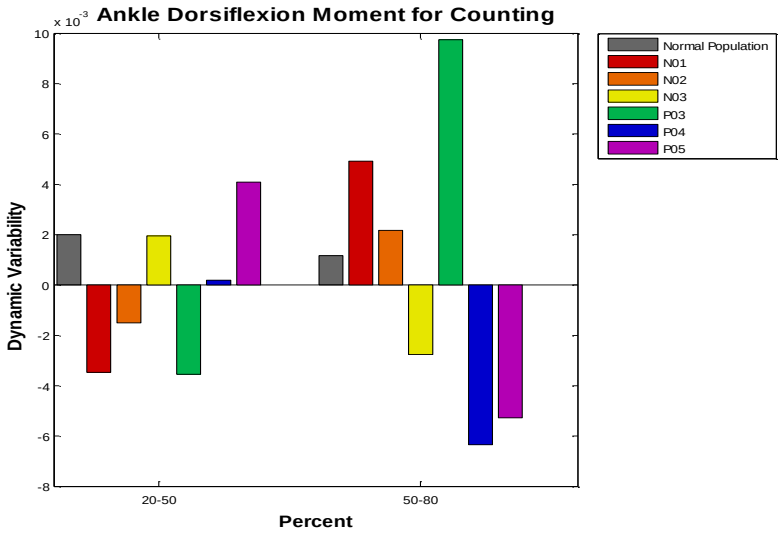

Figure 5-16. Dynamic variability of ankle dorsiflexion/plantar flexion joint moment of the normal population and individual participants during single-support counting.

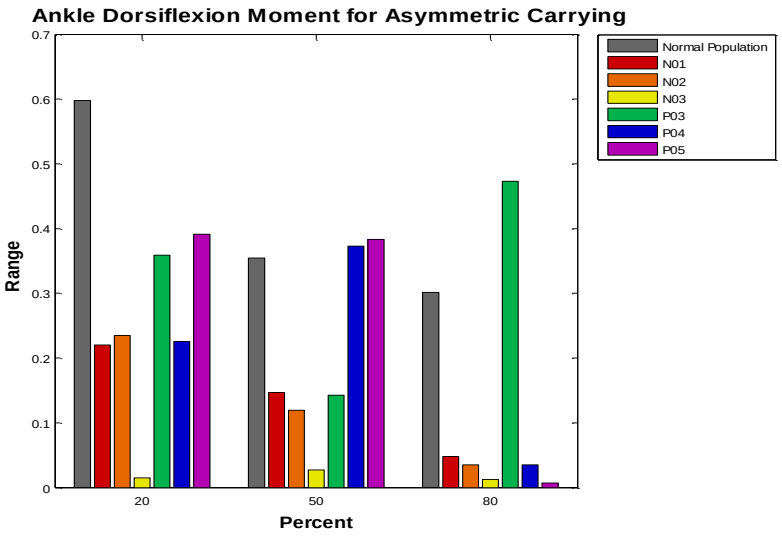

Figure 5-17. Range of ankle dorsiflexion/plantar flexion joint moment of the normal population and individual participants during single-support carrying.

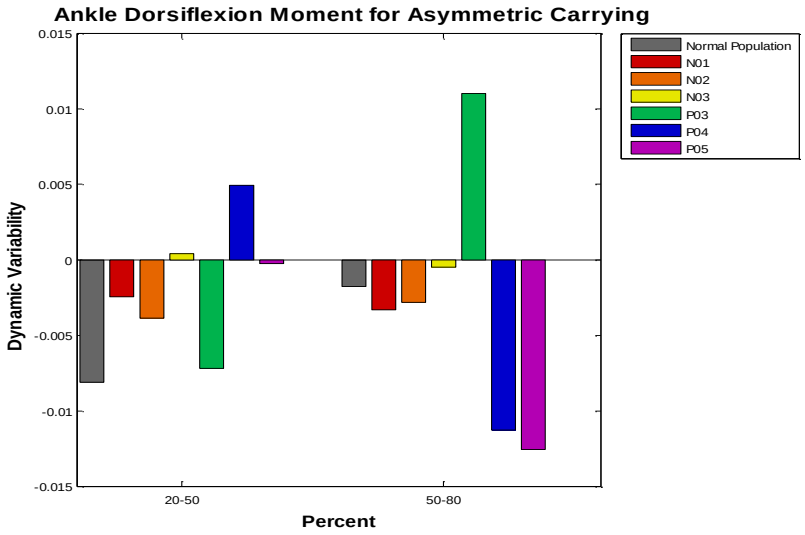

Figure 5-18. Dynamic variability of ankle dorsiflexion/plantar flexion joint moment of the normal population and individual participants during single-support carrying.

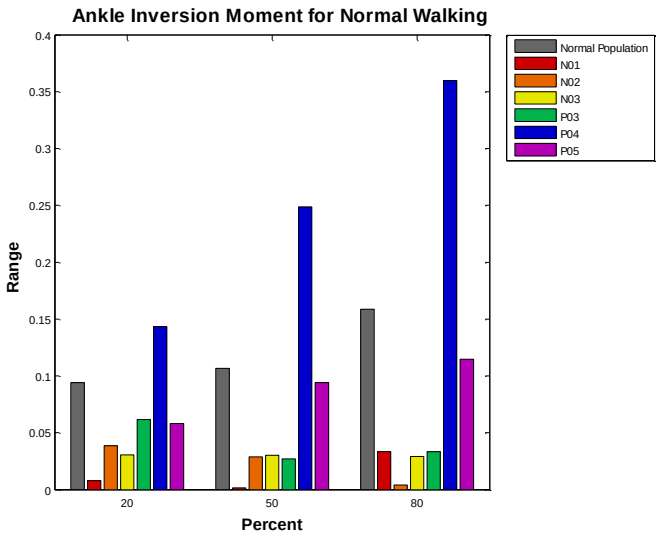

Figure 5-19. Range of ankle inversion/eversion joint moment of the normal population and individual participants during single-support walking.

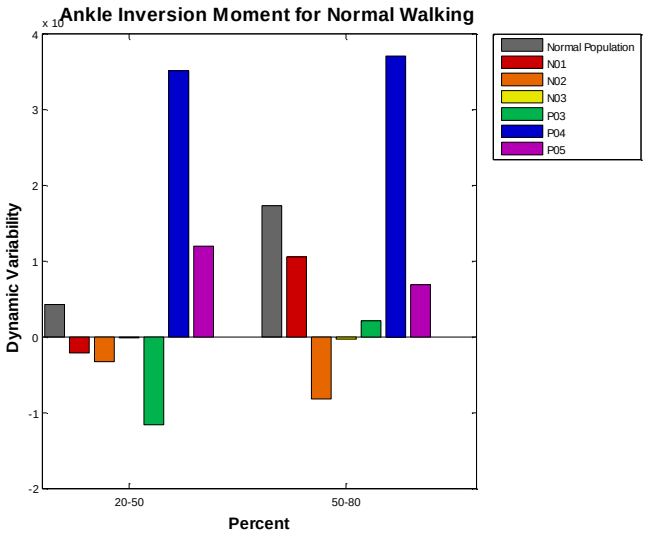

Figure 5-20. Dynamic variability of ankle inversion/eversion joint moment of the normal population and individual participants during single-support walking.

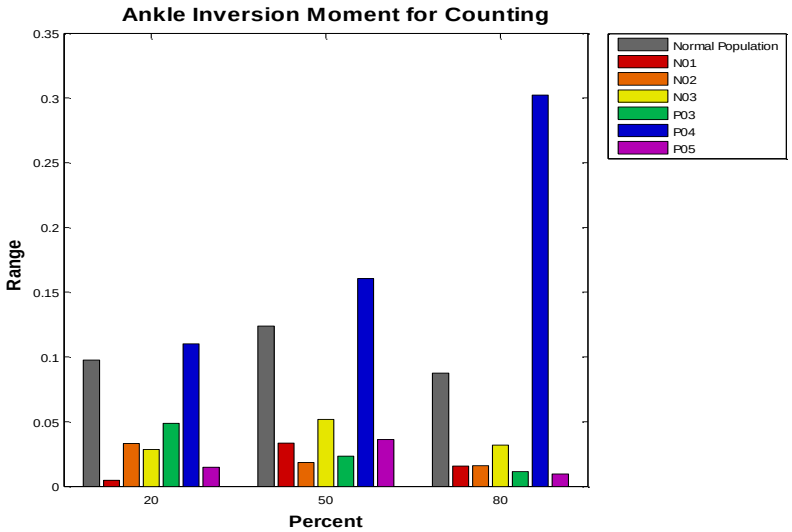

Figure 5-21. Range of ankle inversion/eversion joint moment of the normal population and individual participants during single-support counting.

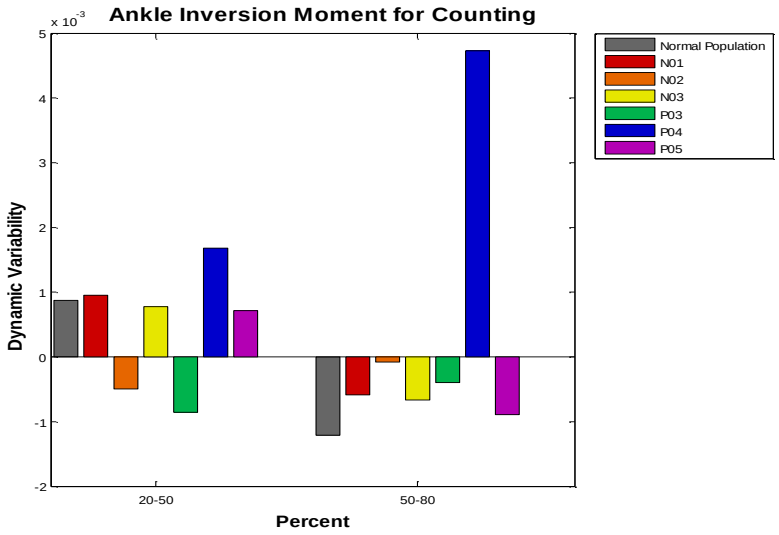

Figure 5-22. Dynamic variability of ankle inversion/eversion joint moment of the normal population and individual participants during single-support counting.

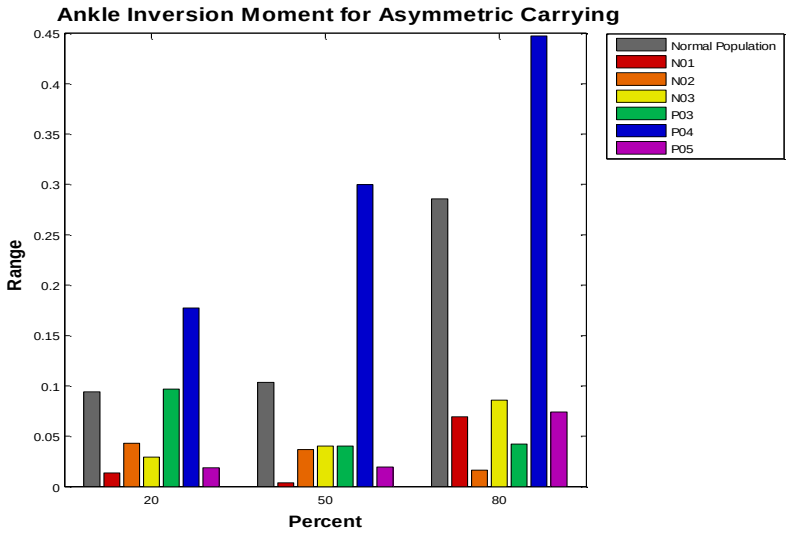

Figure 5-23. Range of ankle inversion/eversion joint moment of the normal population and individual participants during single-support carrying.

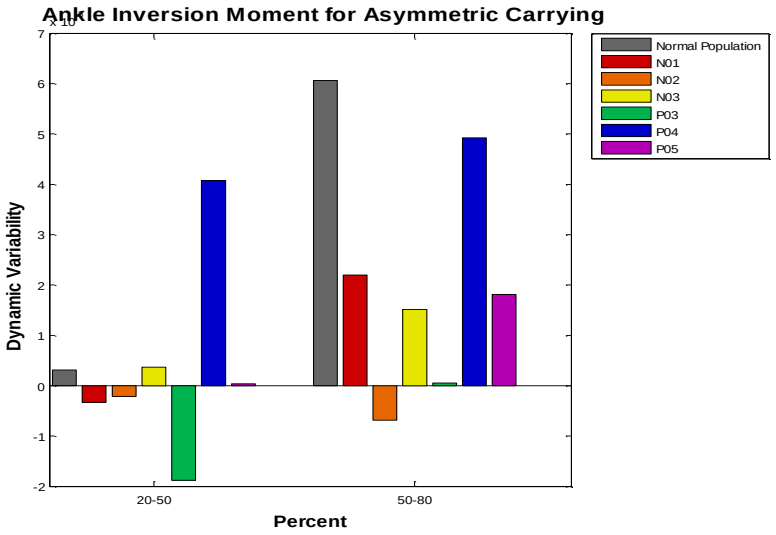

Figure 5-24. Dynamic variability of ankle inversion/eversion joint moment of the normal population and individual participants during single-support carrying.

CHAPTER 6

DISCUSSION

In spite of the relatively small number of patients considered in this work, the results of this work are consistent with the literature in terms of the temporal and spatial gait parameters of MTBI subjects; moreover, this study has added a new variable, the concept of dynamic variability, to the evaluation of MTBI patients.

The temporal and spatial results of single-task walking, as shown in Table 4-2, demonstrate that MTBI patients have reduced gait speed, shortened stride length, and larger step width, similar to prior MTBI studies. These characteristic gait changes reflect caution [29]. Furthermore, the reduced gait speed has also been reported in other patient populations, notably in the elderly, where there is dysfunction in the frontal-subcortical white matter connections [14]. Therefore, a preliminary finding of this study is that the cautious quality of the gait in MTBI subjects is the result of subtle dysfunction in the frontal lobe and its cortical and subcortical white matter tracts connections. This is supported by two lines of evidence: i) MTBI subjects have executive (frontal lobe) dysfunction on cognitive testing [15], and ii) the findings that MTBI subjects have subtle disruption in major white matter tracts as measured by the new technique of Magnetic Resonance Imaging with Diffusion Tensor Imaging, MRI-DTI [26]. In this study, we performed MRI-DTI analysis of the white matter tracts, but the number of subjects was too small to detect the subtle white matter tracts dysfunction. A recent MRI-DTI study of 25 MTBI Iowa City veteran patients (i.e., same population pool as our patients) has confirmed disruption in major white tracts (personal communication, Dr. Jinsuh Kim, University of Iowa).

The second major and novel finding of the study is that MTBI patients had gait variability in moments of their hip and ankle joints. This is a new concept in gait analysis in general and in MTBI patients in particular. Prior studies of gait variability have been

limited to elderly patients and limited to analysis of stride-to-stride variability. These studies in elderly patients have found that stride-to-stride variability correlated with risk of falls [22,43].

Thus, the measurement of joint moments in MTBI is novel; furthermore, the findings that MTBI patients have variable joint moments is also novel. There is no study in the literature that focuses on quantifying and localizing the variability in the joint dynamics (joint motion and joint moments) during gait. The introduction of the concept of dynamic variability for populations and single subjects provides a very powerful tool to capture the variability in a gait parameter and correlate it with muscle activation and possibly brain activity. Further studies will be needed to assess the relationship of gait variability to increased fall risk.

The results overall have shown that the MTBI population has greater variability in their gait measures compared to the normal population. While the normal population does show variability, even when a single subject performs repetitions of a single task, this variability is relatively small compared to the patient population. For example, Figure 4-11 and Figure 4-12 show the hip adduction moment for the normal and patient populations during single-task walking. It is clear from Figure 4-12 that the variability in the range of joint moments for the patients is greater than that of the controls in Figure 4-11 where the normal population shows tighter trends, especially in the first half of single support.

In general terms, one can notice the variability and the trend of the gait parameters in MTBI patients during both single- and dual-task walking; however, due to the small sample size, it is difficult to identify consistent changes using currently available statistical tools. The variability differs from joint to joint and occurs at different times during the gait cycle, such that it becomes very difficult to infer more specific information. Therefore, this work introduced the concept of dynamic variability to localize the variability in the gait parameters at different locations in the gait cycle, and to

quantify the range in the variability at a certain time in the cycle. Further work will be needed to study the relationship between gait variability, as well as the rate of change of this variability and its relationship to the rate of muscle activations and more generally central (brain) commands.

One issue with human gait is the large number of parameters (degrees of freedom) that play a role in balance and stability. However, the amount of data can be reduced by considering parameters that play a larger role than others. For example, according to the literature [47], people use two strategies for their balance and stability during upright posture. One is based on motion of the hip joint, and the other is based on motion of the ankle joint. During gait, the hip flexors/extensors and abductors/adductors control stability in the AP and ML directions, respectively. The ankle dorsiflexors/plantar flexors and invertors/evertors have fine control of the COM acceleration in the AP and ML directions [47]. Based on that, the current work focused on the hip and ankle as two main parameters to discuss the proposed concept of dynamic variability.

The dynamic variability results of the hip adduction joint moment during single-task walking (Figure 4-14) identify differences in how the variability changes immediately following the beginning of single support. The range results in Figure 4-13 show that the normal population range decreases at the beginning of single support and remains small through mid stance. The MTBI population range increases and remains larger during this same time. These observations quantify and locate the tighter trends of the normal population in Figure 4-11 and the greater variability of the MTBI population Figure 4-12. The hip adduction joint moment controls stability in the ML direction and may relate to other motions and force occurring in the ML direction.

Characteristics of the ankle dorsiflexion/plantar flexion moment are similar to those discussed for the hip adduction/abduction joint moment but take place at a later time in the single-support phase. During single-task walking, the normal participants show some variability between repetitions of a single subject and between subjects

(Figure 4-15), but the variability of the patients is greater (Figure 4-16). Dynamic variability captures this variability in Figure 4-18. Dynamic variability is opposite in magnitude and substantially greater in the MTBI population during early and mid single support. The range results in Figure 4-17 have shown a decrease in the normal population as the joint moment trends become tighter until after mid stance at 70% of the single-support phase.

The ankle dorsiflexion moment plays a role in the initial loading response and single-support phase of the gait cycle and affects motion in the direction of progression. Single-task walking differences in the ankle dorsiflexion moment variability may indicate other problems in load bearing and sagittal plane motion.

The results for the GRF have also shown variability between the normal and MTBI populations. Referring to the single-task walking, results for ML GRF for the normal and MTBI populations are in Figure 4-25 and Figure 4-26, respectively, and show that normal participants have variability except between 20% and 30% of the gait cycle, which is immediately before and during mid stance. The trends of the patients show variability throughout the gait cycle, even during the critical mid stance phase.

For the kinematics of the whole-body motion represented by the motion of the COM, the results have shown no significant differences in ML COM acceleration between the normal and MTBI participants during single-task walking (Figure 4-6). However, MTBI participants walked at a slower speed with similar ML COM accelerations. Future work to normalize the data by gait velocity may reveal increased ML COM motion similar to results presented in the literature for MTBI patients [8,33].

Weight acceptance in the MTBI patients peaks at 100% BW following the initial loading response from 0-12%, as shown in Figure 4-28 for the vertical GRF. The normal participants show a quicker loading response with greater peak loading in Figure 4-27. A greater weight-bearing force was observed in patients at mid stance, 30% of the gait cycle. These abnormalities in load bearing disappear by terminal stance, 50% of the gait

cycle, and normal pre-swing forces are measured while the trail limb begins weight acceptance. Similar to the vertical GRF, the peak AP GRF for MTBI patients (Figure 4-24) is lower during weight acceptance compared to the normal participants (Figure 4-23). Although the AP GRF of patients is reduced at the beginning of single support; it correlates well with the controls following mid stance.

The AP COM acceleration is also reduced in patients following the loading response until mid stance (Figure 4-3). Peak acceleration is also reduced at terminal stance, 50%, and during push-off. The initial loading response and braking forces of MTBI patients is reduced compared to normal individuals, although differences are minimized by mid to terminal stance as the trail limb approaches heel strike and the subsequent load-bearing response.

In addition to quantifying and localizing differences in gait variability between two populations, dynamic variability also has the potential to investigate gait abnormality in a specific individual. For example, the individual range and dynamic variability of the hip adduction joint moment during single-task walking were presented in Figure 5-7 and Figure 5-8. P03 (green) had a greater range during early single support and a normal range at mid stance. The dynamic variability between those times from 20% to 50% revealed a faster rate of change in the wrong direction for P03. P05 (purple) had a greater range than normal participants and normal dynamic variability results. P04 (blue) showed a small range during mid and terminal stance with dynamic variability in the opposite direction. The ankle dorsiflexion moment results during single-task walking showed individual patient differences in range (Figure 5-13) and dynamic variability (Figure 5-14). All MTBI patients showed a greater range than normal during early single support. P03 (green) reduced his range by mid stance; the range of P04 (blue) and P05 (purple) was not reduced until terminal stance, where the range of P03 was greater once again. These different locations of variability were captured by the dynamic variability results in Figure 5-14.

It appears obvious from the latter paragraph that each patient has significant differences in their dynamic variability during single-task walking. The changes in dynamic variability of the gait joint moments during gait, which may reflect the changes in the muscle forces and muscle activation, and consequently changes in supraspinal (cortical and subcortical) commands, has great potential to be correlated to the neuromuscular and cerebral systems as mentioned previously in this chapter..

This study used a dual-task methodology in an attempt to magnify subtle abnormalities of the MTBI population. A number of cognitive and motor dual tasks were tested, and the results of two representative tasks were presented in Chapter 4. Counting backwards by a constant number was selected as the cognitive dual task. Other cognitive tests included digit span forward and digit span backward and showed similar effects in magnifying the gait variability. However, the counting task was selected for discussion purposes as a representative of these tasks because it is widely used in clinical testing. The results of the other cognitive tasks are presented in the appendices for future reference, though they are not discussed.

Counting while walking (cognitive dual-task walking) showed trends similar to single-task walking in variability of the hip adduction moment for normal participants in Figure 4-39 and for MTBI patients in Figure 4-40. The range (Figure 4-41) and dynamic variability (Figure 4-42) were similar to single-task walking as shown in Figure 4-13 and Figure 4-14, respectively. Counting magnified the range of the hip adduction moment for P03 (green in Figure 5-9) compared to single-task walking (Figure 5-7). It also affected the dynamic variability of P05 (purple in Figure 5-10) compared to single-task walking (Figure 5-8).

The ankle dorsiflexion moment showed increased variability in the normal population during cognitive dual-task walking (Figure 4-43) as compared to single-task walking (Figure 4-15). The MTBI population had greater variability than normal during single-task walking (Figure 4-16), and this holds for cognitive dual-task walking (Figure

4-44); however, a difference in trend is noted towards terminal stance at the end of single support. The differences in the dynamic variability shown during single-task walking (Figure 4-18) remain between the populations during cognitive dual-task walking (4-46). The increased variability in the normal population is shown in the individual dynamic variability results presented in Chapter 5 in Figure 5-16. P05 (purple) has a smaller range during the cognitive dual-task (Figure 5-15) than single-task walking (Figure 5-13), which affects the dynamic variability in early to mid single support (Figure 5-16) compared to walking (Figure 5-14).

A striking difference between cognitive dual- versus single-task walking was shown in the GRF measures. The vertical GRF for the normal participants during cognitive dual-task walking (Figure 4-55) showed less variability than during single-task walking (Figure 4-27). In addition, the slower and reduced initial peak loading in the MTBI population during single-task walking (Figure 4-28) is magnified during cognitive dual-task walking (Figure 4-56). The effects on AP GRF during single-task walking (Figure 4-23 and Figure 4-24) are also magnified for the normal (Figure 4-51) and MTBI (Figure 4-52) populations during the cognitive dual task. The MTBI patients land with decreased AP force during the initial loading response. Also, during the counting dual task, patients push off with reduced AP GRF later in the gait cycle. The reduced velocity of patients during counting (Table 4-4) may contribute to some of these differences; the normal population did not reduce their velocity compared to single-task walking (Table 4-2). The ML GRF of the normal population was tight at 30% mid stance during single-task walking (Figure 4-25), which was not the case during counting (Figure 4-53). The dual task increased variability of the controls; the MTBI patients showed variability during counting (Figure 4-54), but this was also seen during single-task walking (Figure 4-26).

Asymmetric carrying was selected as the motor dual-task walking because of its practicality and occurrence in daily activity. Symmetric carrying and obstacle crossing

were also tested as motor dual tasks; however, they have large-scale effects on gait patterns and were not discussed. The results for symmetric carrying are presented in the appendices, and the obstacle-crossing results are not considered in this work.

The asymmetric carrying motor dual task increased normal variability (Figure 4-67) from single-task walking (Figure 4-11), particularly for one participant. The range of the MTBI population was reduced in the last half of single support (Figure 4-69) compared to single-task walking (Figure 4-13). The individual dynamic variability results of carrying (Figure 5-12) were similar to walking results shown in Figure 5-8. For the most part, the patients' dynamic variability was closer to the normal population during carrying.

Carrying also produced changes similar to those of counting on the ankle dorsiflexion moment. The normal population had greater variability (Figure 4-71). The trend of the patients (Figure 4-72) more closely matched normal participants, as seen in the range results in Figure 4-73. The dynamic variability during carrying (Figure 4-74) of the MTBI population followed the normal population better except in terminal stance. MTBI individual trends for range and dynamic variability during single-task walking (Figure 5-13 and Figure 5-14) are preserved during carrying and magnified (Figure 5-17 and Figure 5-18).

During carrying, the vertical GRF trends of the MTBI population (Figure 4-84) differed from the normal population (Figure 4-83). This was also shown during single-task walking (Figure 4-27 and Figure 4-28). The MTBI patients had lower peak loading, which was delayed following the initial loading response. The delay was magnified during carrying. The vertical GRF during mid stance was greater in patients than controls. At 50% of the gait cycle, as the trail limb contacts the ground, patients had reduced vertical force with slight peak delay that resulted in later push-off. The AP GRF results for carrying (Figure 4-79 and Figure 4-80) did not differ from single-task walking (Figure 4-23 and Figure 4-24). Patients had reduced peak AP force during loading, but

the difference from the normal participants was minimized by mid stance at 30% of the gait cycle. The majority of MTBI patients measured ML GRF just greater than the normal population average (Figure 4-82). The normal participants were not grouped as closely at mid stance during carrying (Figure 4-81) as they were during single-task walking (Figure 4-25).

In this work, the concept of magnifying the gait variability using a dual task was presented using two dual-task testing scenarios. The first one, counting while walking, was designed to capture the effect of mental tasks on magnifying variability in gait. This may help clinicians if abnormality is found during clinical cognitive testing. The second dual task, asymmetric loading, was designed to work against the motor system of the subject by generating asymmetric loading on the joints and muscles. This test has a potential to capture weaknesses at the muscle levels and asymmetries in gait and to correlate with the magnitude and the speed of muscle recruitment at each joint.

In this work, the dynamic variability analysis was applied to selected joint moments at subjectively chosen times during the single-support phase. However, the methodology provides a tool that can be used to evaluate other gait measures and that can be expanded to the entire gait cycle. Times of interest may be selected based on subjective analysis of the joint or gait measure of interest. In addition, these techniques may be applied to other individuals or patient populations known to experience gait instability or to exhibit subtle gait abnormalities.

Dynamic variability may contribute to the identification of gait abnormalities in cases where data is available only for a small population and statistical methods are not as meaningful. It may also play a role when abnormalities in the patient population of interest are manifested differently in individuals. Then the unique gait variability of an individual may not be captured by the population as a whole.

CONCLUSION

The major contribution of this work is the introduction of a tool to quantify, localize, and show the rate of change of gait variability. This tool, termed dynamic variability, is a new concept developed to capture variability in a small population of chronic MTBI patients who have gait parameters consistent with those present in the literature. Dynamic variability may potentially be correlated to neuromuscular function and provide important information about muscle activation and muscle forces acting on the joints. The results of dynamic variability indicate that slow motion and instability persist following MTBI.

The results of this work, in terms of temporal and spatial parameters, were very similar to those published, in spite of the small number of participants, so the data is considered trustworthy for making analysis and conclusions.

Clinical MRI and gait evaluations do not show abnormalities in MTBI patients with persistent complaints of dizziness. Research imaging using MRI-DTI has shown abnormality in the major white matter tracts of the patient pool considered. White matter tracts dysfunction is presumably related to slow central commands. This is consistent with the findings of gait analysis performed using motion capture technology which have shown slow and delayed motion in the kinetic gait measures of MTBI patients, as well as increased joint moment variability.

APPENDIX A

DUAL-TASK DIGIT SPAN FORWARD

During the digit span forward test, a cognitive dual task, participants were given a series of numbers and asked to repeat them back to the study coordinator. The series of numbers was increased from three to nine digits. The numbers one through nine were used with each number appearing only once in a series. Two sequences were given for each number of digits. One of the two sequences had to be repeated correctly to proceed with the next number of digits. The maximum number of digits repeated correctly was considered a metric. An example of a five digit series of numbers is 7 3 9 5 2.

Table A-1. Number of digits repeated correctly at baseline and during dual-task digit span forward walking.

	# Digits Correct	
	Baseline	Walking
N01	8	5
N02	8	6
N03	8	8
P03	8	9
P04	6	4
P05	9	8

Table A-2. Temporal and spatial parameters of the digit span forward task.

	Velocity (m/s)	Stride Length (m)	Stride Time (s)	Step Width (m)	Step Height (m)
N01	1.32	1.44	1.09	0.067	0.063
N02	1.54	1.51	0.98	0.135	0.047
N03	1.26	1.44	1.15	0.127	0.063
N Avg	1.37	1.46	1.07	0.110	0.058
P03	1.23	1.48	1.20	0.134	0.057
P04	1.03	1.15	1.12	0.090	0.055
P05	1.06	1.19	1.13	0.164	0.050
P Avg	1.11	1.27	1.15	0.129	0.054

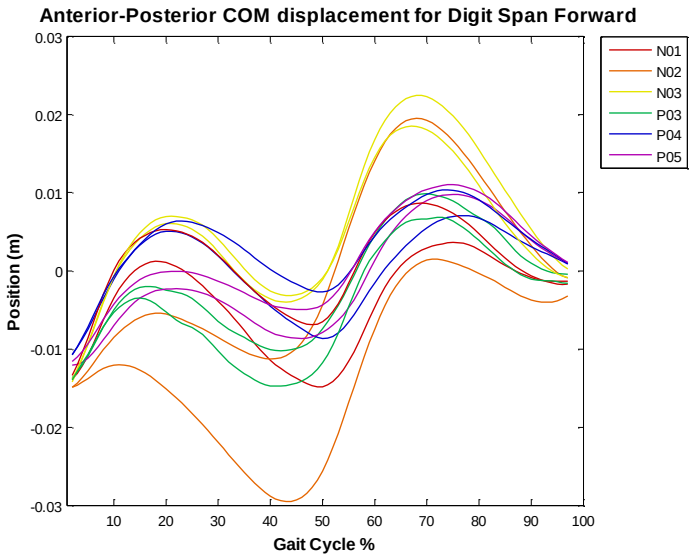

Figure A-1. AP COM displacement during dual-task digit span forward.

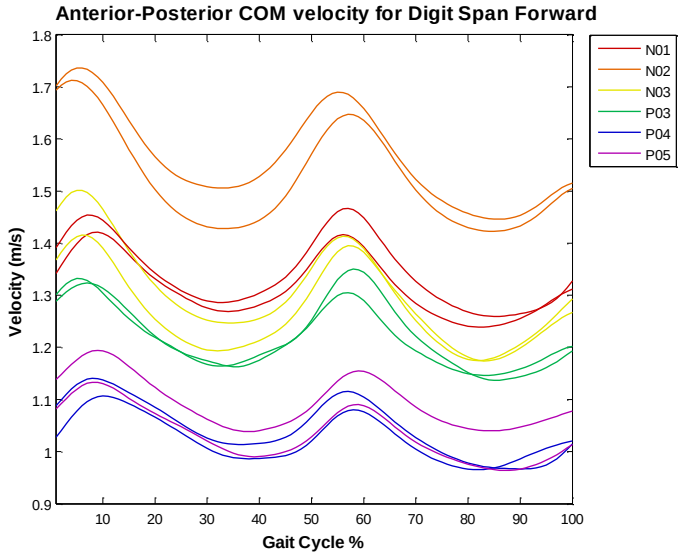

Figure A-2. AP COM velocity during dual-task digit span forward.

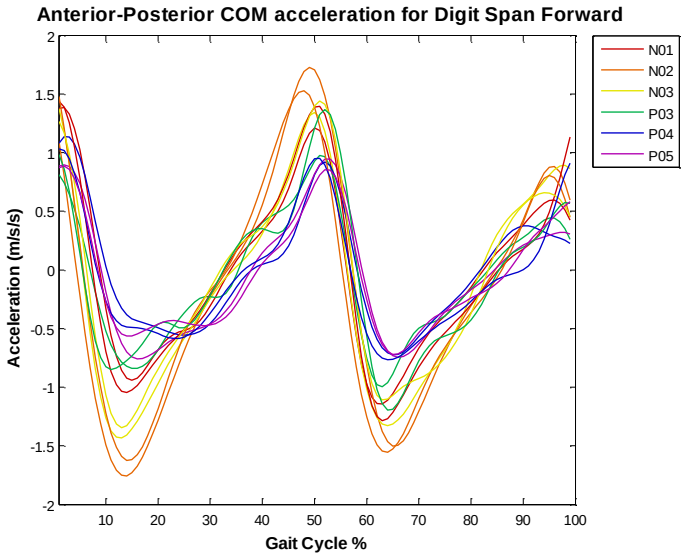

Figure A-3. AP COM acceleration during dual-task digit span forward.

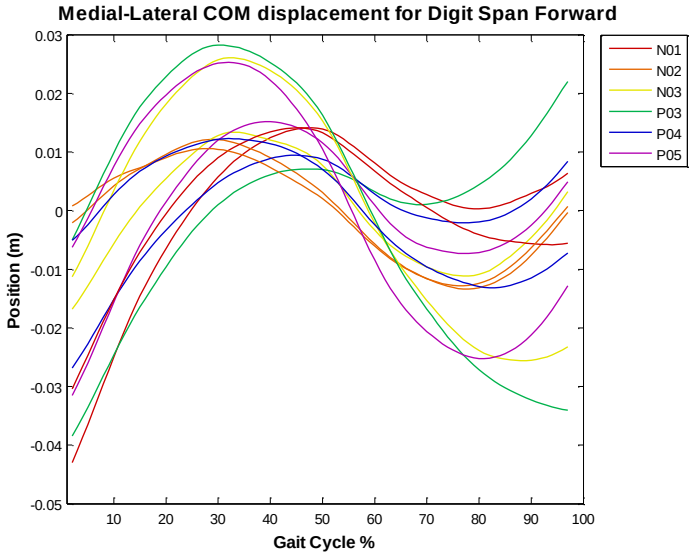

Figure A-4. ML COM displacement during dual-task digit span forward.

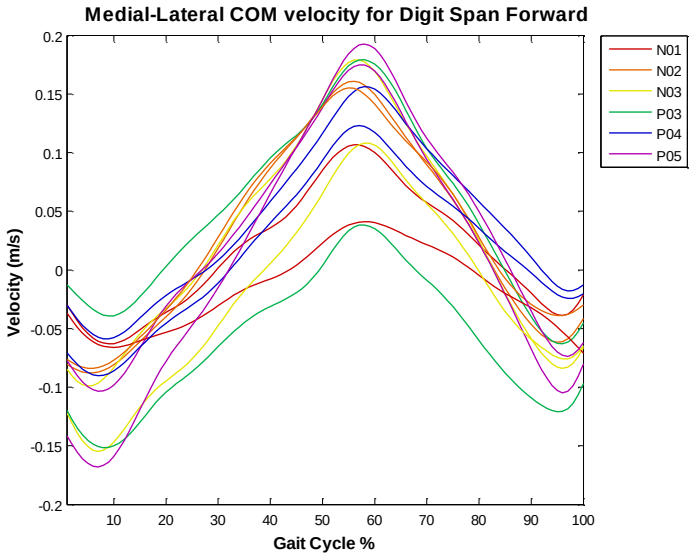

Figure A-5. ML COM velocity during dual-task digit span forward.

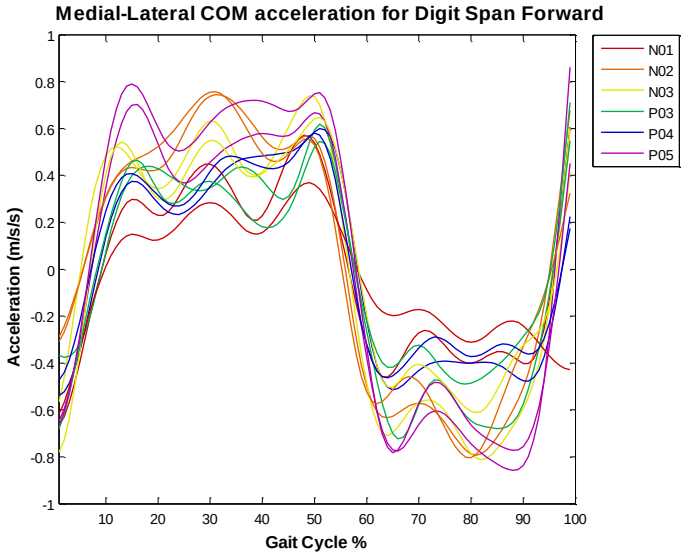

Figure A-6. ML COM acceleration during dual-task digit span forward.

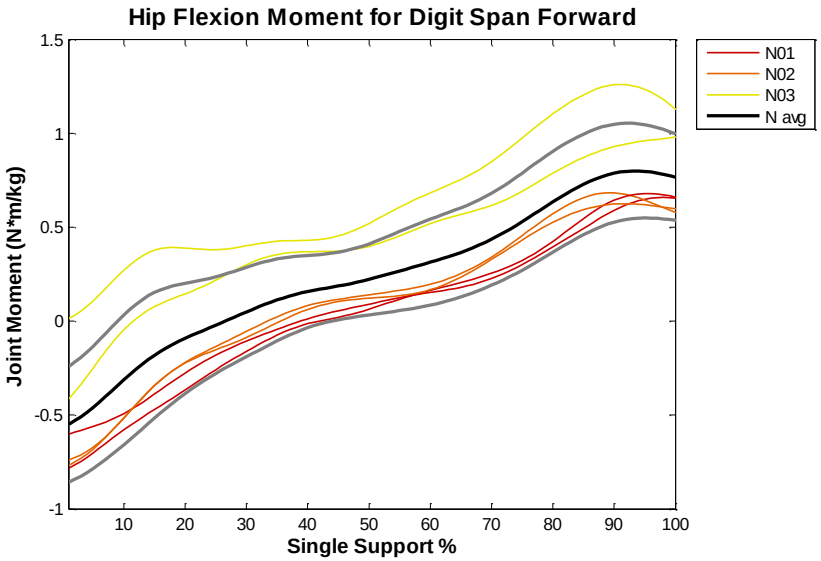

Figure A-7. Hip flexion/extension joint moment of normal participants during dual-task digit span forward.

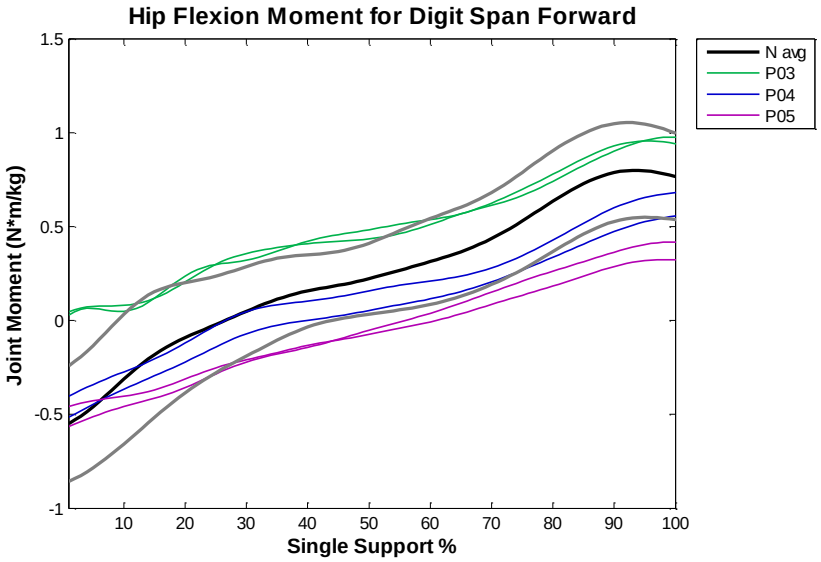

Figure A-8. Hip flexion/extension joint moment of MTBI participants during dual-task digit span forward.

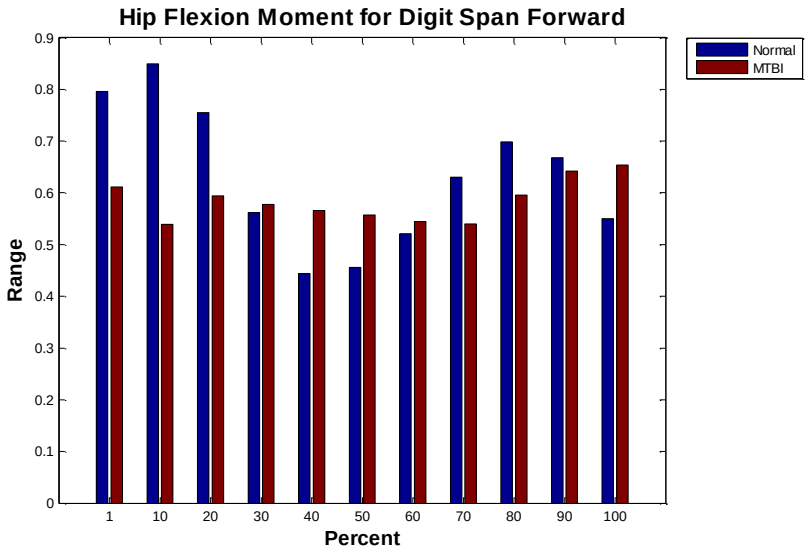

Figure A-9. Range of hip flexion/extension joint moment of the normal and MTBI populations during single-support digit span forward.

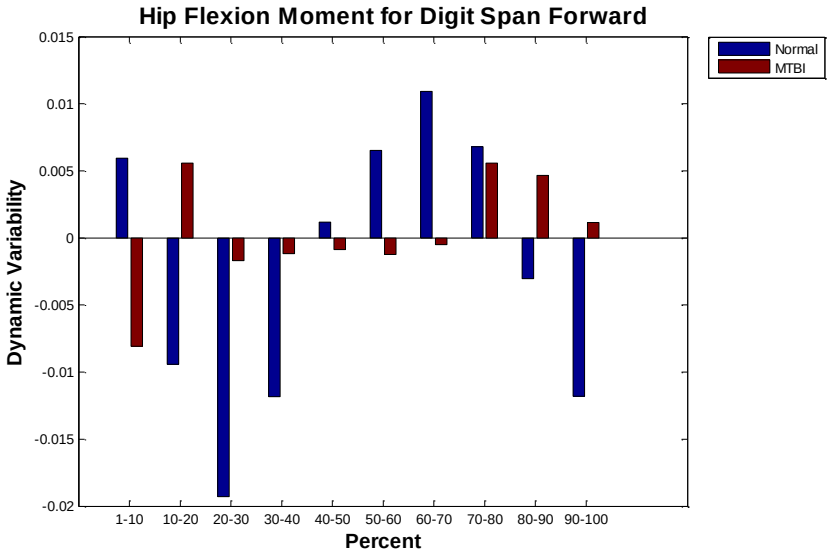

Figure A-10. Dynamic variability of hip flexion/extension joint moment of the normal and MTBI populations during single-support digit span forward.

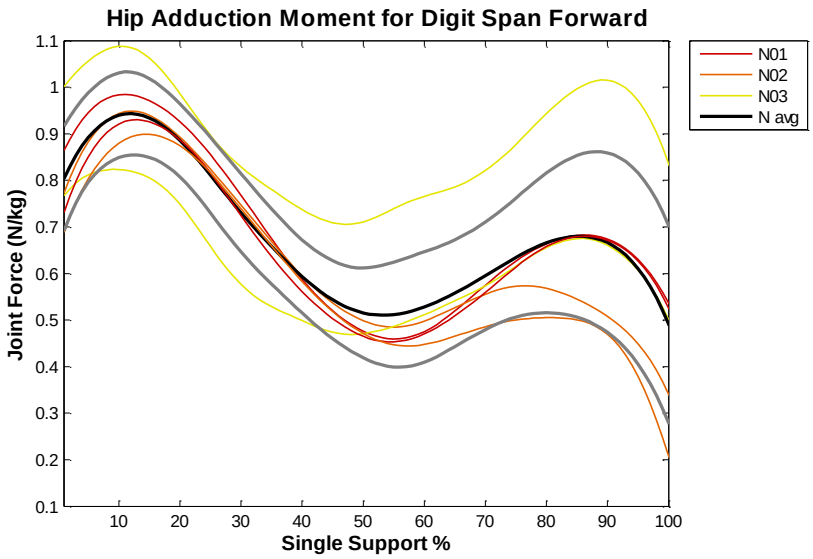

Figure A-11. Hip adduction/abduction joint moment of normal participants during dual-task digit span forward.

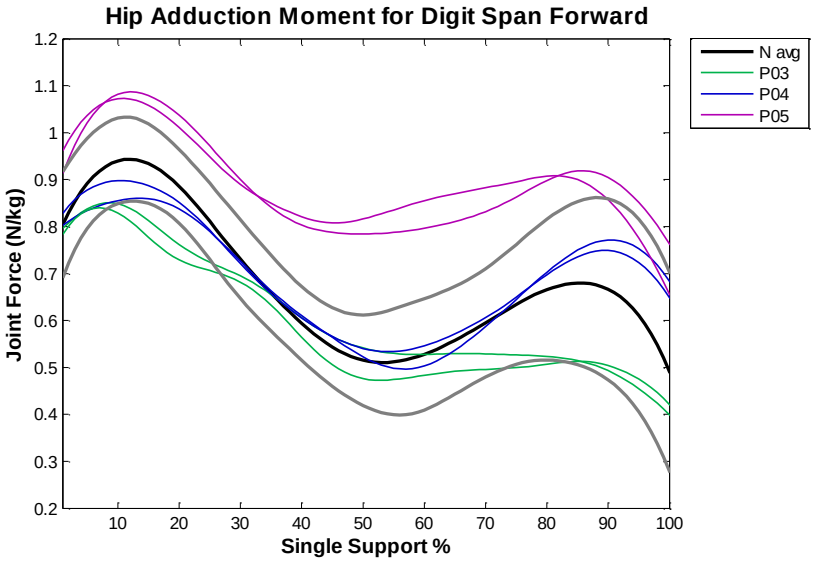

Figure A-12. Hip adduction/abduction joint moment of MTBI participants during dual-task digit span forward.

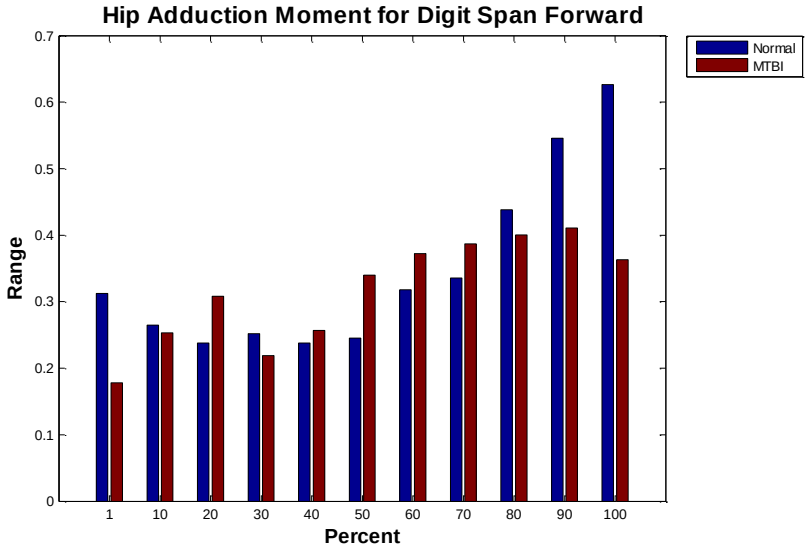

Figure A-13. Range of hip adduction/abduction joint moment of the normal and MTBI populations during single-support digit span forward.

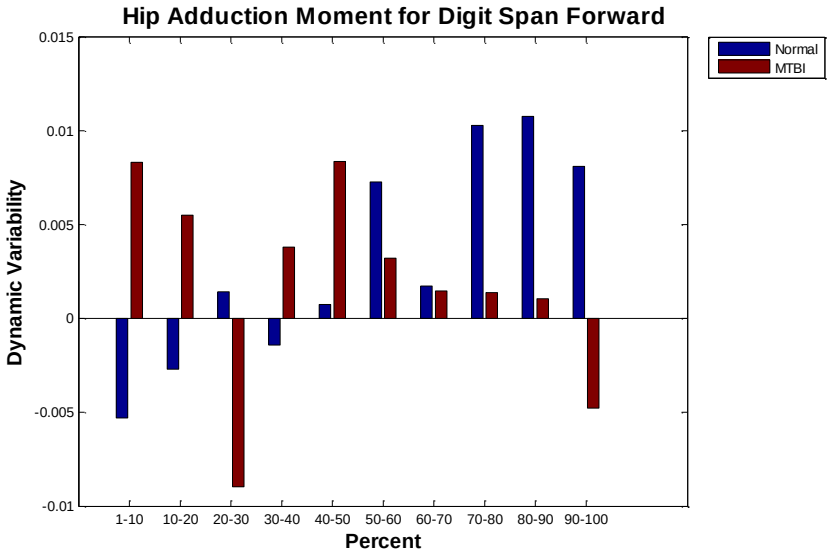

Figure A-14. Dynamic variability of hip adduction/abduction joint moment of the normal and MTBI populations during single-support digit span forward.

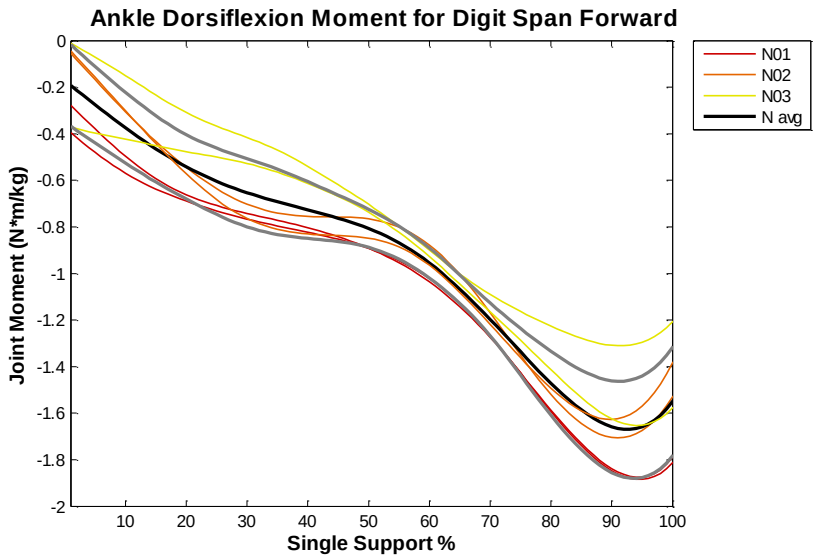

Figure A-15. Ankle dorsiflexion/plantar flexion joint moment of normal participants during dual-task digit span forward.

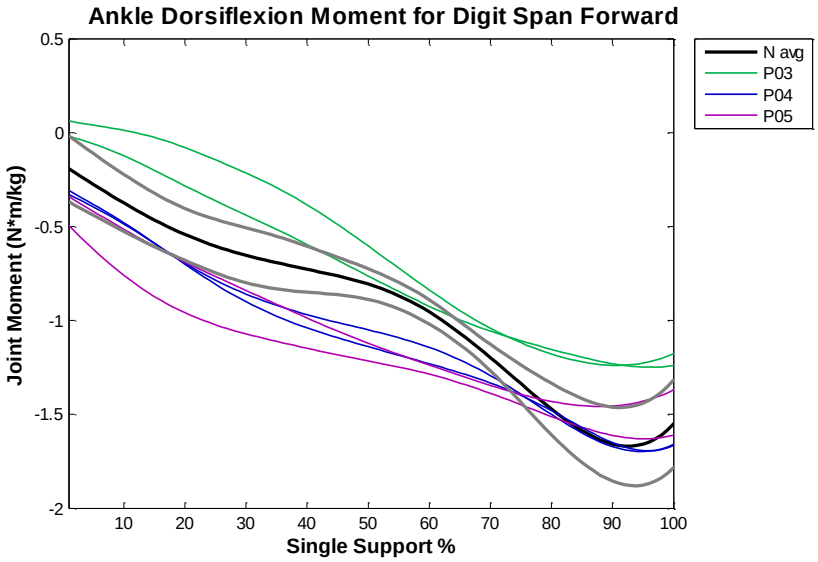

Figure A-16. Ankle dorsiflexion/ plantar flexion joint moment of MTBI participants during dual-task digit span forward.

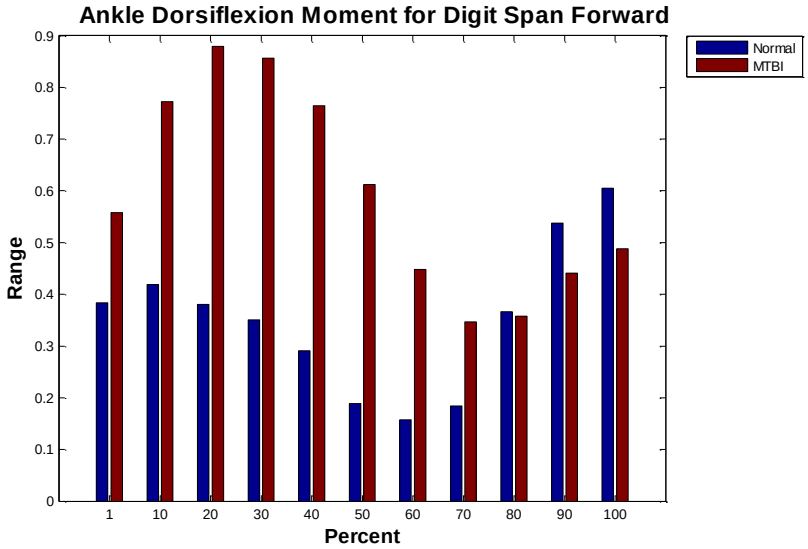

Figure A-17. Range of ankle dorsiflexion/plantar flexion joint moment of the normal and MTBI populations during single-support digit span forward.

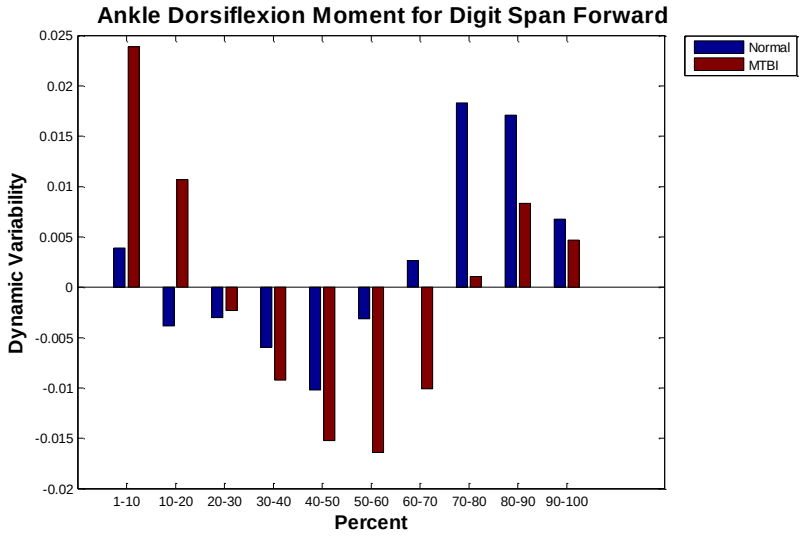

Figure A-18. Dynamic variability of ankle dorsiflexion/plantar flexion joint moment of the normal and MTBI populations during single-support digit span forward.

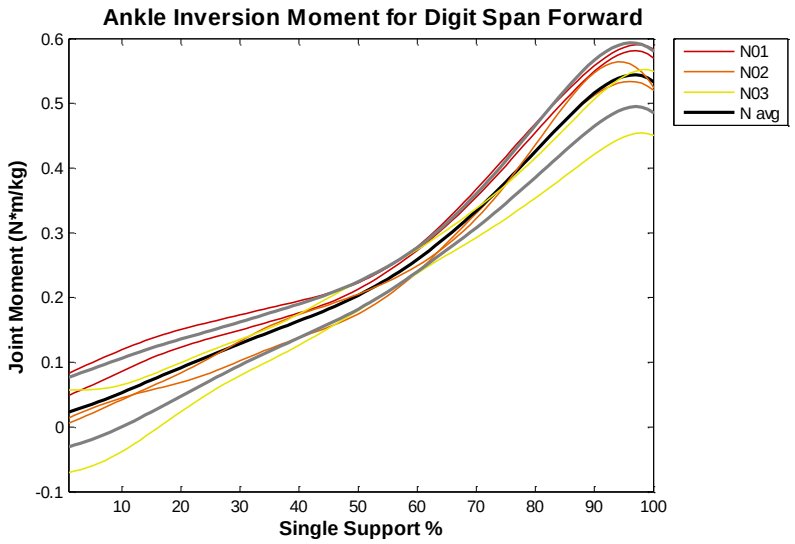

Figure A-19. Ankle inversion/eversion joint moment of normal participants during dual-task digit span forward.

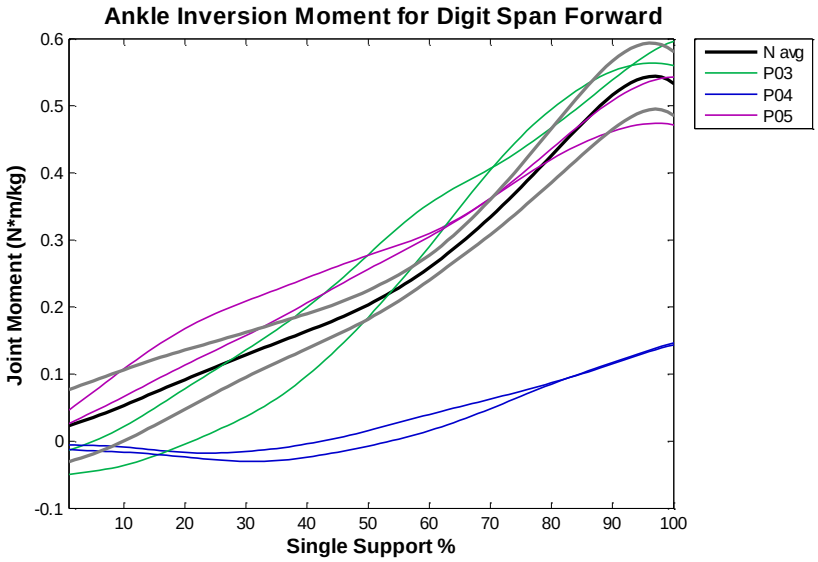

Figure A-20. Ankle inversion/eversion joint moment of MTBI participants during dual-task digit span forward.

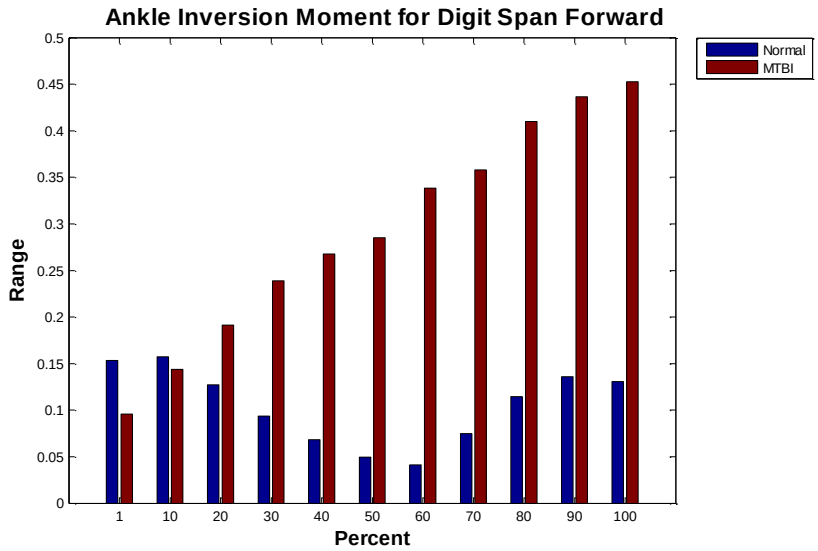

Figure A-21. Range of ankle inversion/eversion joint moment of the normal and MTBI populations during single-support digit span forward.

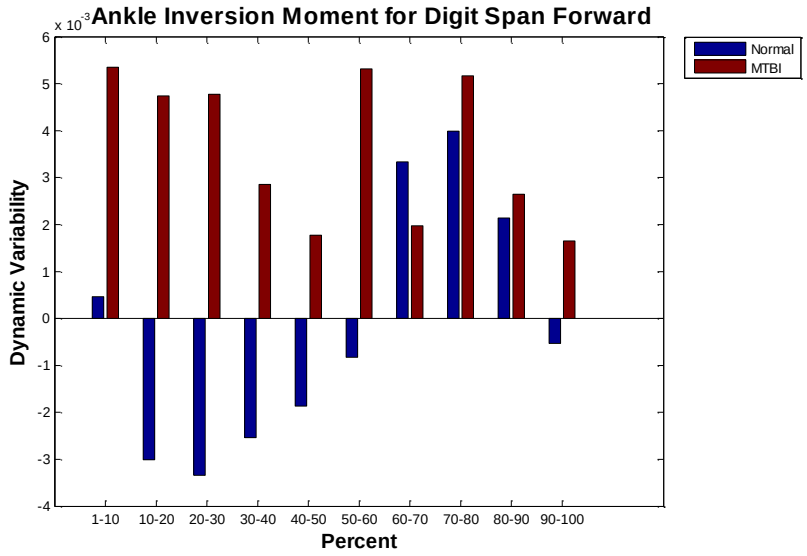

Figure A-22. Dynamic variability of ankle inversion/eversion joint moment of the normal and MTBI populations during single-support digit span forward.

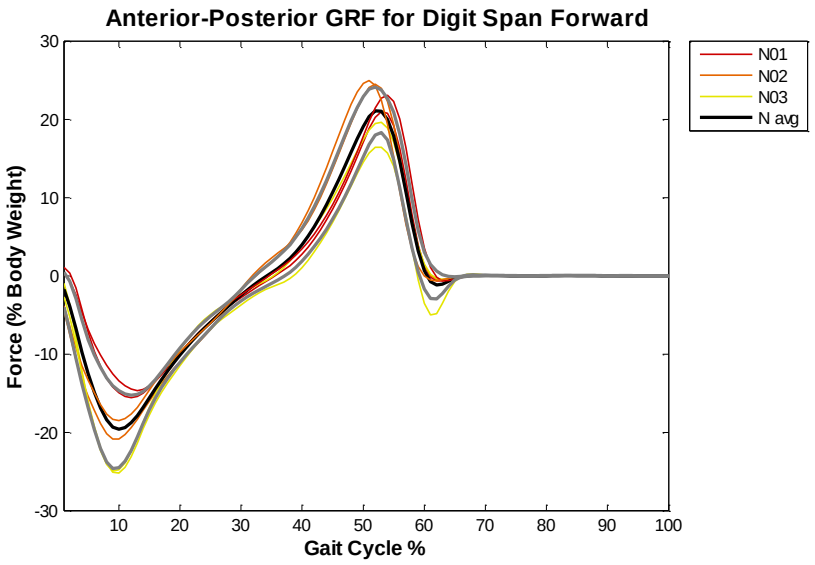

Figure A-23. AP GRF of normal participants during dual-task digit span forward.

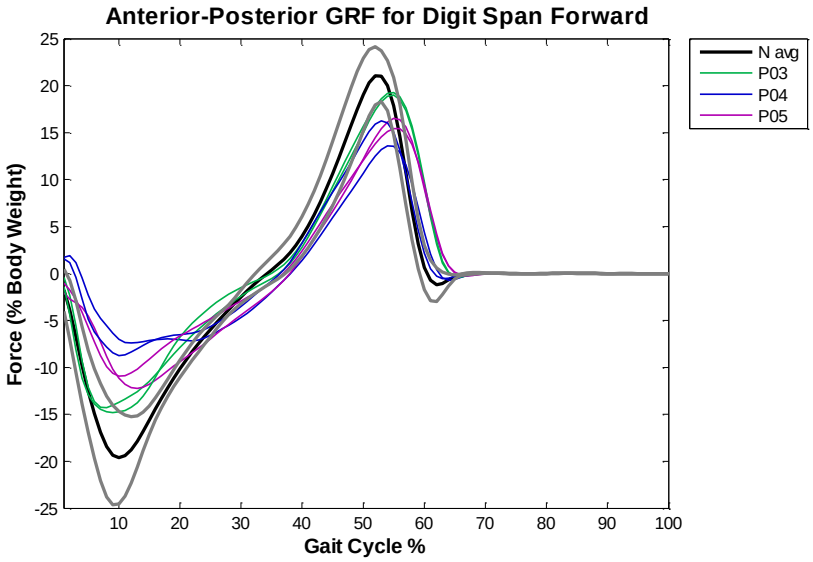

Figure A-24. AP GRF of MTBI participants during dual-task digit span forward.

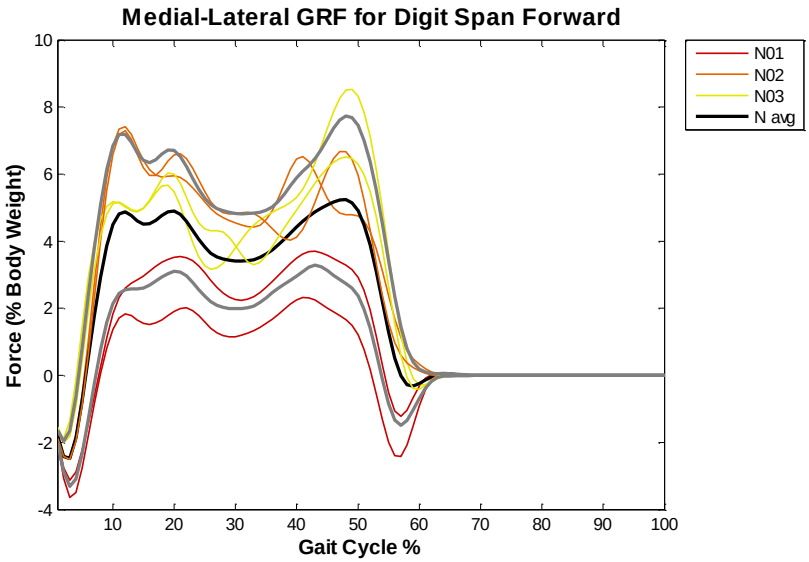

Figure A-25. ML GRF of normal participants during dual-task digit span forward.

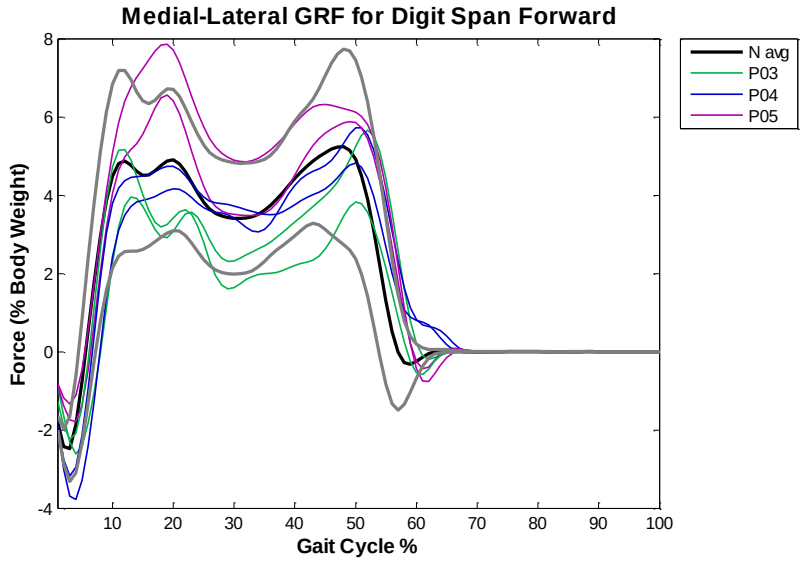

Figure A-26. ML GRF of MTBI participants during dual-task digit span forward.

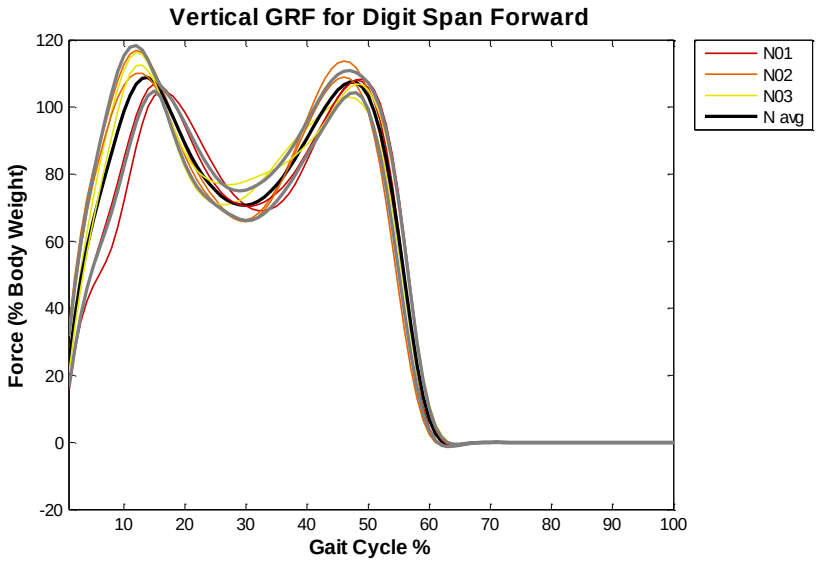

Figure A-27. Vertical GRF of normal participants during dual-task digit span forward.

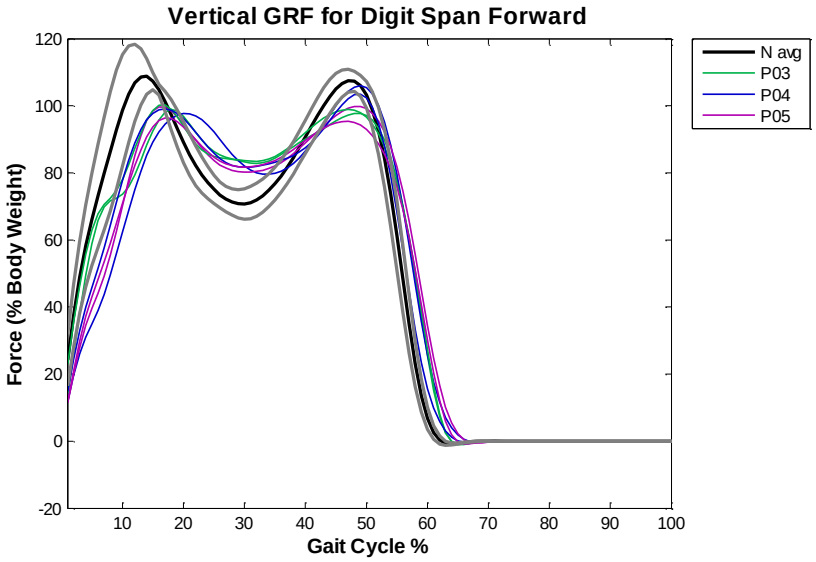

Figure A-28. Vertical GRF of MTBI participants during dual-task digit span forward.

Table A-3. GRF measures for dual-task digit span forward.

	Anterior-Posterior GRF		Vertical GRF		
	Max Loading Time (%)	Max Loading Magnitude (%BW)	Max Loading Time (%)	Min Support Time (%)	Loading-Support Magnitude (%BW)
N01	12.5	-17.2	15.5	31	44.1
N02	9.5	-19.2	13	28.5	44.8
N03	10.5	-24.1	13.5	27.5	40.4
N Avg	10.8	-20.2	14	29	43.1
P03	9	-14.0	17	31.5	14.7
P04	10.5	-10.2	15	33	25.5
P05	10	-13.2	15.5	28.5	22.0
P Avg	9.8	-12.5	15.8	31	20.7

APPENDIX B

DUAL-TASK DIGIT SPAN BACKWARD

During the digit span backward test, a cognitive dual task, participants were given a series of numbers and asked to repeat them back to the study coordinator in reverse order. The series of numbers was increased from three to seven digits. The numbers one through nine were used with each number appearing only once in a series. Two sequences were given for each number of digits. One of the two sequences had to be repeated correctly to proceed to the next number of digits. The maximum number of digits repeated correctly was considered a metric. An example of a five digit series of numbers is 7 2 4 1 8.

Table B-1. Number of digits repeated correctly at baseline and during dual-task digit span backward walking.

	# Digits Correct	
	Baseline	Walking
N01	4	4
N02	5	4
N03	6	5
P03	7	7
P04	3	3
P05	5	4

Table B-2. Temporal and spatial parameters of the digit span backward task.

	Velocity (m/s)	Stride Length (m)	Stride Time (s)	Step Width (m)	Step Height (m)
N01	1.29	1.43	1.11	0.098	0.060
N02	1.48	1.48	1.00	0.128	0.046
N03	1.24	1.43	1.15	0.133	0.056
N Avg	1.34	1.45	1.08	0.120	0.054
P03	1.26	1.51	1.20	0.161	0.055
P04	1.15	1.21	1.05	0.086	0.057
P05	1.02	1.17	1.15	0.164	0.050
P Avg	1.15	1.29	1.13	0.137	0.054

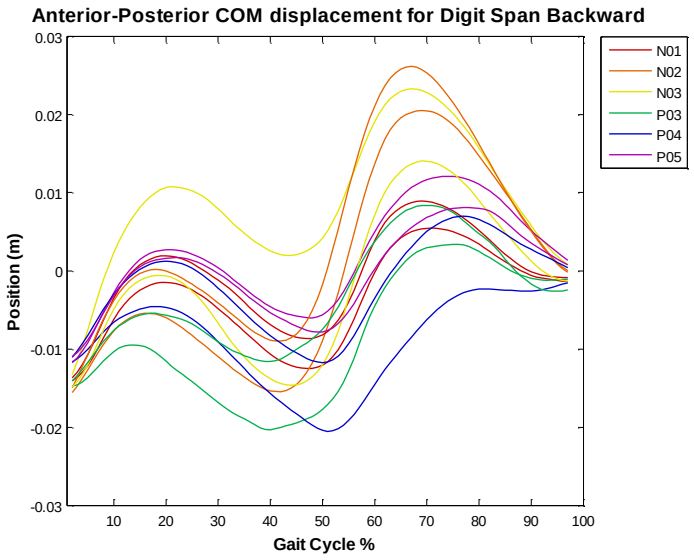

Figure B-1. AP COM displacement during dual-task digit span backward.

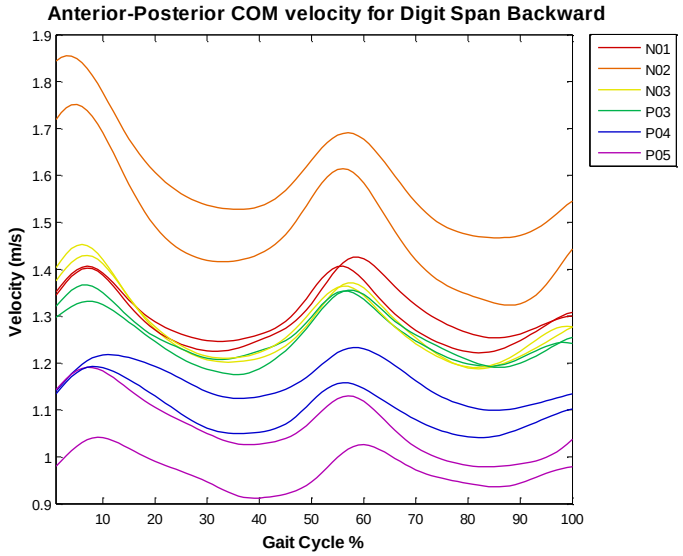

Figure B-2. AP COM velocity during dual-task digit span backward.

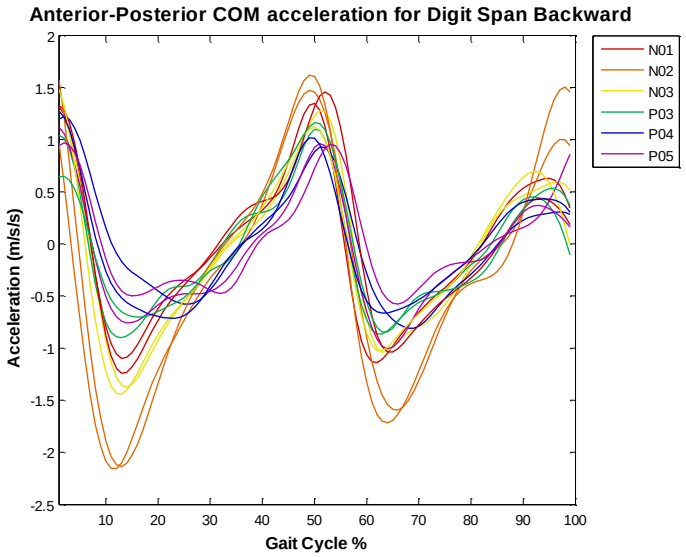

Figure B-3. AP COM acceleration during dual-task digit span backward.

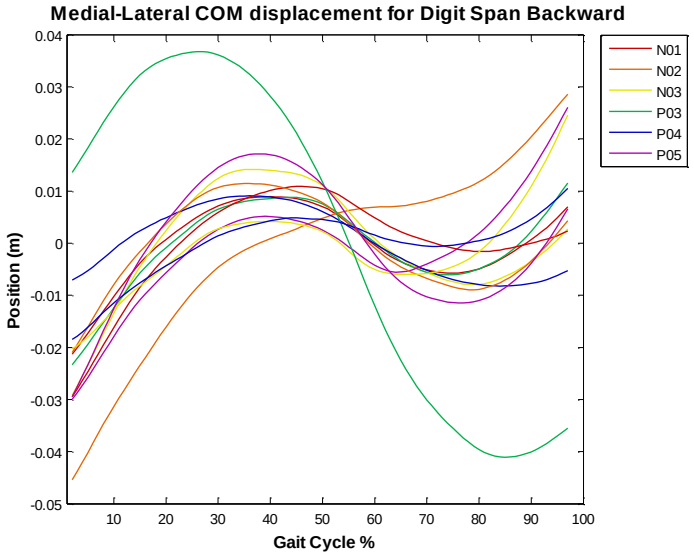

Figure B-4. ML COM displacement during dual-task digit span backward.

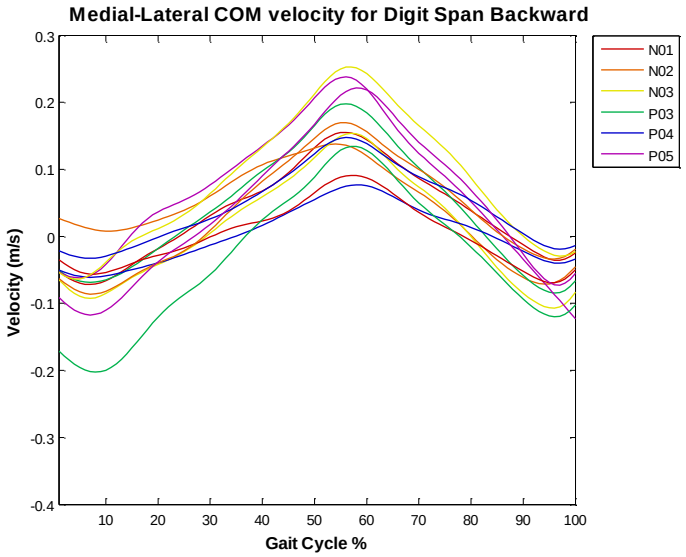

Figure B-5. ML COM velocity during dual-task digit span backward.

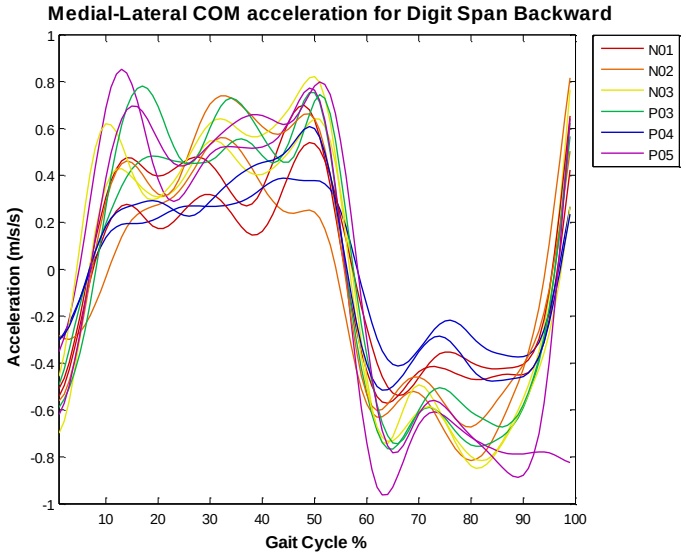

Figure B-6. ML COM acceleration during dual-task digit span backward.

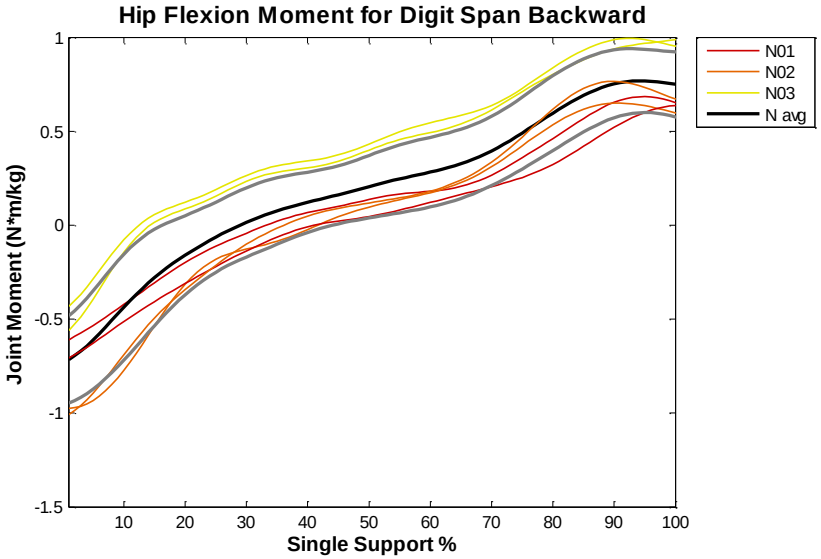

Figure B-7. Hip flexion/extension joint moment of normal participants during dual-task digit span backward.

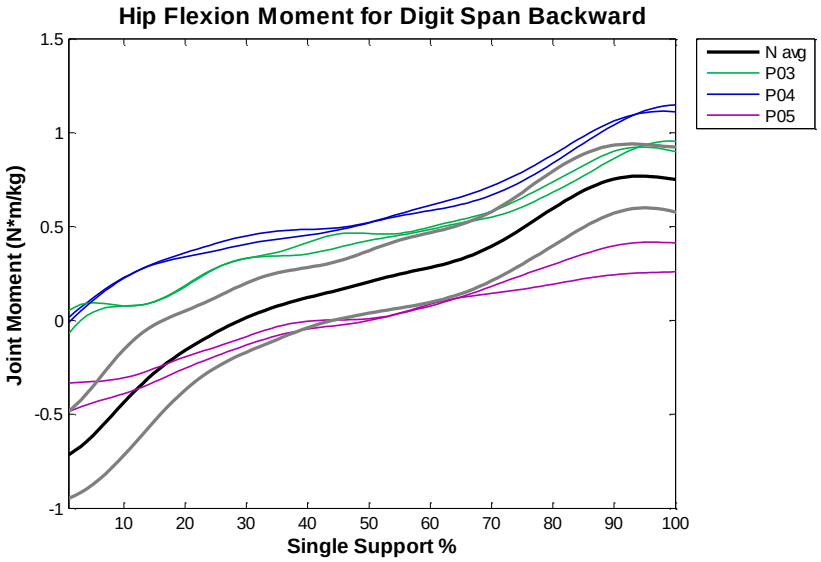

Figure B-8. Hip flexion/extension joint moment of MTBI participants during dual-task digit span backward.

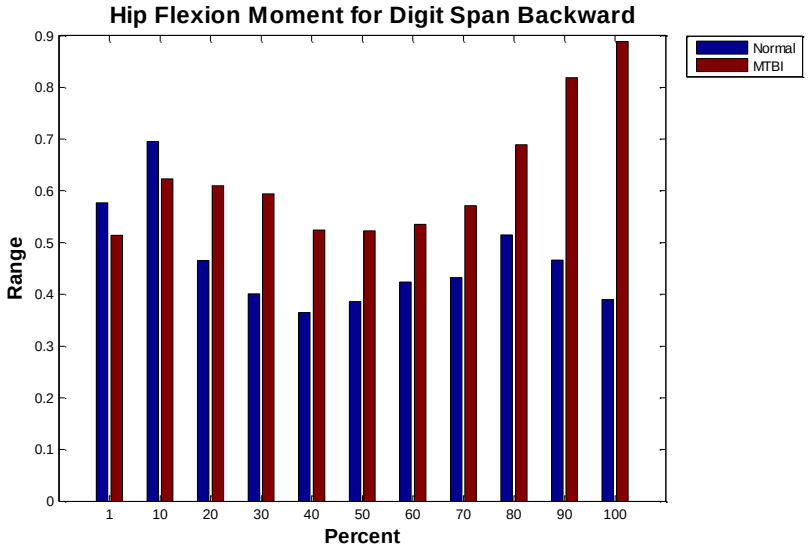

Figure B-9. Range of hip flexion/extension joint moment of the normal and MTBI populations during single-support digit span backward.

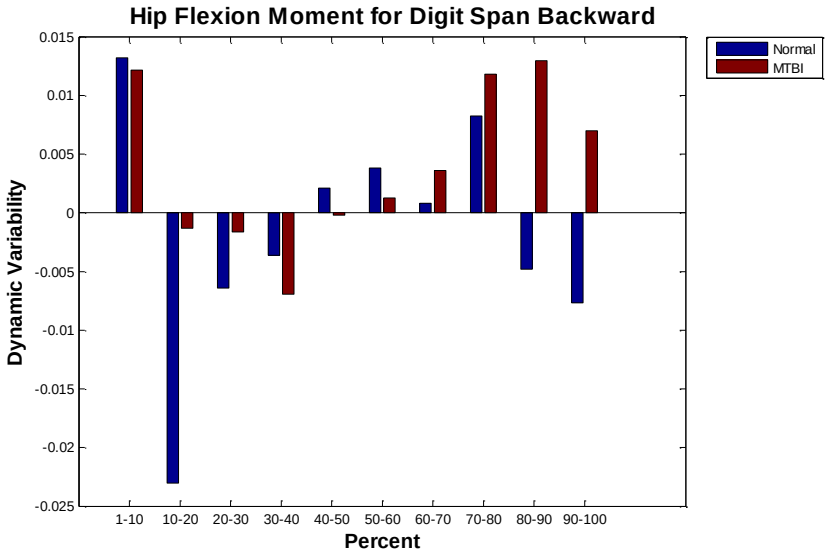

Figure B-10. Dynamic variability of hip flexion/extension joint moment of the normal and MTBI populations during single-support digit span backward.

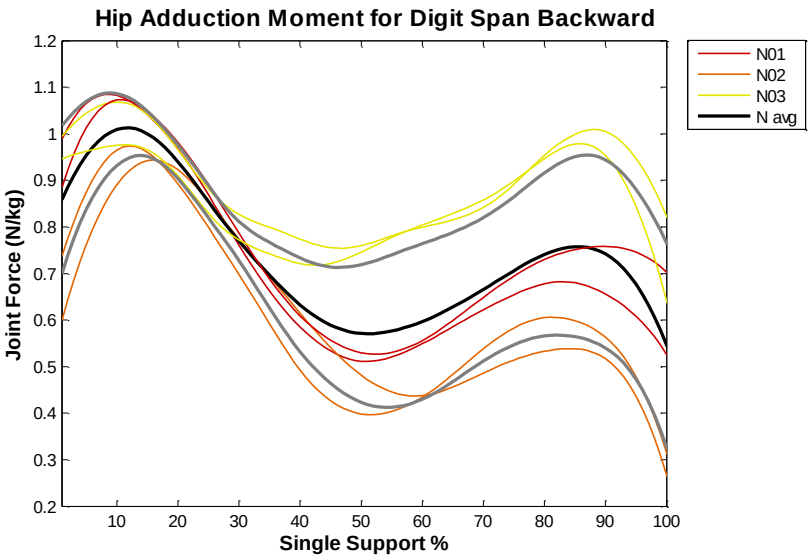

Figure B-11. Hip adduction/abduction joint moment of normal participants during dual-task digit span backward.

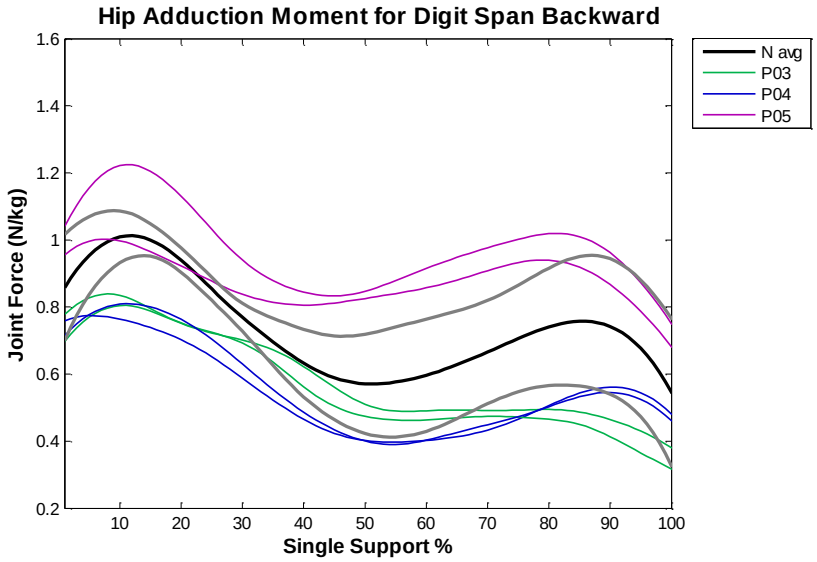

Figure B-12. Hip adduction/abduction joint moment of MTBI participants during dual-task digit span backward.

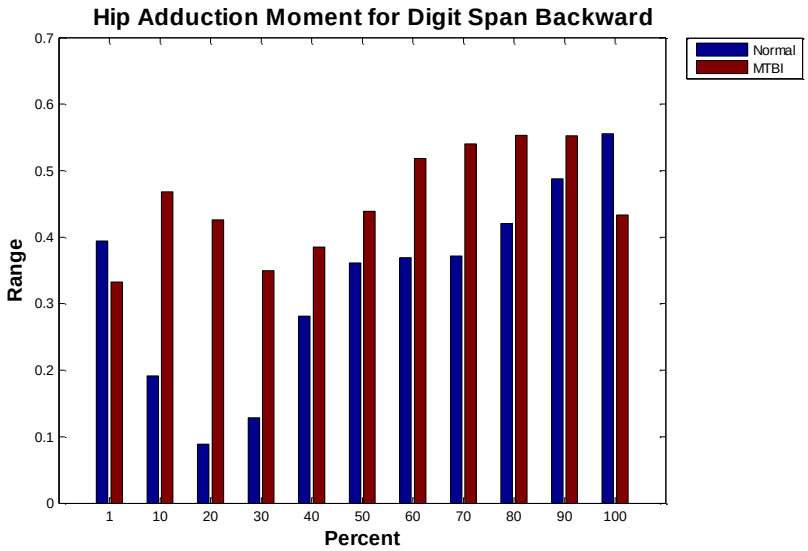

Figure B-13. Range of hip adduction/abduction joint moment of the normal and MTBI populations during single-support digit span backward.

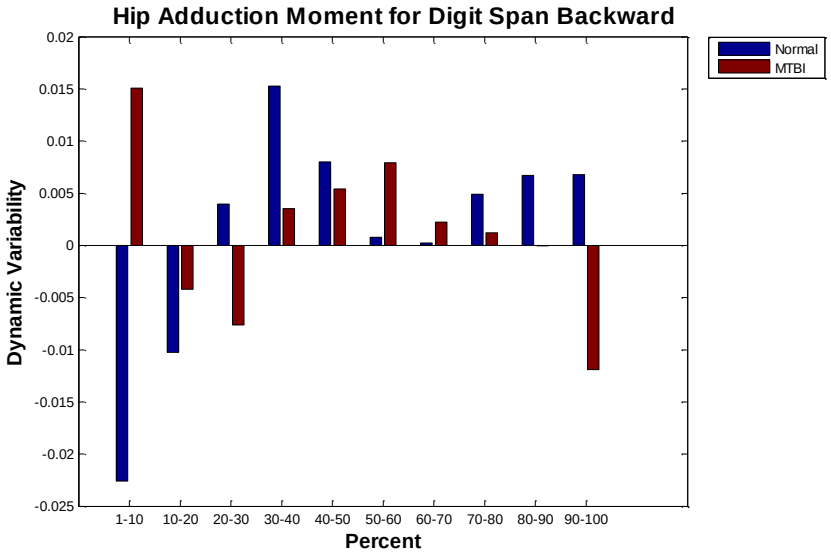

Figure B-14. Dynamic variability of hip adduction/abduction joint moment of the normal and MTBI populations during single-support digit span backward.

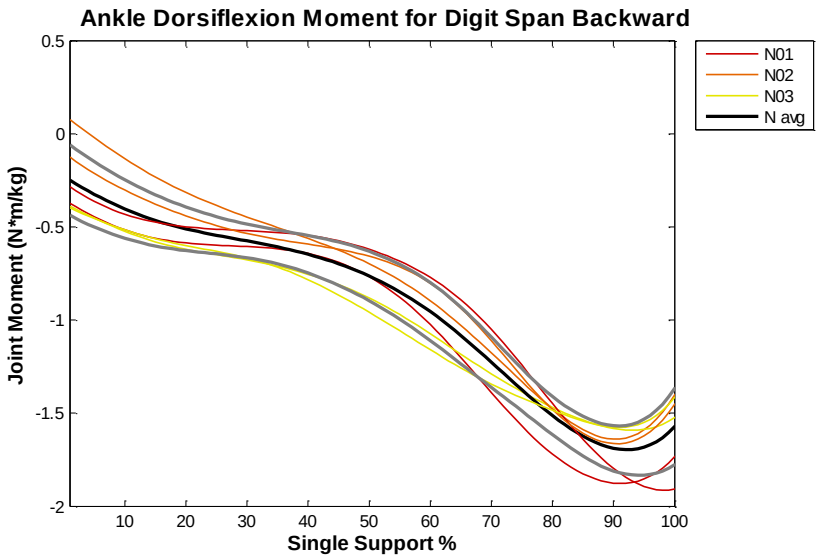

Figure B-15. Ankle dorsiflexion/plantar flexion joint moment of normal participants during dual-task digit span backward.

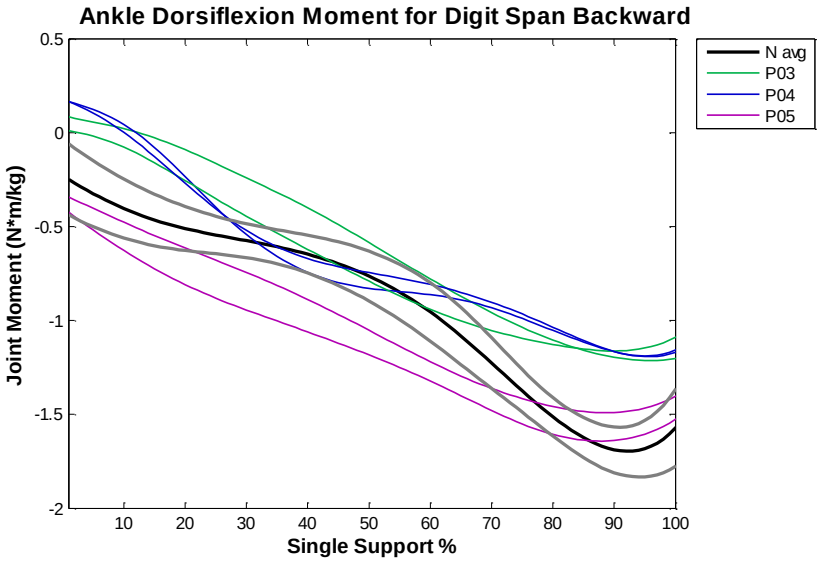

Figure B-16. Ankle dorsiflexion/ plantar flexion joint moment of MTBI participants during dual-task digit span backward.

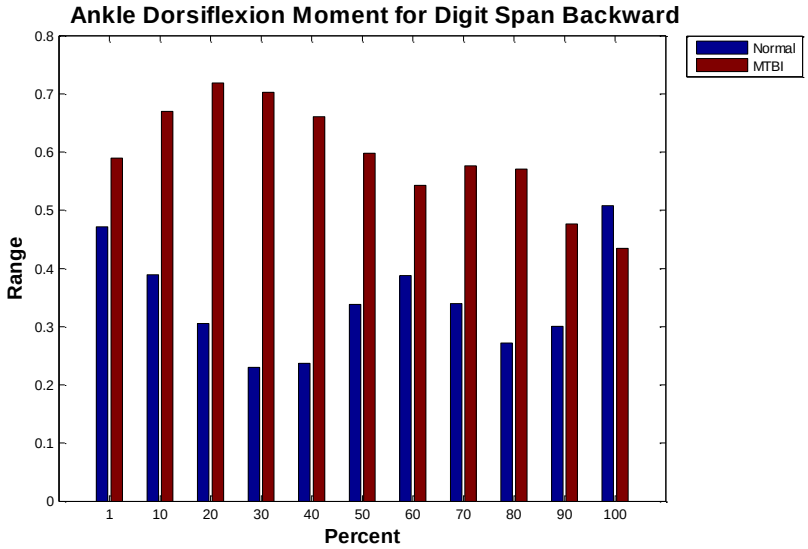

Figure B-17. Range of ankle dorsiflexion/plantar flexion joint moment of the normal and MTBI populations during single-support digit span backward.

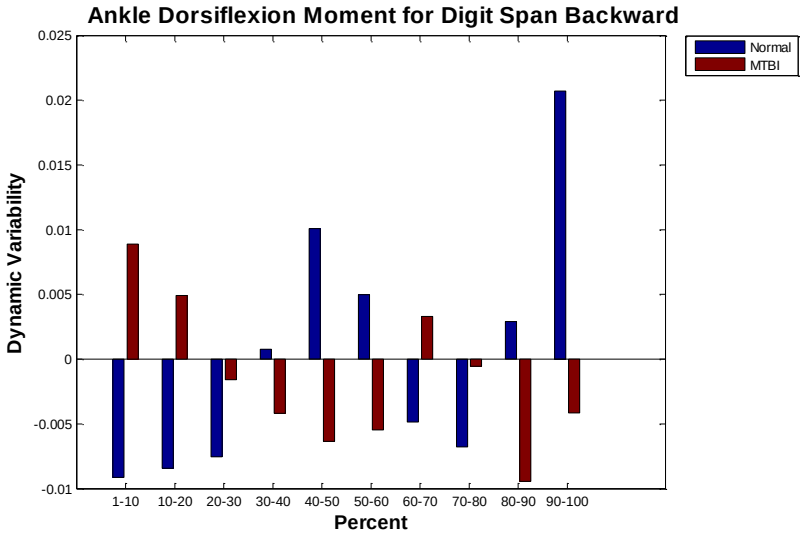

Figure B-18. Dynamic variability of ankle dorsiflexion/plantar flexion joint moment of the normal and MTBI populations during single-support digit span backward.

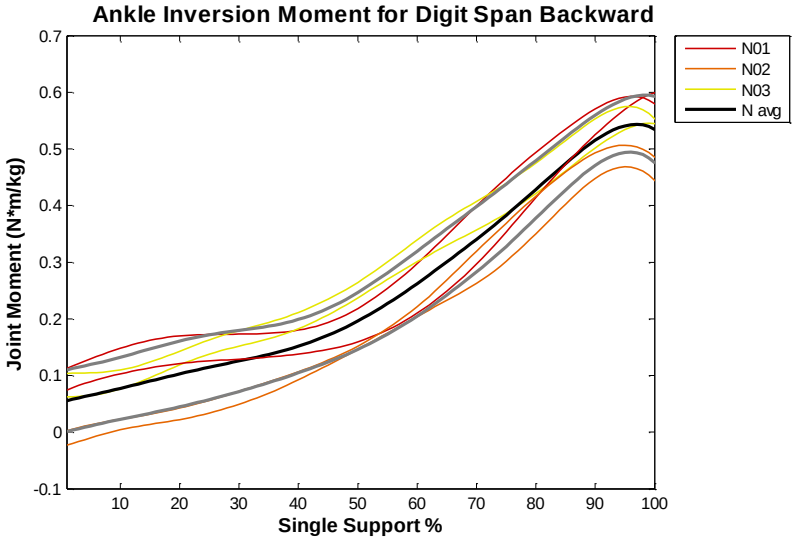

Figure B-19. Ankle inversion/eversion joint moment of normal participants during dual-task digit span backward.

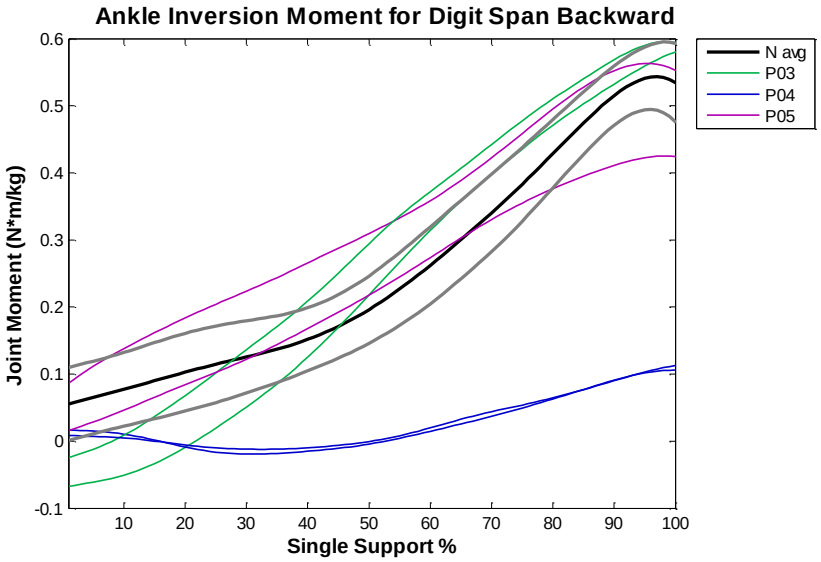

Figure B-20. Ankle inversion/eversion joint moment of MTBI participants during dual-task digit span backward.

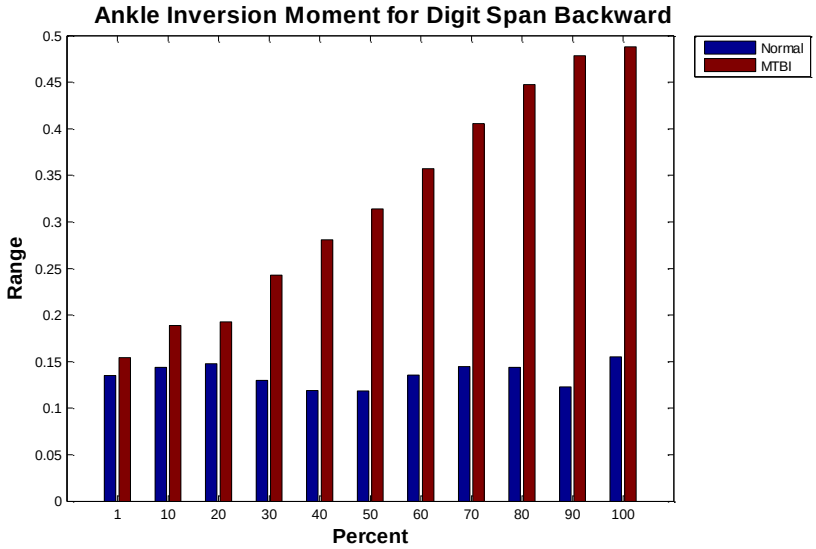

Figure B-21. Range of ankle inversion/eversion joint moment of the normal and MTBI populations during single-support digit span backward.

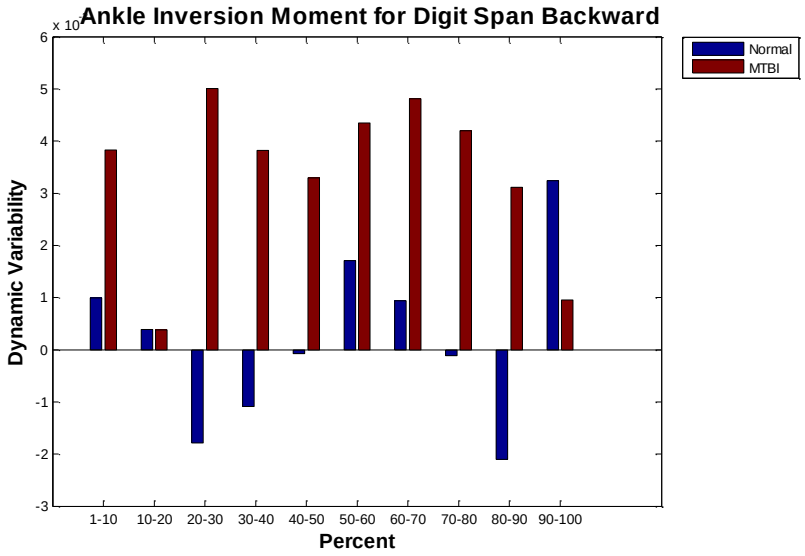

Figure B-22. Dynamic variability of ankle inversion/eversion joint moment of the normal and MTBI populations during single-support digit span backward.

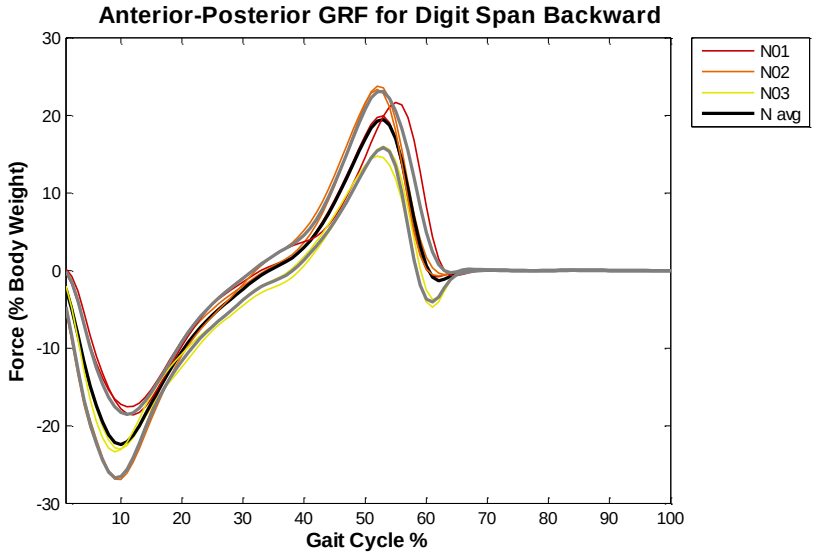

Figure B-23. AP GRF of normal participants during dual-task digit span backward.

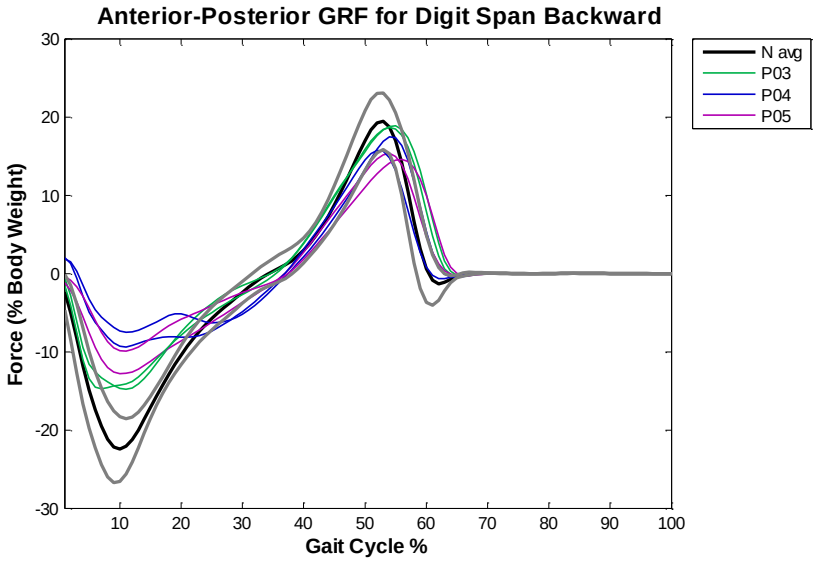

Figure B-24. AP GRF of MTBI participants during dual-task digit span backward.

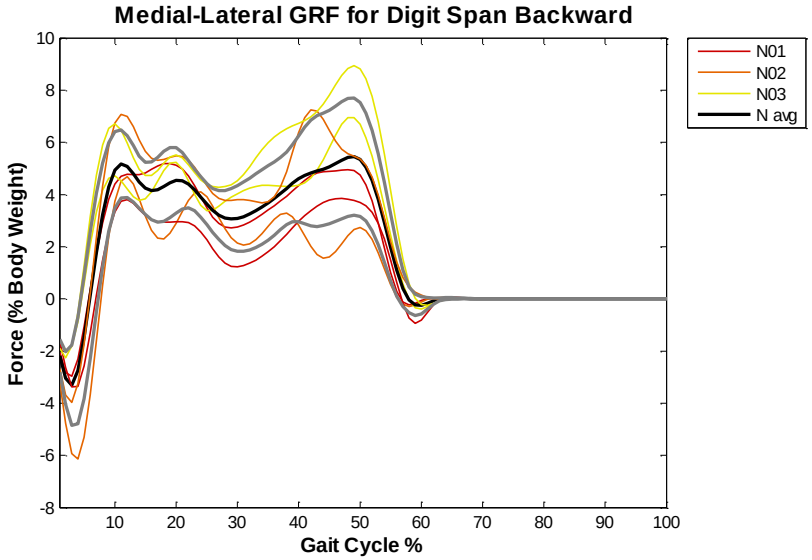

Figure B-25. ML GRF of normal participants during dual-task digit span backward.

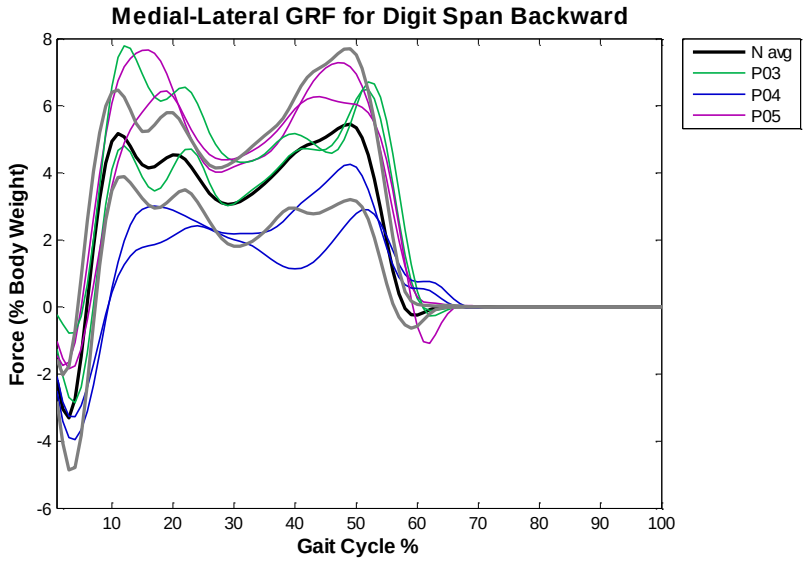

Figure B-26. ML GRF of MTBI participants during dual-task digit span backward.

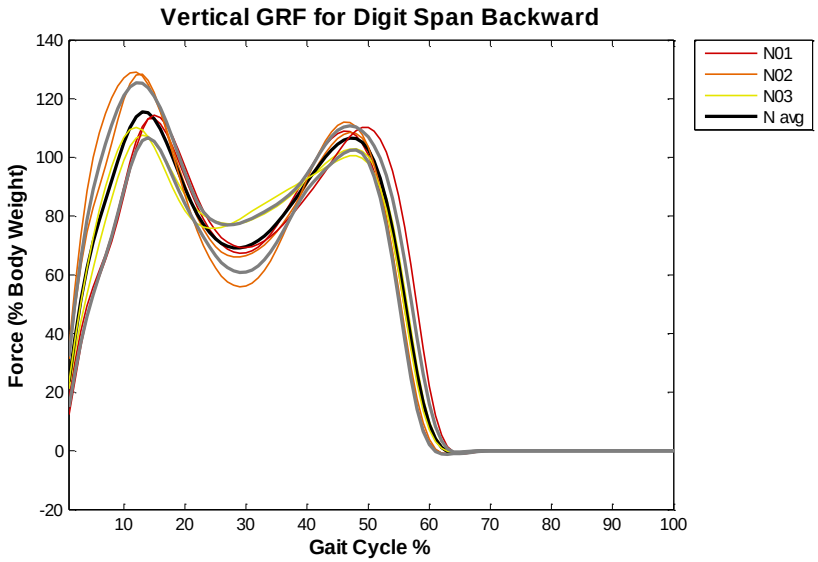

Figure B-27. Vertical GRF of normal participants during dual-task digit span backward.

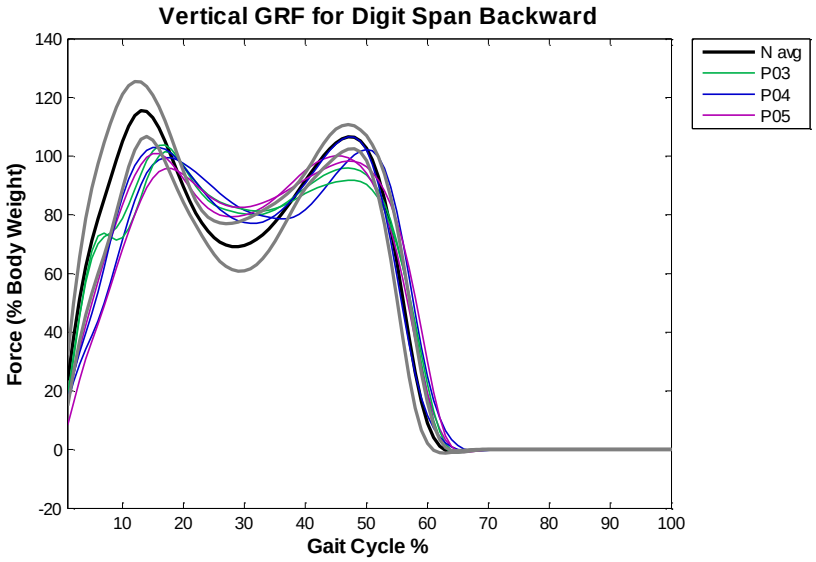

Figure B-28. Vertical GRF of MTBI participants during dual-task digit span backward.

Table B-3. GRF measures for dual-task digit span backward.

	Anterior-Posterior GRF		Vertical GRF		
	Max Loading Time (%)	Max Loading Magnitude (%BW)	Max Loading Time (%)	Min Support Time (%)	Loading-Support Magnitude (%BW)
N01	11.5	-18.1	15	29.5	45.6
N02	9.5	-26.8	12.5	29	67.8
N03	9.5	-23.2	12.5	26.5	32.4
N Avg	10.2	-22.7	13.3	28.3	48.6
P03	9	-14.8	17	32	22.0
P04	11	-8.4	16.5	33.5	23.4
P05	10.5	-11.4	16.5	28.5	17.4
P Avg	10.2	-11.5	16.7	31.3	20.9

APPENDIX C

DUAL-TASK SYMMETRIC CARRYING

The symmetric carrying test, a motor dual task, required participants to carry a 15 pound box with both hands while walking across the platform.

Table C-1. Temporal and spatial parameters of the symmetric carrying task.

	Velocity (m/s)	Stride Length (m)	Stride Time (s)	Step Width (m)	Step Height (m)
N01	1.18	1.27	1.08	0.093	0.063
N02	1.49	1.38	0.93	0.129	0.050
N03	1.38	1.49	1.08	0.143	0.068
N Avg	1.35	1.38	1.03	0.121	0.061
P03	1.27	1.45	1.14	0.142	0.057
P04	1.19	1.13	0.95	0.091	0.056
P05	1.30	1.30	1.00	0.147	0.056
P Avg	1.25	1.29	1.03	0.127	0.056

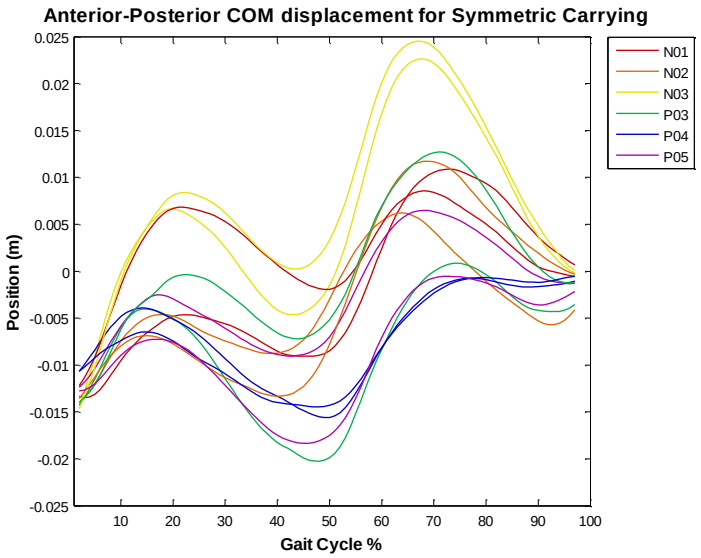

Figure C-1. AP COM displacement during dual-task symmetric carrying.

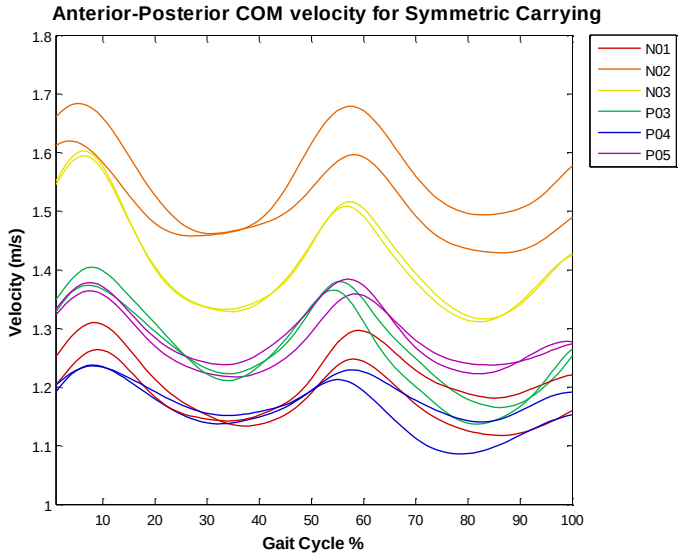

Figure C-2. AP COM velocity during dual-task symmetric carrying.

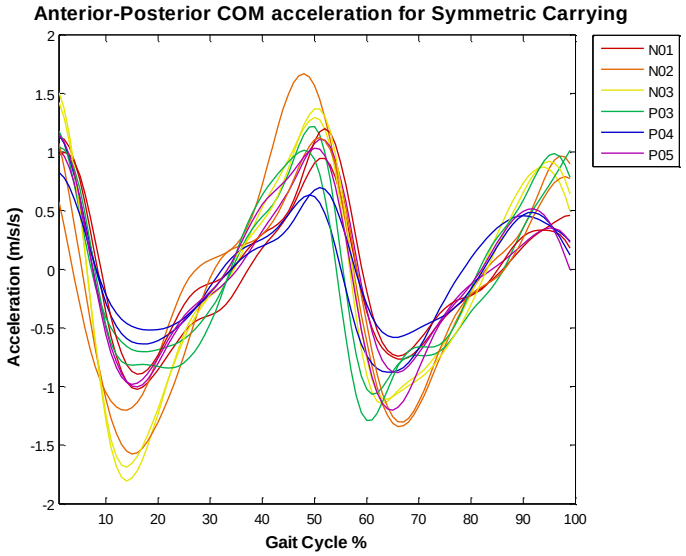

Figure C-3. AP COM acceleration during dual-task symmetric carrying.

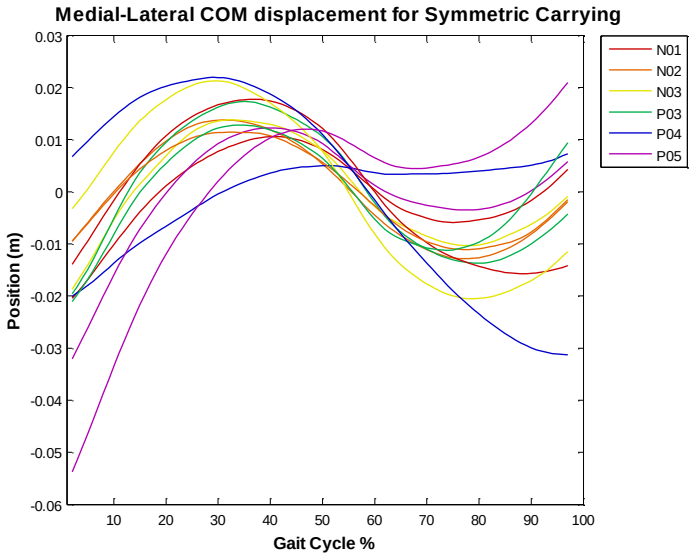

Figure C-4. ML COM displacement during dual-task symmetric carrying.

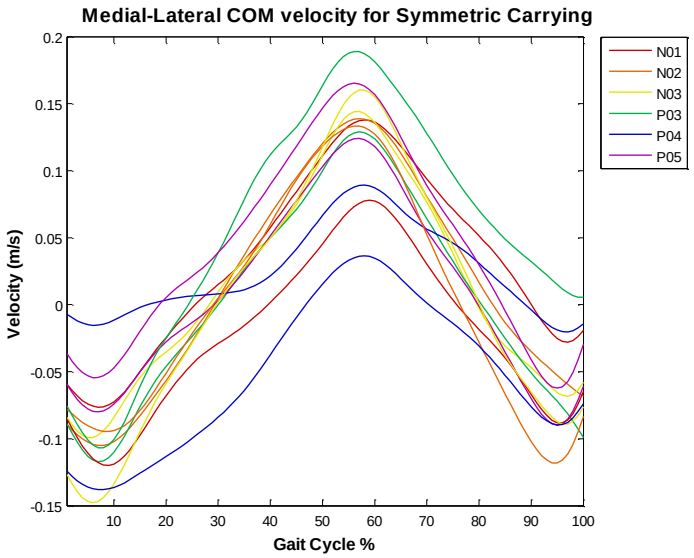

Figure C-5. ML COM velocity during dual-task symmetric carrying.

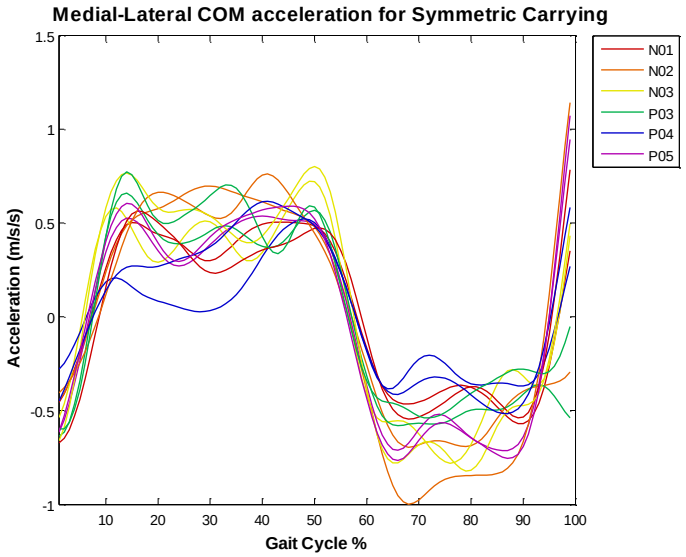

Figure C-6. ML COM acceleration during dual-task symmetric carrying.

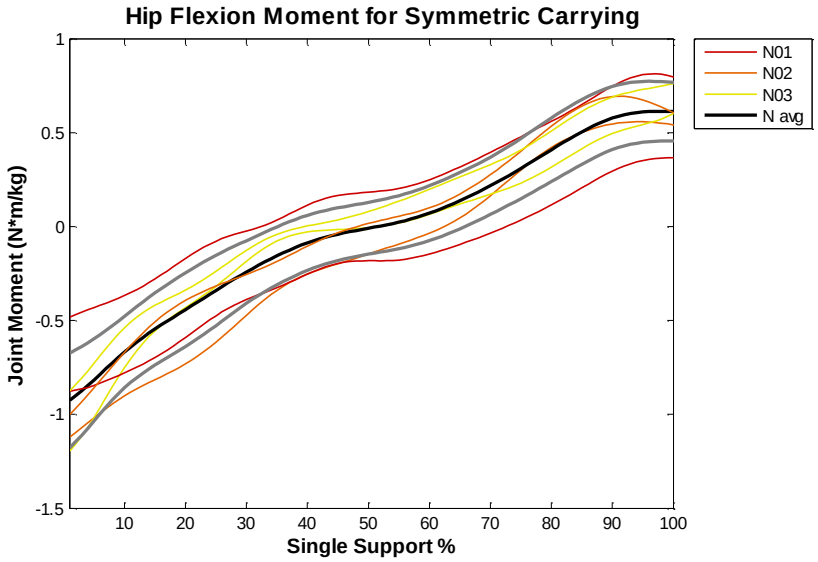

Figure C-7. Hip flexion/extension joint moment of normal participants during dual-task symmetric carrying.

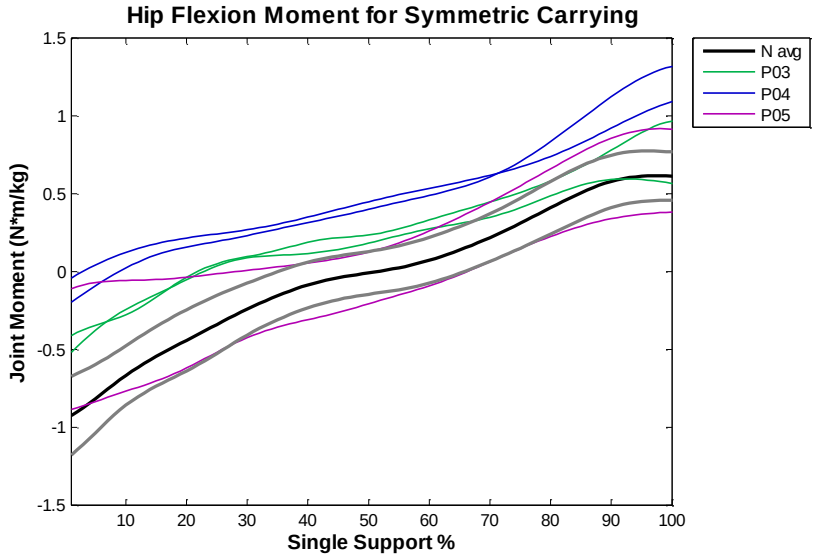

Figure C-8. Hip flexion/extension joint moment of MTBI participants during dual-task symmetric carrying.

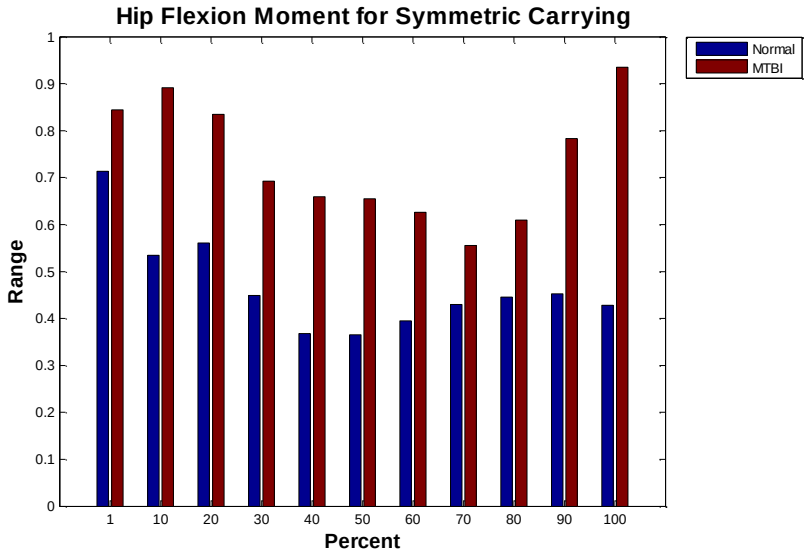

Figure C-9. Range of hip flexion/extension joint moment of the normal and MTBI populations during single-support symmetric carrying.

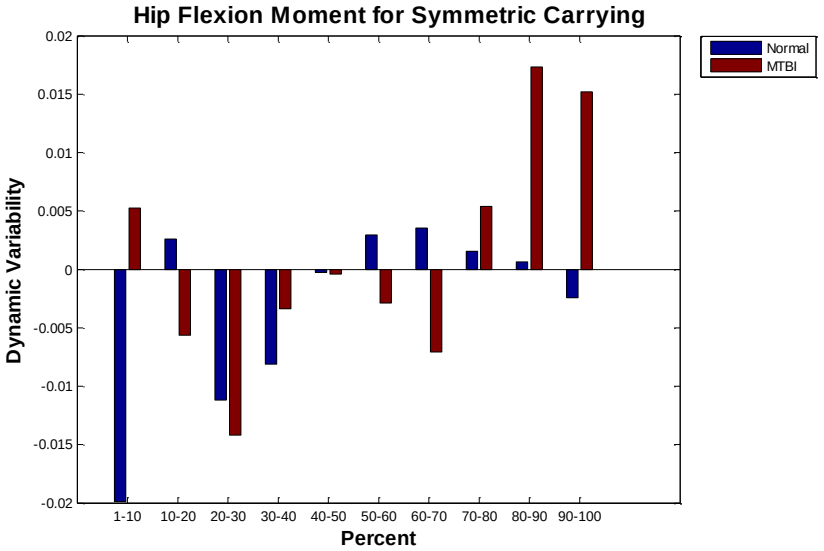

Figure C-10. Dynamic variability of hip flexion/extension joint moment of the normal and MTBI populations during single-support symmetric carrying.

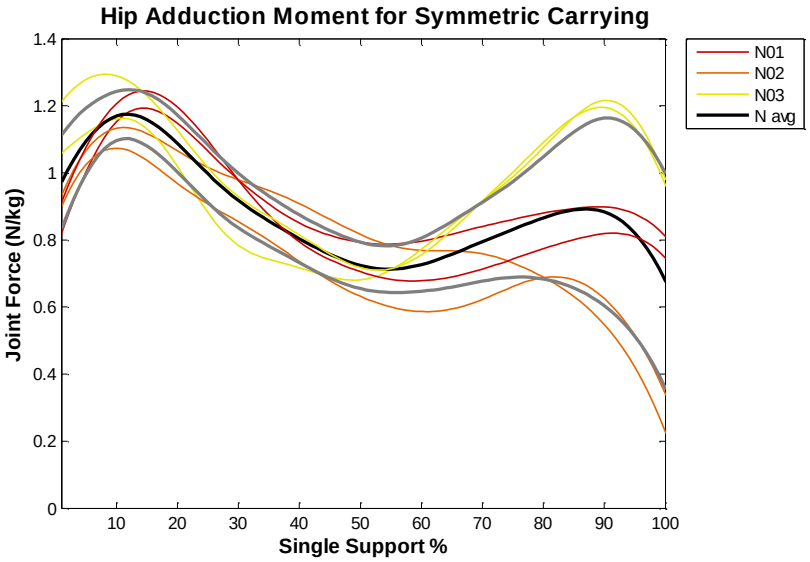

Figure C-11. Hip adduction/abduction joint moment of normal participants during dual-task symmetric carrying.

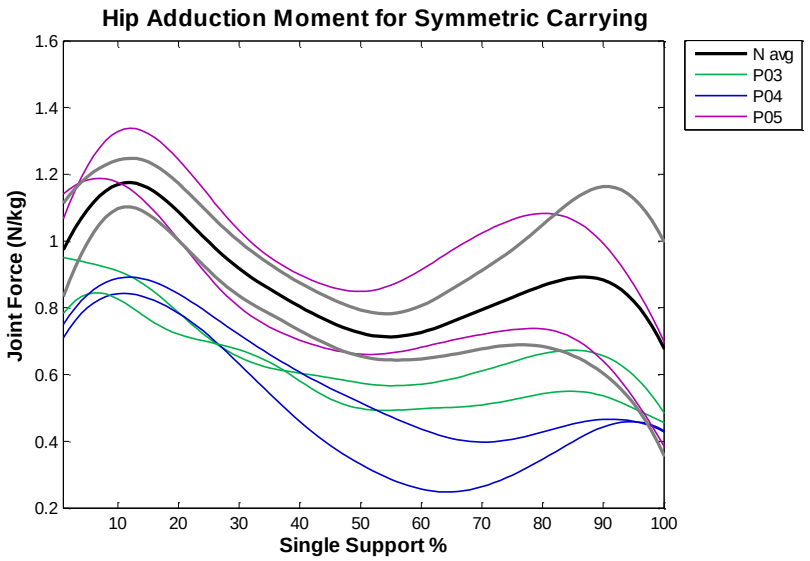

Figure C-12. Hip adduction/abduction joint moment of MTBI participants during dual-task symmetric carrying.

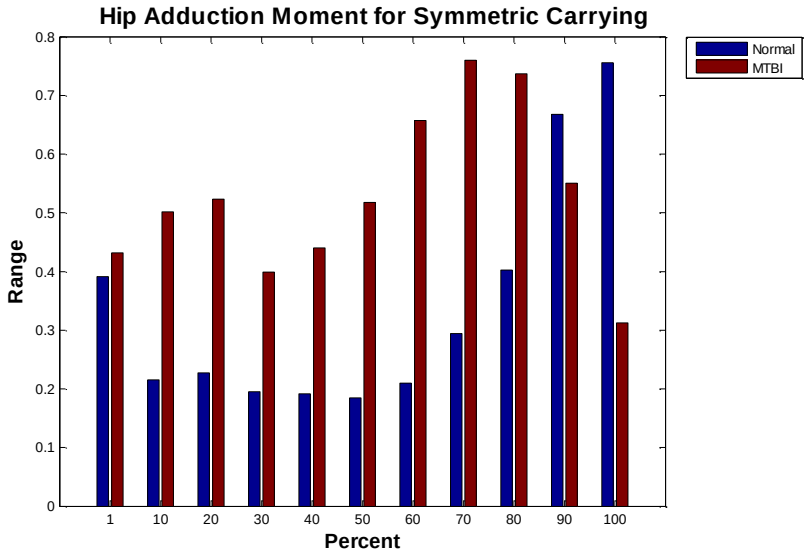

Figure C-13. Range of hip adduction/abduction joint moment of the normal and MTBI populations during single-support symmetric carrying.

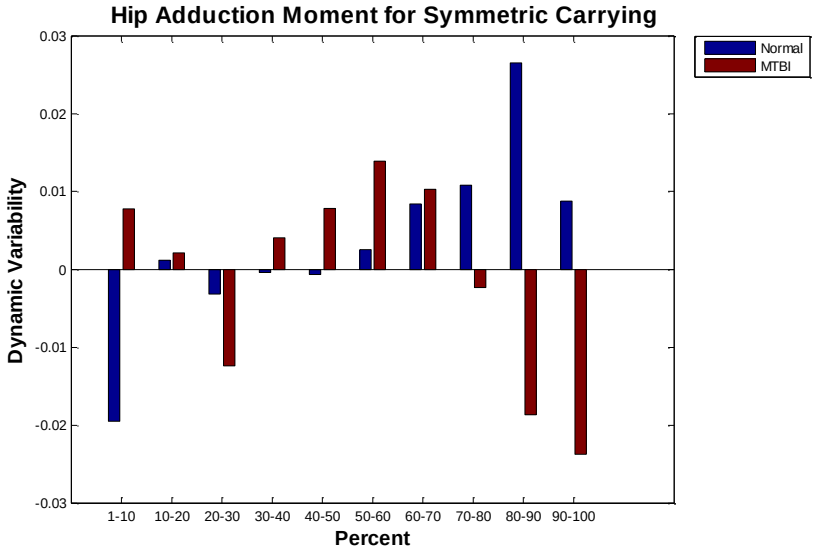

Figure C-14. Dynamic variability of hip adduction/abduction joint moment of the normal and MTBI populations during single-support symmetric carrying.

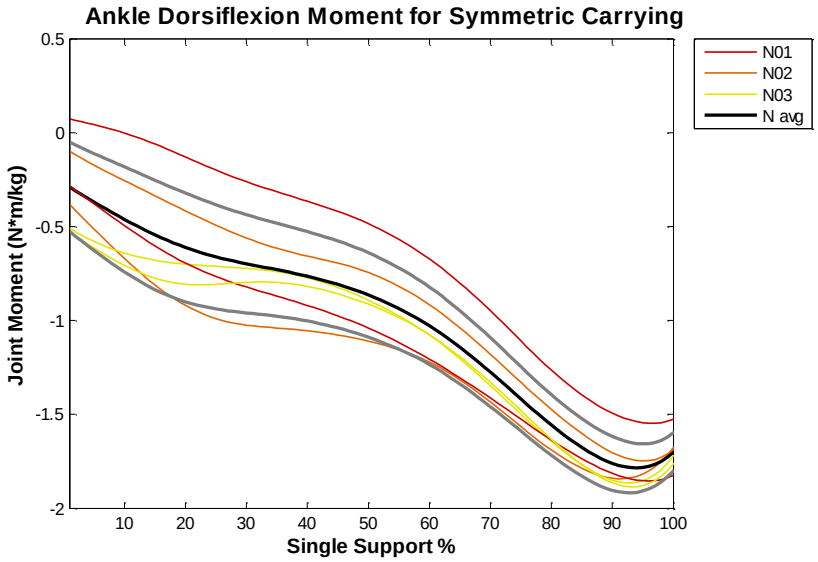

Figure C-15. Ankle dorsiflexion/plantar flexion joint moment of normal participants during dual-task symmetric carrying.

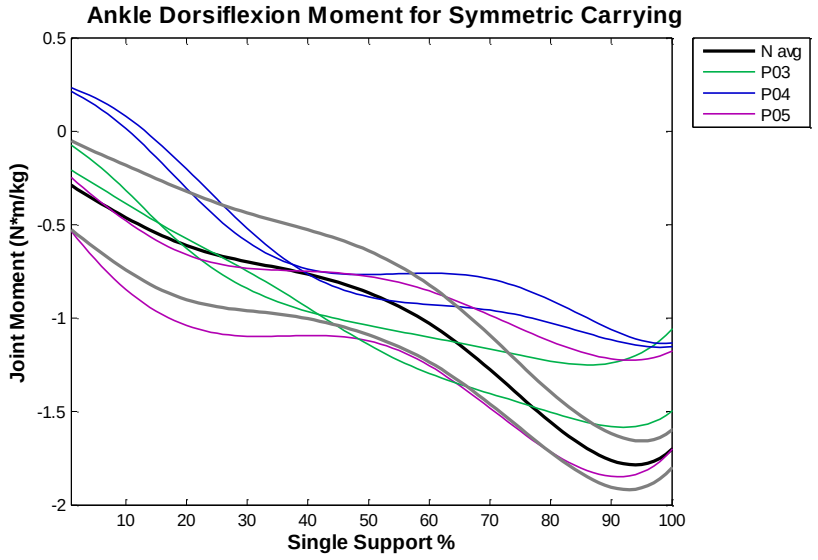

Figure C-16. Ankle dorsiflexion/ plantar flexion joint moment of MTBI participants during dual-task symmetric carrying.

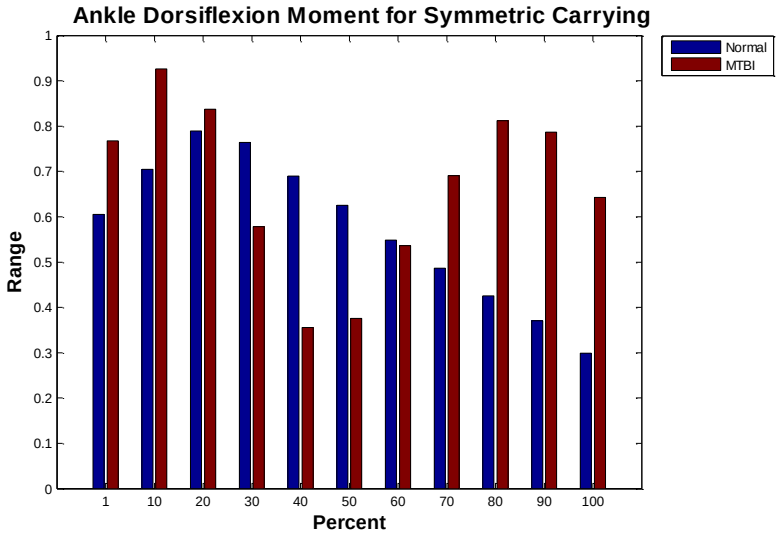

Figure C-17. Range of ankle dorsiflexion/plantar flexion joint moment of the normal and MTBI populations during single-support symmetric carrying.

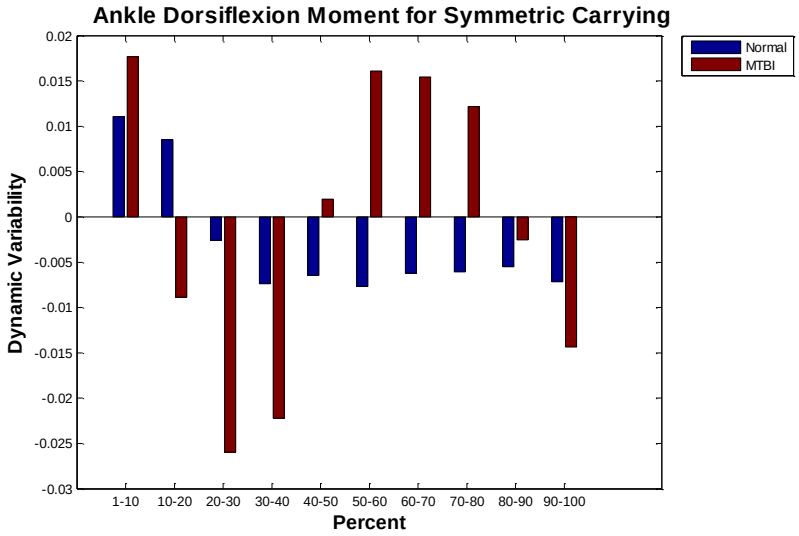

Figure C-18. Dynamic variability of ankle dorsiflexion/plantar flexion joint moment of the normal and MTBI populations during single-support symmetric carrying.

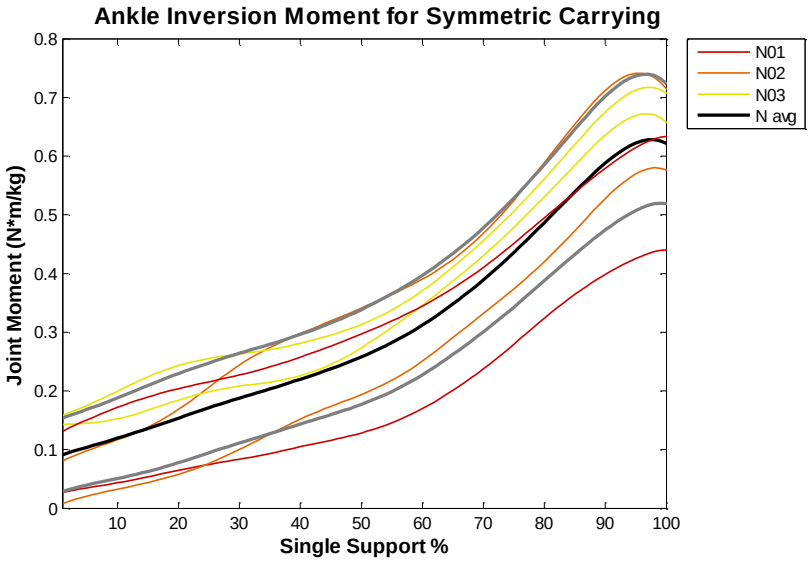

Figure C-19. Ankle inversion/eversion joint moment of normal participants during dual-task symmetric carrying.

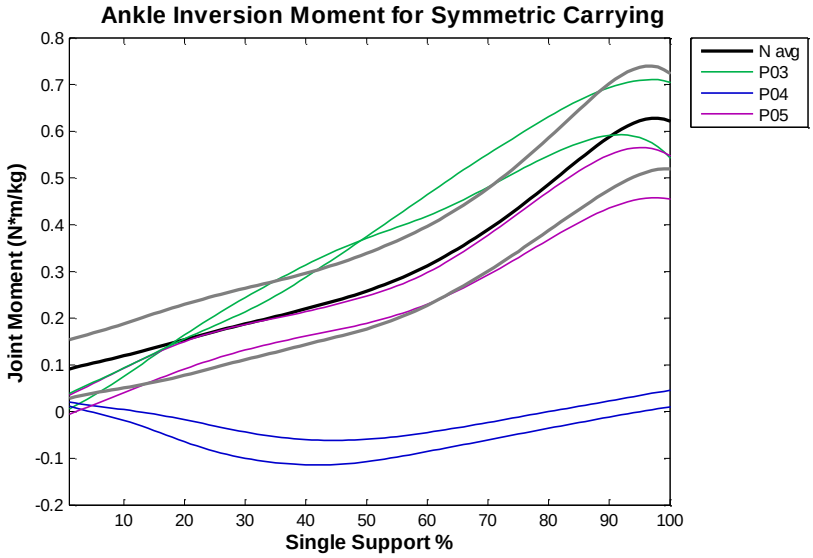

Figure C-20. Ankle inversion/eversion joint moment of MTBI participants during dual-task symmetric carrying.

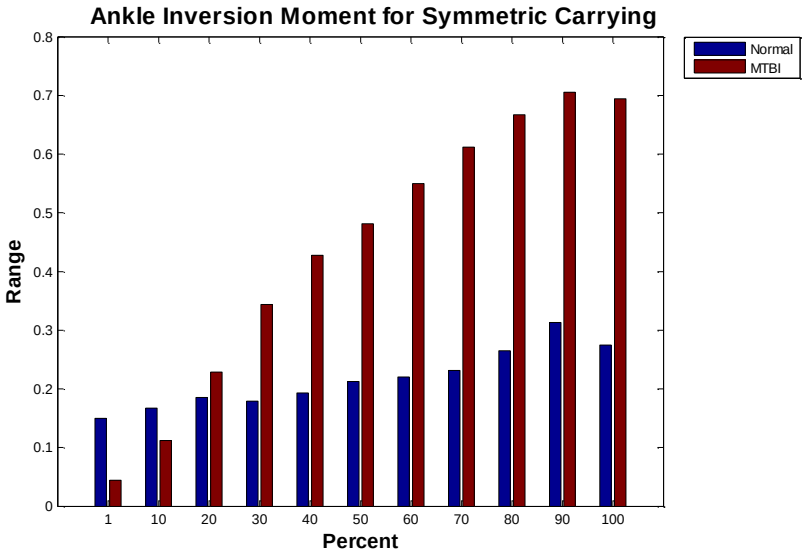

Figure C-21. Range of ankle inversion/eversion joint moment of the normal and MTBI populations during single-support symmetric carrying.

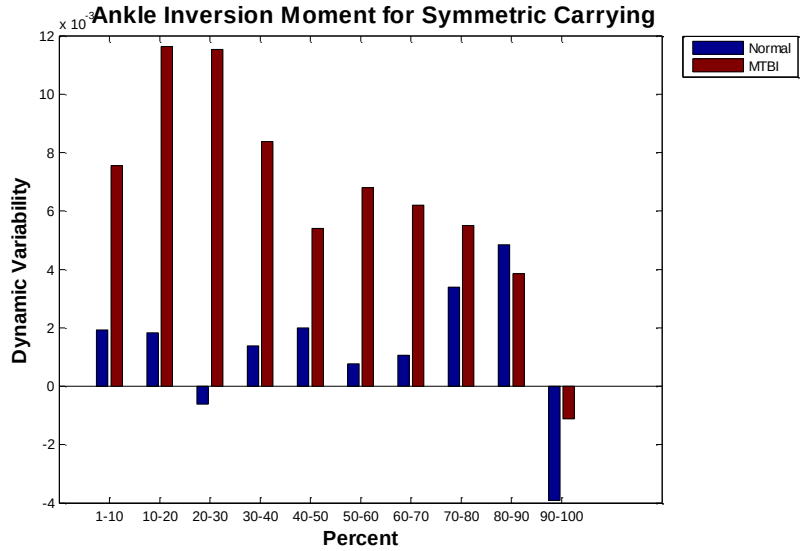

Figure C-22. Dynamic variability of ankle inversion/eversion joint moment of the normal and MTBI populations during single-support symmetric carrying.

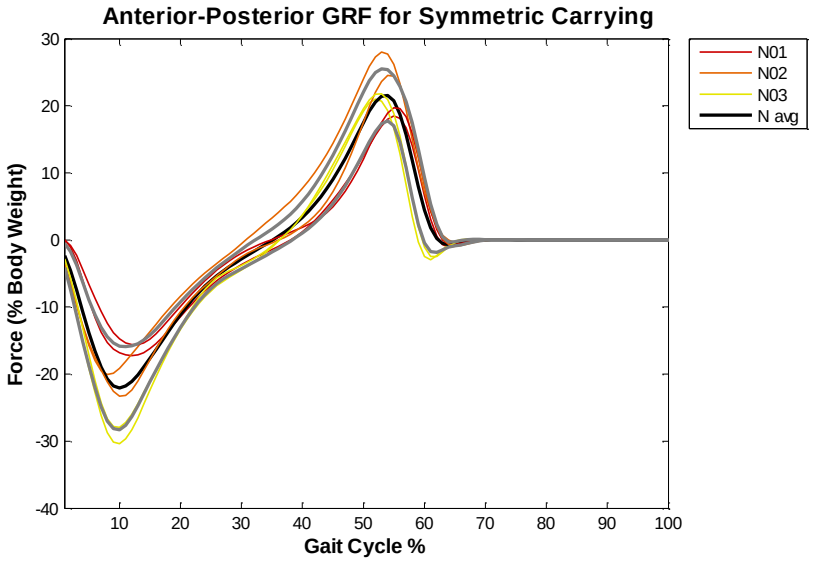

Figure C-23. AP GRF of normal participants during dual-task symmetric carrying.

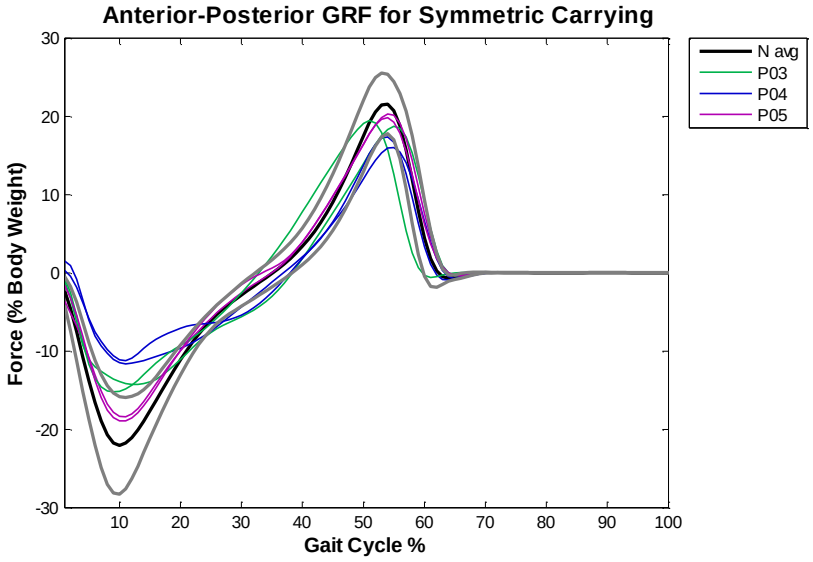

Figure C-24. AP GRF of MTBI participants during dual-task symmetric carrying.

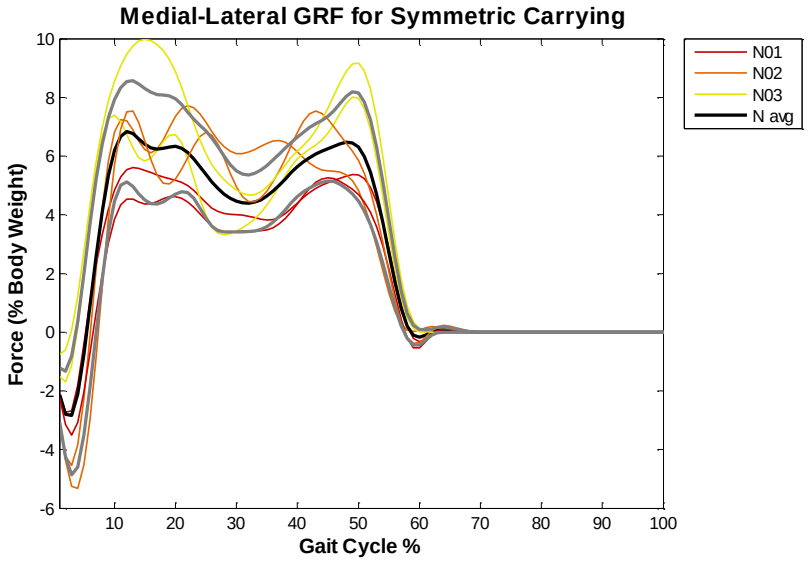

Figure C-25. ML GRF of normal participants during dual-task symmetric carrying.

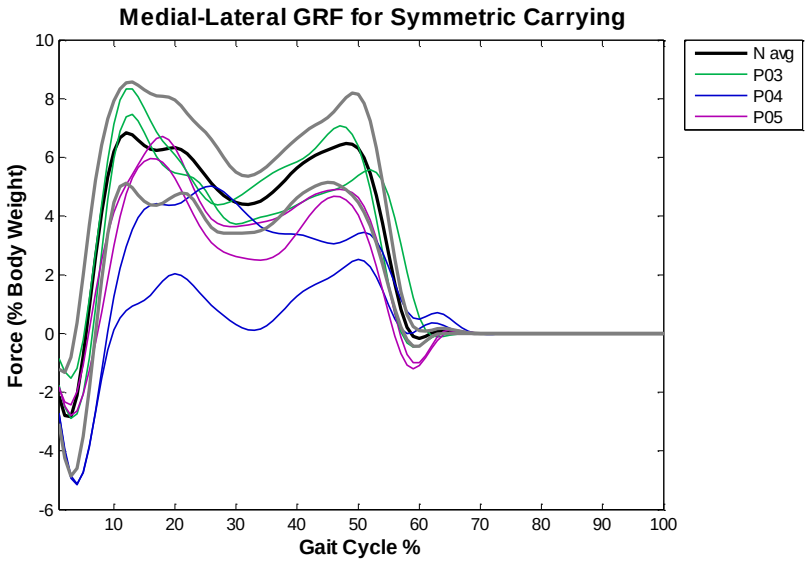

Figure C-26. ML GRF of MTBI participants during dual-task symmetric carrying.

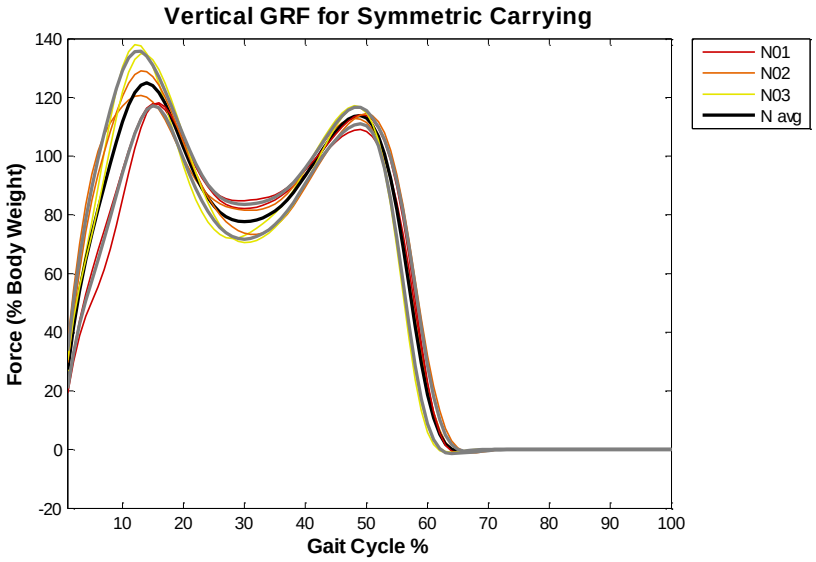

Figure C-27. Vertical GRF of normal participants during dual-task symmetric carrying.

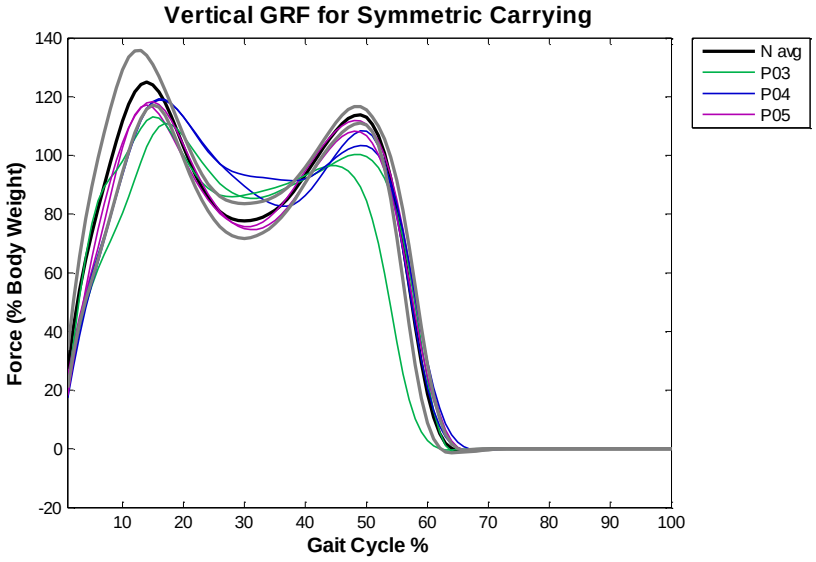

Figure C-28. Vertical GRF of MTBI participants during dual-task symmetric carrying.

Table C-2. GRF measures for dual-task symmetric carrying.

	Anterior-Posterior GRF		Vertical GRF		
	Max Loading Time (%)	Max Loading Magnitude (%BW)	Max Loading Time (%)	Min Support Time (%)	Loading-Support Magnitude (%BW)
N01	12	-16.4	15.5	29.5	34.6
N02	9	-21.7	13	31	47.5
N03	10	-29.2	12.5	29	65.2
N Avg	10.3	-22.4	13.7	29.8	49.1
P03	11	-14.8	16	29.5	26.3
P04	11	-11.4	16	37	32.1
P05	10.5	-18.7	14.5	31	42.5
P Avg	10.8	-14.9	15.5	32.5	33.6

REFERENCES

[1] Alexander MP. Mild traumatic brain injury: Pathophysiology, natural history, and clinical management. *Neurology* 1995;45:1253-60.

[2] Basford JR, Chou L-S, Kaufman KR, Brey RH, Walker A, Malec JF, Moessner AM, Brown AW. An Assessment of Gait and Balance Deficits After Traumatic Brain Injury. *Arch Phys Med Rehabil* 2003;84:343-9.

[3] Cappozzo A, Catani F, Della Croce U, Leardini A. Position and Orientation in Space of Bones During Movement: Anatomical Frame Definition and Determination. *Clinical Biomechanics* 1995;10(4):171-8.

[4] Carroll LJ, Cassidy JD, Peloso PM, Borg J, von Holst H, Holm L, Paniak C, Pépin M. Prognosis for Mild Traumatic Brain Injury: Results of the WHO Collaborating Centre Task Force on Mild Traumatic Brain Injury. *J Rehabil Med* 2004; Suppl 43:84-105.

[5] Carroll LJ, Cassidy JD, Holm L, Kraus J, Coronado VG, WHO Collaborating Centre Task Force on Mild Traumatic Brain Injury. Methodological issues and research recommendations for mild traumatic brain injury: the WHO Collaborating Centre Task Force on Mild Traumatic Brain Injury. *J Rehabil Med* 2004; Suppl 43:113-125.

[6] Cassidy JD, Carroll LJ, Peloso PM, Borg J, von Holst H, Holm L, Kraus J, Coronado VG. Incidence, Risk Factors and Prevention of Mild Traumatic Brain Injury: Results of the WHO Collaborating Centre Taskforce on Mild Traumatic Brain Injury. *J Rehabil Med* 2004; Suppl. 43:28-60.

[7] Catena RD, van Donkelaar P, Chou L-S. Altered Balance control following concussion is better detected with an attention test during gait. *Gait & Posture* 2007;25:406-11.

[8] Catena RD, van Donkelaar P, Chou L-S. Cognitive task effects on gait stability following concussion. *Experimental Brain Research* 2007;176:23-31.

[9] Catena RD, van Donkelaar A, Halterman CI, Chou L-S. Spatial orientation of attention and obstacle avoidance following concussion. *Experimental Brain Research* 2009;194:67-77.

[10] Cheng P, Magnotta VA, Wu D, Nopoulos P, Moser DJ, Paulsen J, Jorge R, Andreasen NC. Evaluation of the GTRACT diffusion tensor tractography algorithm: a validation and reliability study. *Neuroimage* 2006;31(3):1075-85.

[11] Chou L-S, Kaufman KR, Walker-Rabatin AE, Brey RH, Basford JR. Dynamic instability during obstacle crossing following traumatic brain injury. *Gait & Posture* 2004;20:245-54.

[12] Della Croce U, Cappozzo A, Kerrigan DC. Pelvis and lower limb anatomical landmark calibration precision and its propagation to bone geometry and joint angles. *Medical and Biological Engineering and Computing* 1999;37:155-61.

[13] Dikmen S, McLean A, Temkin N. Neuropsychological and psychosocial consequences of minor head injury. *Journal of Neurology, Neurosurgery, and Psychiatry* 1986;49:1227-32.

[14] Fattal D. Balance & Gait Disorders. Medlink Corporation. Retrieved from www.medlink.com/medlinkhome/info_serv.htm., 2009.

[15] Frencham K, Fox A, Maybery M. Neuropsychological studies of mild traumatic brain injury: a meta-analysis review of research since 1995. *Journal of Clinical and Experimental Neuropsychology* 2005;27:334-51.

[16] Galna B, Peters A, Murphy AT, Morris ME. Obstacle crossing deficits in older adults: A systematic review. *Gait & Posture* 2009;30:270-5.

[17] Gerberding JL, Binder S. Steps to Prevent a Serious Public Health Problem. *Report to Congress on Mild Traumatic Brain Injury in the United States* 2003.

[18] Grabiner PC, Biswas ST, Grabiner MD. Age-Related Changes in Spatial and Temporal Gait Variables. *Archives of Physical Medicine & Rehabilitation* 2001;82:31-5.

[19] Gray, H., Lewis, W.H.: Anatomy of the Human Body. Philadelphia, Lea & Febiger (1918).

[20] Guerts ACH, Knoop JA, van Limbeek J. Is postural control associated with mental functioning in the persistent postconcussion syndrome? *Arch Phys Med Rehab* 1999;80:144-9.

[21] Guerts ACH, Ribbers GM, Knoop JA, Limbeek J van. Identification of Static and Dynamic Postural Instability Following Traumatic Brain Injury. *Archives of Physical Medicine & Rehabilitation* 1996;77:639-44.

[22] Hausdorff JM, Rios DA, Edelberg HK. Gait variability and fall risk in community-living older adults: a 1-year prospective study. *Archives of Physical Medicine & Rehabilitation* 2001;82(8):1050-6.

[23] Kaufman KR, Brey RH, Chou LS, Rabatin A, Brown AW, Basford JR. Comparison of subjective and objective measures of balance disorders following traumatic brain injury. *Medical Engineering & Physics* 2006;28:234-9.

[24] Kuhts-Buschbeck JP, Hoppe B, Golge M, Dreesmann M, Damm-Stunitz U, Ritz A. Sensorimotor recovery in children after traumatic brain injury: analyses of gait, gross motor, and fine motor skills. *Developmental Medicine & Child Neurology* 2003;45:821-8.

[25] Kuhts-Buschbeck JP, Stolze H, Golge M, Ritz A. Analysis of gait, reaching and grasping in children after traumatic brain injury. *Archives of Physical Medicine & Rehabilitation* 2003;84:424-30.

[26] Lipton ML, Gulko E, Zimmerman ME, Friedman BW, Kim M, Gellella E, Gold T, Shifteh K, Ardekani BA, Branch CA. Diffusion-tensor imaging implicates prefrontal axonal injury in executive function impairment following very mild traumatic brain injury. *Radiology* 2009;252(3):816-24.

[27] Magnotta VA, Harris G, Andreasen NC, O'Leary DS, Yuh WT, Heckel D. Structural MR image processing using the BRAINS2 toolbox. *Comput Med Imaging Graph* 2002;26(4):251-64.

[28] Maki BE. Gait changes in older adults: predictors of falls or indicators of fear. *Journal of the American Geriatrics Society* 1997;45:313-20.

[29] McFadyen BJ, Swaine B, Dumas D, Durand A. Residual Effects of a Tramatic Brain Injury on Locomotor Capacity: A First Study of Spatiotemporal Patterns During Unobstructed and Obstructed Walking. *Journal of Head Trauma Rehabilitation* 2003;18:512-25.

[30] O'Shea S, Morris ME, Iansek R. Dual Task Interference During Gait in People With Parkinson Disease: Effects of Motor Versus Cognitive Secondary Tasks. *Physical Therapy* 2002;82:888-897.

[31] Ochi F, Esquenazi A, Hirai B, Talaty M. Temporal-Spatial Feature of Gait after Traumatic Brain Injury. *Journal of Head Trauma Rehabilitation* 1999;14:105-15.

[32] Parker TM, Osternig LR, Lee HJ, van Donkelaar P, Chou L-S. The effect of divided attention on gait stability following concussion. *Clinical Biomechanics* 2005;20:389-95.

[33] Parker TM, Osternig LR, Van Donkelaar P, Chou L-S. Gait Stability following Concussion. *Medicine & Science in Sports & Exercise* 2006;38:1032-40.

[34] Parker TM, Osternig LR, van Donkelaar P, Chou L-S. Recovery of cognitive and dynamic motor function following concussion. *British Journal of Sports Medicine* 2007;41:868-73.

[35] Pettersson AF, Olsson E, Wahlund L-O. Effect of Divided Attention on Gait in Subjects With and Without Cognitive Impairment. *Journal Geriatric Psychiatry and Neurology* 2007;20:58-62.

[36] Rees PM. Contemporary Issues in Mild Traumatic Brain Injury. *Arch Phys Med Rehabil* 2003;84:1885-94.

[37] Rimel RW, Giordani B, Barth JT, Boll TJ, Jane JA. Disability Caused by Minor Head Injury. *Neurosurgery* 1981;9:221-8.

[38] Ruff RM, Iverson GL, Barth JT, Bush SS, Broshek DK, NAN Policy and Planning Committee. Recommendations for diagnosing a mild traumatic brain injury: a National Academy of Neuropsychology education paper. *Arch Clin Neuropsychol* 2009;24:3-10.

[39] Schretlen DJ, Shapiro AM. A quantitative review of the effects of traumatic brain injury on cognitive functioning. *International Review of Psychiatry* 2003;15:341-9.

[40] van Iersel MB, Ribbers H, Munneke M, Borm GF, Olde Rikkert MG. The Effect of Cognitive Dual Tasks on Balance During Walking in Physically Fit Elderly People. *Arch Phys Med Rehabil* 2007;88:187-91.

[41] Vanderploeg RD, Curtiss G, Belanger HG. Long-term neuropsychological outcomes following mild traumatic brain injury. *Journal of the International Neuropsychological Society* 2005;11:229-36.

[42] Vereeck L, Wuyts F, Truijen S, Van de Heyning P. Clinical assessment of balance: Normative data, and gender and age effects. *International Journal of Audiology* 2008;47:67-75.

[43] Verghese J, Holtzer R, Lipton RB, Wang C. Quantitative gait markers and incident fall risk in older adults. *J Gerontol A Biol Sci Med Sci* 2009;64:896-901.

[44] Verghese J, Kuslansky G, Holtzer R, Katz M, Xue X, Buschke H, Pahor M. Walking While Talking: Effect of Task Prioritization in the Elderly. *Arch Phys Med Rehabil* 2007;88:50-3.

[45] Williams G, Morris ME, Schache A, McCrory PR. Incidence of Gait Abnormalities After Traumatic Brain Injury. *Arch Phys Med Rehabil* 2009;90:587-93.

[46] Winter, DA. Biomechanics and Motor Control of Human Movement. Third Edition. Hoboken: John Wiley & Sons, Inc., 2005.

[47] Winter DA. Human balance and posture control during standing and walking. *Gait & Posture* 1995;3:193-214.

[48] Woledge RC, Birtles DB, Newham DJ. The Variable Component of Lateral Body Sway During Walking in Young and Older Humans. *Journal of Gerontology* 2005;11:1463-8.

[49] Woollacott M, Shumway-Cook A. Attention and the control of posture and gait: a review of an emerging area of research. *Gait & Posture* 2002;16:1-14.

[50] Yogev-Seligmann G, Hausdorff JM, Giladi N. The role of executive function and attention in gait. *Mov Disord* 2008;23:329-42.